



Technical Letter Report
[TLR-RES/DE/REB-2022-01]

Review of Code Cases Permitting Use of Nickel-Based Alloy 617 in Conjunction with ASME Section III, Division 5

Date: January 31, 2022

Prepared in response to “NRC Non-Light Water Reactor Near-Term Implementation Action Plan” Strategy #4, by:

*Frederick .W. Brust, Prabhat. Krishnaswamy, L.
Hill
Engineering Mechanics Corporation of
Columbus*

*Jeff Poehler, Michael Breach, Mark Yoo
U.S. Nuclear Regulatory Commission*

NRC Project Manager:

*Jeff Poehler
Sr. Materials Engineer
Reactor Engineering Branch*

**Division of Engineering
Office of Nuclear Regulatory Research
U.S. Nuclear Regulatory Commission
Washington, DC 20555–0001**

DISCLAIMER

This report was prepared as an account of work sponsored by an agency of the U.S. Government. Neither the U.S. Government nor any agency thereof, nor any employee, makes any warranty, expressed or implied, or assumes any legal liability or responsibility for any third party's use, or the results of such use, of any information, apparatus, product, or process disclosed in this publication, or represents that its use by such third party complies with applicable law.

This report does not contain or imply legally binding requirements. Nor does this report establish or modify any regulatory guidance or positions of the U.S. Nuclear Regulatory Commission and is not binding on the Commission.

EXECUTIVE SUMMARY

The Nuclear Regulatory Commission (NRC) staff reviewed two code cases permitting the use of nickel-based Alloy 617 in conjunction with the rules of the American Society of Mechanical Engineers Boiler and Pressure Vessel Code (ASME Code), Section III, "Rules for Construction of Nuclear Facility Components," Division 5, "High Temperature Reactors (Section III-5)." The staff is proposing to endorse Section III-5 with some exceptions and limitations as documented in draft regulatory guide DG-1380, "Acceptability of ASME Code, Section III, Division 5, High Temperature Reactors." The technical basis for DG-1380 is NUREG-2245, "Technical Review of the 2017 Edition of ASME Code, Section III, Division 5, High Temperature Reactors." Code Case N-872, "Use of 52Ni–22Cr–13Co–9Mo Alloy 617 (UNS N06617) for Low Temperature Service Construction Section III, Division 5," permits use of Alloy 617 for components operating at temperatures up to 800 degrees F (425 degrees C), and Code Case N-898, "Use of Alloy 617 (UNS N06617) for Class A Elevated Temperature Service Construction Section III, Division 5," allows use of Alloy 617 in components operating at temperatures of 1,750 degrees F (954 degrees C) and below. Code Case N-898 limits service time of these components to 100,000 hours.

Code Case N-872 contains allowable stresses and physical properties for Alloy 617 for use in Section III-5 low temperature components. Code Case N-898 contains allowable stresses, mechanical properties, and physical properties for Alloy 617 to be used at high temperatures, other information needed for high-temperature design such as isochronous stress-strain curves and fatigue curves, and the creep-fatigue design envelope. Code Case N-898 also includes modifications to the design methodologies for of Section III-5 to be used specifically with Alloy 617, such as the elastic-perfectly plastic (EPP) methodology, buckling rules, and multiaxial stress correction (Huddleston equation).

Code Case N-898 essentially uses the same design rules for Alloy 617 as those contained in Section III-5, with the addition of adding provisions to use EPP analysis to demonstrate compliance with the strain limits of Section III-5, HBB-T-1300, the creep-fatigue limits of Section III-5, HBB-T-1400, and provisions for mitigation of stress relaxation cracking. Code Case N-898 also adds specific material parameters and data for Alloy 617 such as fatigue curves, a creep-fatigue design envelope, safety factors, and a multiaxial stress correction parameter. The EPP analysis techniques are similar to those allowed by Code Cases N-861 and N-862 for Type 304 and Type 316 stainless steel, which are endorsed by the NRC in DG-1380. Code Case N-898 also restricts the use of elastic analysis and simplified inelastic analysis to demonstrate compliance with the strain limits of HBB-T-1300 and creep-fatigue limits of HBB-T-1400 to temperatures less than or equal to 650 degrees C. This is because creep strains and plastic strains cannot be distinguished above this temperature. Therefore, full inelastic analysis or EPP analysis are the only options to show compliance with the limits of HBB-T-1300 and HBB-T-1400 for components operating above 650 degrees C. The staff notes that a constitutive material model for use with full inelastic analysis of Alloy 617 is not provided in Code Case N-898. This type of model is under development by the ASME Code committees involved with high-temperature design.

This report recommends endorsement of Code Case N-872 without limitations or exceptions. The basis for the NRC staff's recommendation is that the materials mechanical properties, allowable stresses, and physical properties provided in N-872 are based either on data already tabulated in the ASME Code, Section II, Subpart D, for Alloy 617, or are based on test data from a representative and sufficient database for Alloy 617.

This report recommends endorsement of Code Case N-898 with the following two limitations:

- When applying HBB-T-1710 and HBB-4800 to Alloy 617 components, applicants and licensees should develop their own plans to address the potential for stress relaxation cracking in their designs. These plans should address factors such as weld joint design and controls on welding in addition to the required heat treatment of HBB-4800.
- When applying HBB-T-1836(2)(-b), the equation for plastic strain in the code case should be replaced with the following equation:

$$\text{for } \sigma > \sigma_1, \varepsilon_p = -\frac{1}{\delta} \ln \left(1 - \frac{\sigma - \sigma_1}{\sigma_p - \sigma_1} \right)$$

The following summarizes the basis for these limitations:

- Guidance for mitigation of stress relaxation cracking (SRC) provides a stabilizing heat treatment that should address the metallurgical contributors to SRC and also relieve weld residual stresses and cold work residual stresses that contribute to SRC. The heat treatment required for mitigation of SRC is in addition to the heat treatment for components with greater than 5% cold work. However, the staff found that heat treatment alone may not be sufficient to mitigate the potential for SRC; therefore, the staff identified the following limitation:
 - When applying HBB-T-1710 and HBB-4800 to Alloy 617 components, applicants and licensees should develop their own plans to address the potential for stress relaxation cracking in their designs. These plans should address factors such as weld joint design and controls on welding in addition to the required heat treatment of HBB-4800.
- The staff determined that the isochronous stress-strain curves (ISSC) for Alloy 617 (HBB-T-1800) provide conservative predictions of stress and strain compared to the data for the same temperature and time as shown in Section 3.10 and Appendix I where spot checks on the curves were made. The ASME Code has identified a typographical error in the equation for plastic strain in HBB-T-1836. The correct equation is provided in Section I.2 as Equation I-1 and a limitation is recommended that this equation be used instead of the equation in Code Case N-898, HBB-T-1836(2)(-b).

For the portions of Code Case N-898 recommended for endorsement without limitations, the bases are as follows:

- The permitted material specifications for base and weld material are recognized ASME material specifications and the permitted weld material is consistent with material used in testing done to qualify the code case.
- The mechanical properties and allowable stresses are based upon analysis of a sufficient and representative database and were evaluated using methodology consistent with that used to determine the corresponding properties for the materials permitted by Section III-5. Additionally, confirmatory analysis by the NRC staff yielded consistent properties to those of the code case.
- The physical properties are based on sufficient and representative data or are the same as properties for Alloy 617 in Section II-D.
- Satisfaction of strain limits for Alloy 617 (Section 3.7) is assured because the standard tests apply below 650 degrees C where creep and plasticity can be separated, which is a requirement for the elastic analysis and simplified inelastic analysis design approach in the code. In addition, the simplified EPP analysis methods for satisfying strain limits can be used as an alternative at any temperature. The EPP methods are based on well-established bounding theorems. Full inelastic analysis methods can always be used to satisfy strain design limits. These rules are recommended for endorsement because predictions using the elastic and EPP analysis methods provide conservative predictions when compared to either test data or results of full inelastic analyses.
- The creep-fatigue rules of HBB-T-1400 (Section 3.8) provide conservative results because the fatigue and creep-fatigue data is conservative, and the methodologies provide conservative results. Specifically, the fatigue design curves for Alloy 617 are conservative because the curves are constructed by reducing the best-fit curve of continuous cycling fatigue data by a factor of two on total strain range or a factor of 20 on life, whichever results in a minimum value, which is consistent with the lower temperature rules in Subsection NB. In addition, the creep-fatigue design envelope is consistent with the data from creep-fatigue tests of Alloy 617. The evaluation methods are appropriate and conservative because they provide a multiaxial stress correction, and also include a procedure for evaluating creep-fatigue damage using EPP analysis. Certain bounding theorems ensure conservative results with the EPP method for Alloy 617. In addition, full inelastic analysis methods can be used to satisfy creep-fatigue design limits and rules ensure conservative design.
- The rules for buckling for Alloy 617 are the same as those in Section III-5. These rules consider time independent and time-dependent buckling and the distinctions between load-controlled conditions, which are most severe, and strain-controlled buckling. The rules permit use of NB buckling rules when creep buckling is not a concern. These rules are equally applicable to Alloy 617 as they are for the other Section III-5 materials. Based on experimental validation of the buckling rules discussed in Section 3.9, and applicability to Alloy 617, the buckling rules are recommended for endorsement.

- The staff determined that the isochronous stress-strain curves (ISSC) for Alloy 617 (HBB-T-1800) provide conservative predictions of stress and strain compared to the data for the same temperature and time as shown in Section 3.10 and Appendix I where spot checks on the curves were made. The cognizant ASME Code working group has identified a typographical error in the equation for plastic strain in HBB-T-1836. The correct equation is provided in Section I.2 as Equation I-1 and a limitation is recommended that this equation be used instead of the equation in Code Case N-898, HBB-T-1836(2)(-b).

Finally, Code Case N-872 and Code Case N-898 do not address degradation of Alloy 617 caused by environmental effects such as irradiation or corrosion. This is consistent with Section III-5, which also does not address such effects. The effects of the environment on Alloy 617 components will therefore have to be addressed separately by applicants.

ACKNOWLEDGMENTS

The authors would like to acknowledge the support provided by Dr. T. L. Sham and of Idaho National Laboratory and Richard N. Wright, Structural Alloys, LLC. for their assistance in creating and providing a publicly available version of the technical bases for Code Cases N-872 and N-898, and also for providing independent consultation on the NRC staff's review of the code cases. In addition, the authors would like to thank Dr. Mark Messner of Argonne National Laboratory and Bob Jetter, Consultant, for helpful discussions during the course of this review.

TABLE OF CONTENTS

Executive Summary.....	i
Acknowledgments	v
Table of Contents	vi
List of Tables	ix
List of Figures	x
Acronyms and Abbreviations	xi
1 Introduction	1
2 Code Case N-872	3
2.1 Background.....	3
2.2 Review Process	3
2.3 Table 1 – Product Specification	4
2.4 Table 2 – Design Stress Intensity Values and Yield and Tensile Strength Values for Section III, Division 5 Class A.....	4
2.4.1 Tensile and Yield Strength Values.....	4
2.4.2 Design Stress Intensity Values	4
2.5 Table 3 - Maximum Allowable Stress Values and Yield and Tensile Strength Values for Section III, Division 5, Class B.....	5
2.6 Table 4/4M – Thermal Expansion for Alloy 617	6
2.7 Table 5/5M – Nominal Coefficients of Thermal Conductivity and Thermal Diffusivity for Alloy 617	7
2.8 Summary – Code Case N-872.....	9
3 Code Case N-898	10
3.1 Background.....	10
3.2 Article HBB-2000, Material.....	12
3.2.1 HBB-2160 Deterioration of Material in Service	12
3.2.2 Article HBB-3000, Design	12
3.2.3 HBB-3210 Design Criteria	12
3.2.4 HBB-3225 Level D Service Limits.....	13
3.2.5 HBB-3225-1 Tensile Strength Values, S_u	13
3.2.6 Table HBB-3225-2, Tensile and Yield Strength Reduction Factors.....	15
3.3 Article HBB-4000	17

3.3.1	HBB-4212 Effects of Forming and Bending Processes	17
3.3.2	HBB-4800 Relaxation Cracking	19
3.4	Mandatory Appendix HBB-I-14 Tables and Figures	22
3.4.1	Table HBB-I-14.1(a) Permissible Base Materials	23
3.4.2	Table HBB-I-14.1(b) Permissible Weld Materials	24
3.4.3	Table HBB-I-14.2 s_o — Maximum Allowable Stress Intensity	24
3.4.4	Figure and Table HBB-I-14.3F S_{mt} – Allowable Stress Intensity Values.....	26
3.4.5	Figure and Table HBB-I-14.4 S_t – Allowable Stress Intensity Values.....	27
3.4.6	Table HBB-I-14.5 Yield Strength Values, S_y	32
3.4.7	Figure and Table HBB-I-14.6G S_r - Minimum Stress-to-Rupture.....	33
3.4.8	Table HBB-I-14.10F Stress Rupture Factors for Welded Alloy 617.....	34
3.5	Physical Properties	38
3.5.1	Coefficient of Thermal Expansion.....	38
3.5.2	Thermal Conductivity and Thermal Diffusivity	38
3.5.3	Nonmandatory Appendix C, Modulus of Elasticity	39
3.6	ALARA Considerations (Cobalt)	40
3.7	HBB-T-1300 Deformation and Strain Limits for Structural Integrity	40
3.7.1	HBB-T-1320 Satisfaction of Strain Limits Using Elastic Analysis	41
3.7.2	HBB-1322, HBB-T-1323, HBB-T-1324 Tests A-1, A-2 and A-3.....	43
3.7.3	HBB-T-1330 Satisfaction of Strain Limits Using Simplified Inelastic Analysis	44
3.8	Article HBB-T-1400 Creep-Fatigue Evaluation	49
3.8.1	HBB-T-1411 Huddleston Parameter for Multiaxial Creep Failure Criterion	50
3.8.2	Figure HBB-T-1420-2, Creep-Fatigue Damage Diagram	52
3.8.3	HBB-T-1420 Limits Using Inelastic Analysis.....	54
3.8.4	HBB-T-1430 Limits Using Elastic Analysis	56
3.8.5	HBB-T-1440 Limits Using Elastic-Perfectly Plastic Analysis – Creep-Fatigue Damage 58	
3.9	Article HBB-T-1500 Buckling and Instability	60
3.9.1	HBB-T-1510 General Requirements.....	60
3.9.2	HBB-T-1520 Time-Dependent Buckling	61
3.10	HBB-T-1820 Isochronous Stress-Strain Relations.....	64
4	Conclusions.....	67
4.1	Code Case N-872 Conclusions.....	67

4.2	Code Case N-898 Conclusions.....	67
4.2.1	Limitations.....	67
4.2.2	Material Properties and Allowable Stresses	68
4.2.3	ALARA Considerations	69
4.2.4	HBB-T Strain Limits and Creep-Fatigue	69
5	References.....	72
APPENDIX I MATERIAL PROPERTY ASSESSMENT OF ISSC FOR ALLOY 617		I-1
I.1	Alloy 617 Data Source	I-3
I.2	Alloy 617 Curves Validation.....	I-4
I.3	Spot Checks of ISSC for Alloy 617 with other data	I-7

LIST OF TABLES

Table 3-1 Topics and Reference Numbers for ASME Records for Code Case N-898.....	10
--	----

LIST OF FIGURES

Figure 2-1	Thermal conductivity of Alloy 617 from INL, 2021b	8
Figure 2-2	Thermal conductivity of Alloy 617 (Heat 1) as a function of temperature, compared to other alloys. (Reproduced from Rabin et. al., 2013, Figure 11)	8
Figure 3-1	Actual vs. expected rupture stress for weld tests reported in INL, 2021h, all test temperatures	36
Figure 3-2	Actual vs. expected rupture stress for welds tests reported in INL, 2021h, for temperatures < 1562 degrees F (850 degrees C)	37
Figure 3-3	Actual vs. expected rupture stress for welds tests reported in INL, 2021h, for temperatures \geq 1562 degrees F (850 degrees C)	37
Figure 3-4	Creep-fatigue damage envelope for Alloy 617.	53
Figure I-1	Schematic of isochronous stress-strain curves	I-2
Figure I-2	Calculated ISSC for Alloy 617 at 1,749 degrees F (954 degrees C).	I-5
Figure I-3	Calculated ISSC for Alloy 617 at 1,400 degrees F (760 degrees C).	I-6
Figure I-4	Calculated ISSC for Alloy 617 at 1,099 degrees F (593 degrees C).	I-7
Figure I-5	Comparison of Code Case N-898 ISSC curve at 1292 degrees F (700 degree C) to data from Narayanan, et. al., 2017 (Davies) and Knezevic, 2013.....	I-8
Figure I-6	Comparison of Code Case N-898 ISSC curve at 1200 degrees F (649 degree C) to model predictions from Corum et. al., 1991.	I-9
Figure I-7	Comparison of Code Case N-898 ISSC curve at 1701 degrees F (927 degree C) to model predictions from Jetter et. al., 2004.	I-10
Figure I-8	Comparison of Code Case N-898 ISSC curve at 982 degree C to model predictions from Corum et. al.,1991.	I-11

ACRONYMS AND ABBREVIATIONS

ADAMS	Agencywide Documents Access and Management System
ALARA	as low as reasonably achievable
ANLWR	advanced nonlight-water reactor
ANL	Argonne National Laboratory
ART	Advanced Reactor Technologies
ASME	American Society of Mechanical Engineers
BPVC	Boiler and Pressure Vessel Code
C	Celsius
CTE	coefficient of thermal expansion
DDS	Demonstration Reactor Design Standard
DOE	U.S. Department of Energy
E	modulus of elasticity
Emc ²	Engineering Mechanics Corporation of Columbus
EPP	elastic-perfectly plastic
EPRI	Electric Power Research Institute
F	Fahrenheit
FEA	finite element analysis
GTAW	gas tungsten arc welding
HTGR	high-temperature gas-cooled reactor
HTR	high-temperature reactor
INL	Idaho National Laboratory
IRSN	Institut De Radioprotection et de Surete Nucleaire
ISSC	isochronous stress-strain curves
ksi	kilopound per square inch
L-M	Larson-Miller
LMP	Larson-Miller Parameter
LWR	light water reactor
mm	millimeter
MPa	megapascal
NIMS	Busshitsu-zairyō kenkyū kikō (National Institute of Materials Science)
NMDA	New Material Data Analysis
NRC	U.S. Nuclear Regulatory Commission

NUMARK	NUMARK Associates, Inc.
ORNL	Oak Ridge National Laboratory
PNNL	Pacific Northwest National Laboratory
PHWT	post-weld heat treatment
PVRC	Pressure Vessel Research Council
RCC-MR	Regles de Conception et de Construction des Materiels Mecaniques des ilots nucleaires (Rules for Design and Construction of Fast-Breeder Liquid-Metal-Cooled Reactors)
RG	regulatory guide
SG	subgroup
SMT	simplified model test
SRC	stress relaxation cracking
SRF	stress rupture factor
SS	stainless steel
TC	thermal conductivity
TD	thermal diffusivity
U.K.	United Kingdom
WRC	Welding Research Council

1 INTRODUCTION

In 2019 the Nuclear Regulatory Commission (NRC) initiated a project to review for endorsement the American Society of Mechanical Engineers (ASME) Boiler and Pressure Vessel Code (ASME Code), Section III, Division 5, “High Temperature Reactors” (Section III-5). The staff is proposing to endorse Section III-5 with some exceptions and limitations as documented in draft regulatory guide DG-1380, “Acceptability of ASME Code, Section III, Division 5, High Temperature Reactors.” (NRC 2021a). The technical basis for DG-1380 is NUREG-2245, “Technical Review of the 2017 Edition of ASME Code, Section III, Division 5, High Temperature Reactors” (NRC 2021b). In 2016, ASME published Code Case N-872, which covers the use of Alloy 617 in Class A and B Section III-5 components with service temperatures up to 800 degrees F (425 degrees C). In 2019, ASME published Code Case N-898, which covers the use of Alloy 617 in Class A Section III-5 components with service temperatures greater than 800 degrees F (425 degrees C) up to 1,750 degrees F (954 degrees C). These code cases represent the first new material to be allowed for Section III-5 use since it was initially published in 2011. Alloy 617 also has better high-temperature strength compared to other materials allowed by Section III-5, which may be important for some advanced non-light water reactor (ANLWR) designs. Due to the timing of the Alloy 617 high temperature code case publication, review of the two code cases was not included in the initial NRC project to review and endorse Section III-5 initiated in 2019.

Code Case N-872 contains allowable stresses and physical properties for Alloy 617 for use in Section III-5 low temperature components. Code Case N-898 contains allowable stresses and physical properties for Alloy 617 to be used at high temperatures, other information needed for high-temperature design such as isochronous stress-strain curves (ISSC) and fatigue curves, and the creep-fatigue design envelope. Code Case N-898 also includes modifications to the design methodologies for of Section III-5 to be used specifically with Alloy 617, such as the elastic-perfectly plastic (EPP) methodology, bucking rules, and multiaxial stress correction (Huddleston equation).

Due to the size and complexity of the draft code case for use of Alloy 617 in high-temperature applications, multiple ASME records were created for various aspects of the code case. Therefore, the original technical basis for Code Case N-898 was contained in background documents for ASME Code Record Numbers 16-994 through 16-1001. The original background documents are not publicly available but are contained in ASME’s C&S Connect Database and are available to ASME Code committee members.

A publicly available version of the technical bases for Code Case N-872 and N-898 is contained in Wright, Richard., “Draft ASME Boiler and Pressure Vessel Code Cases and Technical Bases for Use of Alloy 617 for Construction of Nuclear Components Under Section III, Division 5,” INL/EXT-21-15-36305, Revision 2 (INL, 2021a). INL, 2021a contains the same technical content as the background documents for Records 16-994 through 16-1001, with some editorial corrections. Appendix 3 to INL, 2021a (INL, 2021b) contains a publicly available version of the single technical basis document for Code Case N-872.

Appendix 5 to INL, 2021a (INL, 2021c), contains the compiled technical bases for Code Case N-898. For ease of referencing, the individual background documents for different topics within this compilation have been included as separate references INL, 2021d through INL, 2021s.

2 CODE CASE N-872

2.1 Background

Code Case N-872 (ASME 2016) provides materials properties and allowable stresses for using Alloy 617 (UNS N06617) in components constructed to the requirements of Section III, Division 5, Subsection HB, Subpart A, Class A and Subsection HC, Subpart A, Class B. N-872 allows the use of Alloy 617 up to a maximum temperature of 800 degrees F (425 degrees C). This temperature range is appropriate for the lower temperature components of high-temperature reactors constructed to Section III-5.

Subsection HB, Subpart A (HBA) addresses Class A metallic pressure boundary component in low temperature service, as defined in Section III-5. For austenitic materials, the upper limit of low temperature is defined in Section III-5 Table HAA-1130-1 as 800 degrees F (425 degrees C). HBA allows low temperature Class A components to essentially be constructed to Section III, Division 1 (Section III-1), Subsection NB rules, which pertain to Class 1 components in Section III-1. NUREG-2245 (NRC 2021b), Section 3.5 discusses the technical basis for the staff's review of HBA, which is endorsed without exceptions or limitations in DG-1380 (NRC 2021a)

Subsection HC, Subpart A (HCA) addresses Class B metallic pressure boundary components in low temperature service. The same temperature limits apply as for Class A low temperature components. HCA allows low temperature Class B components to essentially be constructed to Section III-1, Subsection NC rules, which pertain to Class 2 components in Section III-1. NUREG-2245 (NRC 2021b) Section 3.12 discussed the technical basis for the staff's review of HCA, which is endorsed without exceptions or limitations in DG-1380 (NRC 2021a).

2.2 Review Process

Since the provisions of N-872 are intended to be used with Section III-5, HBA and HCA which are essentially similar to Section III-1, Subsection NB and NC rules for Class 1 and Class 2 components, the staff evaluated the provisions of N-872 for appropriateness to use with the Section III-1 provisions. Essentially, the properties and allowable stresses should be acceptable up to and including the maximum use temperature of 800 degrees F (425 degrees C). Additionally, if allowable stresses are taken from Section II-D, these allowable stresses should be appropriate for the equivalent safety class in Section III-5; e.g. allowable stresses for Class 1 in Section III-1 for Section III-5 Class A components and allowable stresses for Class 2 in Section III-1 for Section III-5 Class B components.

Appendix 3 to INL, 2021a, Background for Draft Code Case: Use of Alloy 617 (UNS N06617) for Low Temperature Service Construction, documents ASME's technical basis for the draft code case which became Code Case N-872 (INL, 2021b).

2.3 Table 1 – Product Specification

Summary of Code Case Content

N-872 Table 1 lists the product specifications allowed by the code case. These include SB-166, for rod, bar and wire, SB-167, for seamless pipe and tube, SB-168, for plate sheet and strip, and SB-564 for forgings.

Staff Evaluation

No specific technical basis is provided for the permitted specifications. The staff finds the listed specifications acceptable because they are ASME material specifications, all of which have properties listed in Section II-D/II-D-M and are generally allowed for use in other code books such as Section III-1.

2.4 Table 2 – Design Stress Intensity Values and Yield and Tensile Strength Values for Section III, Division 5 Class A

Summary of Code Case Content

Table 2 and Table 2M of N-872 contains the Design Stress Intensity Values and Yield and Tensile Strength Values for Section III, Division 5 Class A for metal temperatures from 100-800 degrees F and 40-425 degrees C.

2.4.1 Tensile and Yield Strength Values

Technical Basis

INL, 2021b indicates that the proposed yield and tensile strength values for N-872 are taken from Tables Y-1 and U of Section II-D.

Staff Evaluation

The staff verified the tensile and yield strength values for temperatures from 100 degrees F through 800 degrees F in Table 2 of N-872 are identical to those in Section II-D, 2019 edition, Table U and Y-1, respectively (for Customary Units), and Section II-D-M from 40 degrees C up to 425 degrees C (for Systeme International (SI) Units). This is appropriate since the Section II-D and Section II-D-M tensile and yield strength values are appropriate for Section III-1 use, which is appropriate for Section III-5 Class A low temperature components, and the staff thus finds these values acceptable.

2.4.2 Design Stress Intensity Values

Summary of Code Case Content

Table 2 and Table 2M of N-872 include design stress intensity values for metal temperatures from 100-800 degrees F and 40-425 degrees C.

Technical Basis

INL, 2021b notes that since Alloy 617 is not currently allowed for Section III-1 use, the design stress intensity, S_m is not shown in Table 2B for this alloy and the values must be determined. INL, 2021b further notes that the criteria to be evaluated to determine S_m are given in Table 2-100(a) of Mandatory Appendix 2 of Section II-D. INL, 2021b also notes that, as specified in Note (1) to Table 2-100(a), a yield strength multiplication factor of either $2/3$ or 0.9 must be selected for austenitic and nickel alloys when determining the yield strength criteria above room temperature, and that examination of tabulated S_m values in Table 2A and B of the Code revealed that 0.9 was used for nickel alloys 600, 690 and 800 as well as Types 304 and 316 stainless steels. INL, 2021b indicates that the factor of $2/3$ was used for Alloy 625 apparently because of its higher strength. The staff notes that Note 1 to Table 2-100 states that for austenitic stainless steels, nickel alloys, copper alloys, and cobalt alloys having a specified minimum room temperature yield strength to specified minimum room temperature tensile strength (S_y/S_T) ratio less than 0.625, the design stress intensity values in Tables 2A and 2B may exceed two-thirds and may be as high as 90% of the yield strength at temperature. For Alloy 617 this ratio is less than 0.5 in the temperature range covered by Division 5.

Staff Evaluation

Design stress intensity values, S_m , are shown in Table 2B of Section II-D/II-D-M of the ASME Code for nonferrous alloys allowed for Section III, Division 1, Class 1 design. The design stress intensity values for Alloy 617, Class A low temperature components should be the same as those that would be allowed for Section III-1, Class 1 components in Section II-D, Table 2B.

The staff calculated the S_m values using the criteria of Section II-D/II-D-M Table 2-100(a) as described above, using the tensile and yield strength values given in Table 2 of the Code Case. The staff calculated nearly identical values to the values in Code Case Table 2. The staff therefore considers the code case values to be verified and finds the S_m values acceptable.

2.5 Table 3 - Maximum Allowable Stress Values and Yield and Tensile Strength Values for Section III, Division 5, Class B

Summary of Code Case Content

Table 3 and Table 3M provide maximum allowable stress values and yield and tensile strength values for Section III-5, Class B components for metal temperatures from 100-800 degrees F and 40-425 degrees C. The table provides two different allowable stress values for each temperature, as explained below.

Technical Basis

INL, 2021b, states that the proposed maximum allowable stress values for this code case are taken from Section II-D Table 1B. In Section II-D, Table 1B, the allowable stress, S , is

determined as the minimum of the values calculated using the criteria listed in Table 1-100 of Mandatory Appendix 1 of Section II-D. Note (1) to Table 1-100 states for austenitic steels and some nickel alloys two sets of allowable stress values may be listed. The lower values are controlled by the $\frac{2}{3}S_Y$ criteria, while if a small amount of deformation can be tolerated in the part, $0.9S_Y$ can be used resulting in higher allowable stress. Table 3 and Table 3M of N-872 each provide two sets of maximum allowable stress values, one of which is identical to the higher set of values from Section II-D/II-D-M, and the other identical to the lower set of values from Section II-D/II-D-M. The higher set of values in N-872 references Note (1) to Table 3, which states:

Due to the relatively low yield strength of this material, the higher stress values were established at temperatures where stress values in this range exceed 66- $\frac{2}{3}$ % but do not exceed 90% of the yield strength at temperature. Use of these stresses may result in dimensional changes due to permanent strain. These stress values are not recommended for the flanges of gasketed joints or other applications where slight amounts of distortion can cause leakage or malfunction. For Section III applications, Table Y-2 lists multiplying factors that, when applied to the yield strength values shown in this table, will give allowable stress values that will result in lower levels of permanent strain.

INL, 2021b indicates that Alloy 617 is one of the nickel alloys with two sets of allowable stress in Table 1B, and that the higher values meet the $0.9S_Y$ criteria and is denoted by the footnote G5 to Table 1B, which the staff notes is essentially identical to Note (1) to N-872 Table 3/3M.

Staff Evaluation

The staff confirmed that the maximum allowable stress values of N-872, Table 3/3M are identical to the maximum allowable stress values for Alloy 617 (UNS Number N06617), in Section II-D/II-D-M, Table 1B, 2019 edition.

The staff finds that maximum allowable stress values for Section III-5, Class B components in low temperature service are acceptable because they are identical to the maximum allowable stress values of Section II-D/II-D-M, Table 1B, 2019 edition. This is appropriate because Section III-5, HCA essentially references the rules of Section III-1, Subsection NC for Class 2 components, and Section II-D/II-D-M Table 1B provides maximum allowable stress values for Section III, Class 2 components (among other code books/classes).

2.6 Table 4/4M – Thermal Expansion for Alloy 617

Summary of Code Case Content

N-872 Table 4 and Table 4M provides instantaneous, mean, and linear coefficients of thermal expansion (CTE) for Alloy 617 from 70-800 degrees F and 20-425 degrees C.

Technical Basis

The CTE values were based on physical measurements, which are reported in Rabin et. al., 2013. INL, 2021b indicates that physical measurements were made from 20 degrees C up to 1,000 degrees C and the change in length per unit length ($\Delta l/l_0$) versus temperature was fit to a third-order polynomial, which provided a good fit to the data. INL, 2021b also noted that the calculated CTE values for Alloy 617 were compared to those for other nickel-based alloys, Alloy 230 and Hastelloy-X, that have tabulated values in Section II-D Table TE-4. The CTE values for these other alloys are in reasonable agreement with the calculated values for Alloy 617. The proposed CTE values were also compared in INL, 2021b to the proposed values in a draft code case for Alloy 617 from 1992, and a Special Metals data sheet for Alloy 617, finding reasonable agreement with both.

Staff Evaluation

The staff reviewed the graphs comparing the values to the other nickel alloys and other values for Alloy 617 and agrees that the proposed code case values are in reasonable agreement. Since the CTE values are based on physical measurements and were calculated via a model providing a good fit to this data and are in reasonable agreement with both previously determined values for Alloy 617 and similar alloys, the staff finds these values acceptable.

The staff notes that INL, 2021b provides CTE values from 20-1000 degrees C (70-1800 degrees F); however, N-872 only provides CTE values through 425 degrees C (800 degrees F). The same fit equations were used for both the high temperature and low temperature values. The basis document for the CTE values for N-898 (16-995) includes these same fit equations.

2.7 Table 5/5M – Nominal Coefficients of Thermal Conductivity and Thermal Diffusivity for Alloy 617

Summary of Code Case Content

Table 5 and 5M provide nominal coefficients of thermal conductivity and thermal diffusivity for Alloy 617 from 70-800 degrees F and 20-425 degrees C.

Technical Basis

INL, 2021b, provides the technical basis for the proposed thermal conductivity and thermal diffusivity values. The staff notes that N-872 provides thermal conductivity and thermal diffusivity values from 20-425 degrees C (70-800 degrees F). However, the technical basis in INL, 2021b provides proposed values of thermal conductivity and thermal diffusivity from 20-1000 degrees C (70-1800 degrees F). Both thermal conductivity and thermal diffusivity were based on physical measurements. Polynomial fits to the data were used to determine the relationship of thermal conductivity to temperature and thermal diffusivity to temperature. Both thermal diffusivity and thermal conductivity show an essentially linear relationship to temperature except in the temperature range of about 600-800 degrees C (1112-1472 degrees F), where non-monotonic behavior is observed, with a peak at around 1,300 degrees F (700 degrees C)(Figure 2-1).

However, Rabin et. al., 2013, shows actual test data for several nickel-based alloys, including Alloy 230, which shows similar non-monotonic behavior (Figure 2-2). INL, 2021b also showed a comparison of the proposed thermal conductivity values to the values for two other nickel-based alloys (Alloy 230 and Hastelloy-X) from Section II-D Table TCD. The proposed values are in good agreement with the other two alloys except that the Section II-D values for the other two alloys do not reflect the non-monotonic behavior.

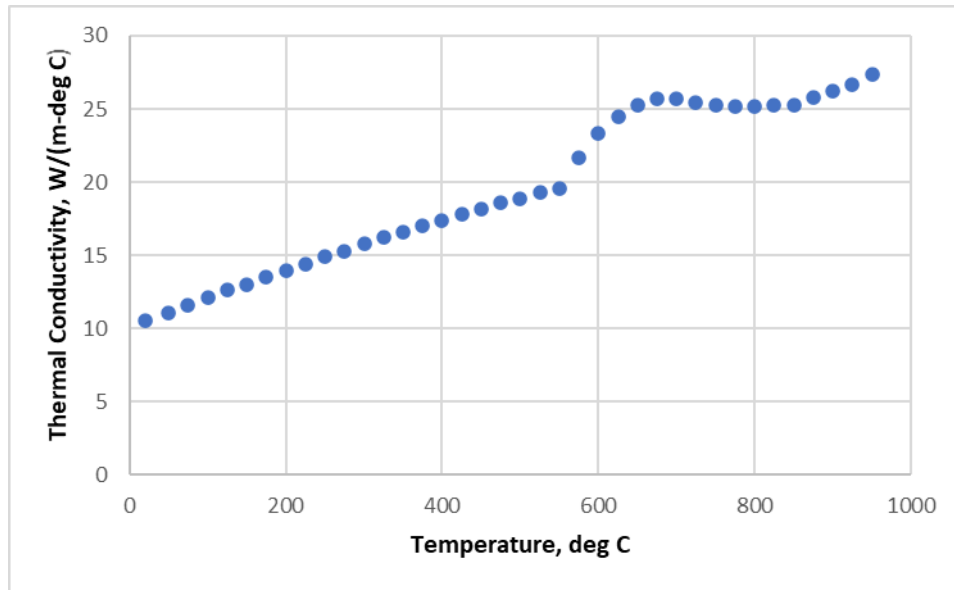


Figure 2-1 Thermal conductivity of Alloy 617 from INL, 2021b

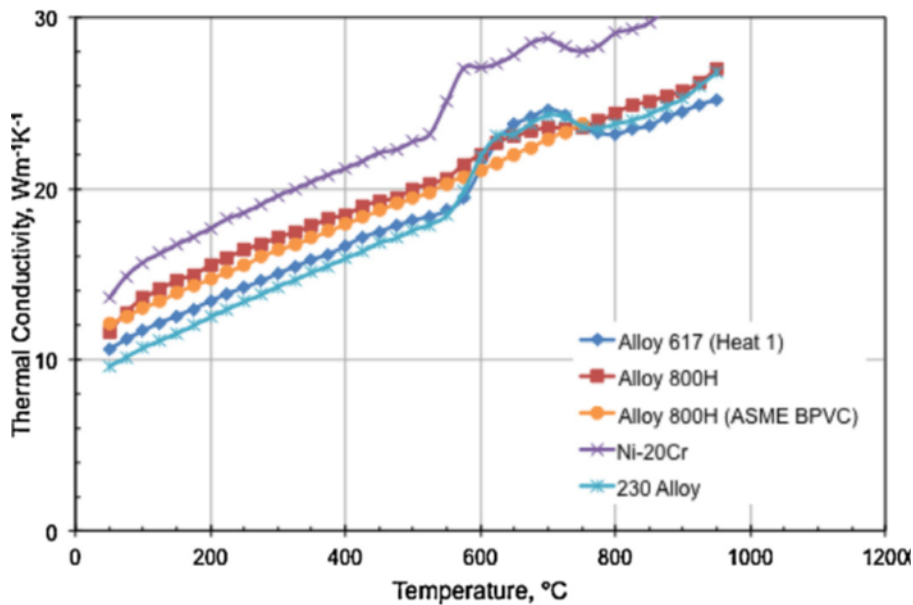


Figure 2-2 Thermal conductivity of Alloy 617 (Heat 1) as a function of temperature, compared to other alloys. (Reproduced from Rabin et. al., 2013, Figure 11)

INL, 2021b notes that although the deviation is not shown in either the vendor data for Alloy 617 or in Section II-D for the other nickel solid solutions, the magnitude of the local peak in conductivity is nearly 20% compared to a monotonic curve, and the local peak lies within the temperature range where it is anticipated that Alloy 617 will be used for nuclear heat exchanger design. Rabin et. al, 2013, ascribes this behavior primarily to short-range order/disorder phenomena known to occur in the nickel-chromium system. INL, 2021b states that it therefore seems reasonable to include the non-monotonic behavior in the proposed thermal properties. The staff notes that the non-monotonic behavior occurs at temperatures above 800 degrees F (425 degrees C); therefore, this behavior does not affect the values of thermal diffusivity and thermal conductivity included in Code Case N-872, which only includes values up to 800 degrees F (425 degrees C). However, the non-monotonic behavior is pertinent to the thermal properties in Code Case N-898, since the same technical basis is used for the thermal properties in the high-temperature code case.

Staff Evaluation

The staff finds the proposed thermal conductivity and thermal diffusivity acceptable because the values are based on physical measurements, the mathematical fit to the data seems reasonable, and a plausible physical explanation has been given for the non-monotonic behavior occurring in the 600-800 degrees C (1112-1472 degrees F).

2.8 Summary – Code Case N-872

The staff reviewed Code Case N-872, which provides permissible product specifications, allowable stresses, mechanical and physical properties for use in construction of low temperature Alloy 617 components for Section III, Division 5, Subsection HB Subpart A (Class A) and Subsection HC, Subpart B (Class B). Allowable stresses include the design stress intensity values and maximum allowable stresses. Mechanical properties include yield and tensile strength. Physical properties include CTE, thermal conductivity, and thermal diffusivity.

The staff finds the permissible product specifications acceptable because they are ASME material specifications, all of which have properties listed in Section II-D/II-D-M and are generally allowed for use in other code books such as Section III-1.

The staff found all the proposed allowable stresses and mechanical properties acceptable because these are generally consistent with the corresponding values of these properties and allowable values in Section II-D, for design of components of equivalent safety significance, or have been determined consistently with the procedures of Section II-D, when explicit values were not included in Section II-D.

The staff found the proposed thermal properties acceptable, because the properties are generally based on a sufficient amount of experimental data, reasonable mathematical fits to the data are used to define the temperature versus property relationship, and the proposed properties have been benchmarked against values of these properties for similar alloys, or other investigations of Alloy 617.

3 CODE CASE N-898

3.1 Background

The primary reference for the staff's review is a publicly available version of the technical basis for Code Case N-898 contained in INL, 2021a, Appendix 5, "Background for Draft Code Case: Use of Alloy 617 (UNS N06617) For Class A Elevated Temperature Service Construction" (INL, 2021c). INL, 2021c compiles individual background documents which are references INL, 2021d through INL, 2021s. These individual background documents are essentially identical to the non-publicly available background documents in ASME Code Record Numbers 16-994 through 16-1001. For Records 16-994 and 16-995, this report identifies multiple references for each since the background documents for these records are further subdivided into smaller background documents which have their own set of references. Table 3-1 provides a cross-reference between the reference numbers in this report to the corresponding ASME Record Numbers, and a list of topics addressed in each ASME Record Number.

Table 3-1 Topics and Reference Numbers for ASME Records for Code Case N-898

ASME Record No.	Topic(s)	Reference Number(s)
16-994	Permissible Base Metals, Permissible Weld Materials, Yield and Ultimate Strength, Allowable Stress Values, Stress Rupture Factors, Relaxation Cracking, Strength Reduction Factor due to Long Time Prior Elevated Temperature Service, Effects of Forming and Bending Processes	INL, 2021d-INL, 2021k
16-995	Physical Property tables, Modulus of Elasticity tables	INL, 2021l, INL, 2021m
16-996	Buckling and Instability	INL, 2021n
16-997	Huddleston Parameter, Isochronous Stress-Strain Relationships	INL, 2021o
16-998	Strain limits, Creep-Fatigue Damage Diagram and Temperature Limits, Creep-Fatigue Limits using EPP Analysis	INL, 2021p
16-999	HBB-T-1340 Satisfaction of Strain Limits Using EPP Analysis	INL, 2021q
16-1000	HBB-T-1420-1 Design Fatigue Strain Range	INL, 2021r

ASME Record No.	Topic(s)	Reference Number(s)
16-1001	Abridged Background for Overall Alloy 617 code case	

Code Case N-898, “Use of Alloy 617 (UNS N06617) For Class A Elevated Temperature Service Construction,” (N-898) (ASME 2019a) was published by ASME in 2019. N-898 allows the use of nickel-based Alloy 617, also known as 52Ni-22Cr-13Co-9Mo, in the construction of components conforming to the requirements of Section III-5, Subsection HB, Subpart B “Elevated Temperature Service,” for service temperatures up to 1,750 degrees F (954 degrees C) and service times out to 100,000 hours. N-898 was written to be used in conjunction with Section III-5, Subsection HB, Subpart B. In the reply to the inquiry, N-898 states that all requirements of Subsection HB, Subpart B shall be met except:

- when these requirements are modified by the corresponding numbered paragraphs of this Code Case, or
- when new requirements are added with new numbered paragraphs of this Code Case.

N-898 modifies several areas of Section III-5. In the area of materials, N-898 modifies the allowable materials specifications for base and weld materials, allowable stresses, other material properties (yield strength and ultimate strength), stress rupture factors for weldments, and strength reduction factors due to long-term aging. N-898 also provides rules related to stress relaxation cracking (SRC) and forming and bending. In the area of mechanical design, N-898 modifies portions of Section III-5 Nonmandatory Appendix HBB-T including the rules for buckling and instability, creep-fatigue, and strain range. N-898 also adds methodology for EPP analysis as an alternative for demonstrating compliance with the strain limits of Section III-5 HBB-T-1300 and the creep-fatigue limits of HBB-T-1400. The EPP methodology is similar to the methodology of Code Cases N-861 and N-862.

For components that operate with temperatures and loadings conditions where creep effects are significant, Section III-5 addresses structural failure modes considering time-dependent materials properties including ductile rupture from short term loadings, creep-rupture from long-term loadings, creep-fatigue failure, and gross distortion due to incremental collapse and ratcheting. Section III-5 also provides guidelines for preventing loss of function due to excessive deformation, bucking due to short-time loadings, and creep bucking due to long-term loadings. Code Case N-898 addresses these same failure modes. Neither Section III-5 nor Code Case N-898 address deterioration that may occur in service due to corrosion, mass transfer phenomena, radiation effects, or other materials instabilities. Therefore, such environmental effects are outside the scope of the staff’s review of Code Case N-898.

The staff’s review of the topics listed above are detailed in Sections 3.2 through 3.10.

3.2 Article HBB-2000, Material

Code Case N-898 adds information on Deterioration of Material in Service (HBB-2160) to Section III-5, including a reference to tensile and yield strength reduction factors to be added to Table HBB-3225-2 for Alloy 617. NUREG-2245, Section 3.6.2 contains more explanation of these factors and how they are generally determined by ASME, as well as the staff's review of these properties for the five¹ materials allowed by Section III-5 for Class A, high-temperature components. The primary technical basis document for these properties is in the Background Document - HBB-1-14.1(a) Permissible Base Materials for Structures other than Bolting (INL, 2021d).

3.2.1 HBB-2160 Deterioration of Material in Service

This subparagraph addresses reduction of yield and tensile strength resulting from long-term aging, or exposure to high temperatures for a certain time period. A new item (g) is added to HBB-2160 in Section III-5, which refers to the yield and tensile strength reduction factors of Table HBB-3225-2 of the code case, which are reviewed in Section 3.2.2 of this report. The staff finds HBB-2160 acceptable because it found the tensile and yield strength reduction factors of Table HBB-3225-2 acceptable, as detailed in Section 3.2.2 of this report.

3.2.2 Article HBB-3000, Design

Code Case N-898 provides temperature dependent tensile strength values in Table HBB-3225-1 and tensile and yield strength reduction factors due to long time prior elevated temperature service in Table HBB-3225-2. NUREG-2245 (NRC, 2021b), Section 3.6.2 and 3.7.8 discuss the review of the tensile strength values and tensile and yield strength reduction factors for the five materials allowed by Section III-5 for Class A, high-temperature components. The primary technical basis document for these properties is found in INL, 2021d.

3.2.3 HBB-3210 Design Criteria

N-898, Paragraphs HBB-3212 and HBB-3214 provide additional information regarding the mechanical behavior of Alloy 617 at high temperatures.

Summary of Code Case Content

HBB-3212, Basis for Determining Stress, Strain, and Deformation Quantities, points out two unique characteristics of the mechanical behavior of Alloy 617: 1) the lack of a clear distinction between time independent elastic-plastic behavior and time-dependent creep behavior; 2) Flow stresses are strongly strain rate sensitive at elevated temperatures.

¹ One additional material, Alloy 718, is allowed for Class A, high temperature bolting.

HBB-3214, Stress Analysis adds a new paragraph to HBB-3214.2 that cautions that decoupling of plastic and creep strains in the classical constitutive framework is generally a poor representation of the true material behavior. The new paragraph recommends that unified constitutive equations, which do not distinguish between rate-dependent plasticity and time-dependent creep, represent the rate dependence and softening that occur, particularly at higher temperatures.

Technical Basis

Background for Draft Code Case: Use of Alloy 617 (UNS N06617) For Class A Elevated Temperature Service Construction (INL, 2021n) provides the technical basis for HBB-3212 and HBB-3214. INL, 2021n states that the use of unified, or visco-plastic constitutive material models appropriately accounts for the lack of independence between plasticity and creep as discussed in J. M. Corum and J. J. Blass, "Rules for Design of Alloy 617 Nuclear Components to Very High Temperatures," (Corum et. al, 1991).

Staff Evaluation

The staff reviewed the information in Corum et. al, 1991, which states that constitutive models of inelastic behavior are typically based on classical concepts of time independent plasticity and time-dependent creep. In such models, inelastic strain is considered the sum of separately evaluated plastic and creep strains. Corum et al, 1991, further state that for Alloy 617 at temperatures close to 982 degrees C (1,800 degrees F), this distinction between plasticity and creep is unrealistic; inelastic behavior is always significantly time- or rate-dependent. Finally, Corum et. al, 1991 states that to properly characterize this behavior, a so-called unified, or visco-plastic constitutive model is much more appropriate. Such a model can provide a useful description of both short- and long-term behavior as a function of loading rate.

The information in HBB-3212 and HBB-3214 of the code case does not contain any requirements but provides useful information and recommendations. Therefore, the staff finds HBB-3212 and HBB-3214 acceptable.

3.2.4 HBB-3225 Level D Service Limits

The additions to Paragraph HBB-3225 in N-898 consist of references to Table HBB-3225-1 for ultimate strength of Alloy 617, S_u and Table HBB-3225-2, for tensile and yield strength reduction factors for Alloy 617.

3.2.5 HBB-3225-1 Tensile Strength Values, S_u

Summary of Code Case Content

Tensile strength values (S_u) from Section II-D, Table U for Alloy 617 are used up to 1,000 degrees F (525 degrees C).

Technical Basis

The technical basis for the S_u values is provided in Background Document – Yield and Ultimate Strength (INL, 2021f). INL, 2021f states that the New Material Data Analysis (NDMA) Excel Spreadsheet for time independent material properties was used to determine S_u for temperatures greater than 977 degrees F (525 degrees C). INL, 2021f indicates that the current ASME Code values at 1,000 degrees F and 525 degrees C are used in Table HBB-3225-1 of the code case, and above that temperature new values based on this analysis are proposed. The NDMA spreadsheet produces a fit to the ratio values of elevated temperature to room temperature values of the yield and ultimate strengths, R_Y and R_T . The ratios were represented by a polynomial in terms of $T-T_{RT}$ where T is the temperature and T_{RT} is room temperature, both in degrees F or degrees C. For the tensile ratio, a fifth-order polynomial was fit to the tensile ratio. The ratio was then multiplied by the specified room temperature ultimate tensile strength S_T to obtain the proposed values of S_u . Figure 4 of INL, 2021f is a plot showing the fit along with the data for each heat. The staff reviewed the plot of the fits and finds it to be reasonable.

The tensile data (including both tensile and yield strength) is provided in Appendix I of the Background Document for Tensile and Yield Strength in INL, 2021f.

Staff Evaluation

Nonmandatory Appendix HBB-Y provides guidance on the information related to tensile properties that should be included in the data package for time independent data for each heat and representative product, per Section II-D, Mandatory Appendix 5.

- Yield strength from room temperature at 100 degrees F (50 degrees C) intervals to 100 degrees F (50 degrees C) above maximum use temperature
- Ultimate tensile strength from room temperature at 100 degrees F (50 degrees C) intervals to 100 degrees F (50 degrees C) above maximum use temperature
- Tensile elongation from room temperature at 100 degrees F (50 degrees C) intervals to 100 degrees F (50 degrees C) above maximum use temperature
- Reduction of area from room temperature at 100 degrees F (50 degrees C) intervals to 100 degrees F (50 degrees C) above maximum use temperature

HBB-Y also recommends that a minimum of three commercial heats are required to be tested.

The data used to determine S_u in INL, 2021f comprises 208 data points from 13 material heats. The product forms represented are rod, sheet, bar, forgings, and plate. The temperatures ranges from room temperature up to 1,093 degrees C, which is more than 50 degrees C above the maximum use temperature of 950 degrees C. Not all of the heats have elongation and reduction in area data, or cover the entire temperature range recommended by HBB-Y. However, four of 13 heats have a complete set of tensile data (ultimate tensile strength, yield strength, elongation, and reduction in area), and cover the temperature range recommended by HBB-Y, for all data points. Therefore, the data set meets the criteria of HBB-Y for sufficient data

and number of heats. Only data from heats of material with known chemistry was included. The staff judges that the database for the tensile and yield strength determination is sufficient in terms of number of data, number of heats and product forms represented, and temperature range.

General Note (b) to Table U of Section II-D states in part:

The tabulated values of tensile strength are those which the Committee believes are suitable for use in design calculations. At temperatures above room temperature, the values of tensile strength tend toward an average or expected value which may be as much as 10% above the tensile strength trend curve adjusted to the minimum specified room temperature tensile strength. The tensile strength values do not correspond exactly to "average" as this term is applied to a statistical treatment of a homogeneous set of data.

The trend line given by the fit in Figure 4 appears to be consistent with the tendency toward the tensile strength roughly corresponding to an average value.

Figure 5 of INL, 2021f shows the proposed S_u values for temperatures above 1,000 degrees F (525 degrees C) along with the Section II-D, Table U values for lower temperatures. The figure shows a smooth transition from the Section II-D, Table U values to the code case values for higher temperatures.

Based on the sufficient database of tensile data, plus the reasonable fit of the tensile ratio R_T to the data, the staff finds the proposed S_u values to be acceptable.

3.2.6 Table HBB-3225-2, Tensile and Yield Strength Reduction Factors

Summary of Code Case Content

The tensile and yield strength reduction factors in Table HBB-3225-2 of the code case are both 1.0 for all temperatures ≥ 800 degrees F (425 degrees C), indicating no reduction in tensile or yield strength due to long time elevated temperature service.

Technical Basis

The technical basis for the tensile and yield strength reduction factors is described in Background Document - HBB-3225-2 – Strength Reduction Factor Due to Long Time Prior Elevated Temperature Service (INL, 2021j) related to the aging factors. ASME reviewed some data from previous testing in W. Ren and R. Swindeman, "A Review Paper on Aging Effects in Alloy 617 for Gen IV Nuclear Reactor Applications" (Ren et. al 2009), and also conducted some testing. Materials were aged at a variety of temperatures up to 1,472 degrees F (800 degrees C), and a variety of times out to 32,000 hours. All aged specimens tested at room temperature showed an increase in yield and tensile strength compared to the unaged materials. Additional data from Special Metals Corporation (SMC) and ORNL covered temperatures up to 1,600 degrees F (871 degrees C). A slight decrease in room temperature tensile strength is noted for

an aging temperature of 1,600 degrees F (871 degrees C), while tensile strength increased at all lower aging temperatures.

Figure 4 of INL, 2021j also presents additional room temperature test data on aged tensile and yield strength for temperatures up to 1,000 degrees C and times up to 1,000 hours from H. E. McCoy and J. F. King (Oak Ridge National Laboratory), *Mechanical Properties of Inconel 617 and 618* (McCoy et. al, 1985), Special Metals Corporation, "Inconel Alloy 617" Publication Number SMC-029 (Special Metals, 2005), Ren et. al, 2009, and K. Mo, G. Lovicu, H. M. Tung, X. Chen and J. F. Stubbins, "High Temperature Aging and Corrosion Study on Alloy 617 and Alloy 230" (Mo et. al, 2011). This data shows no reduction in strength compared to unaged material.

INL, 2021j also presents graphs of aged tensile and yield strength data measured at the aging temperature for temperatures from 1,200 degrees F (650 degrees C) up to 1832 degrees F (1,000 degrees C), and times out to 20,000 hours. These data also showed the strength generally increased or was no lower than the unaged strength, with no decreasing trend in strength with increased aging time.

INL, 2021j stated that the time-temperature transformation diagram for Alloy 617 from Q. Wu, H. Song, R. W. Swindeman, J. P. Shingledecker, and V. K. Vasudevan, "Microstructure of Long-Term Aged in 617 Ni-Base Superalloy"(Wu et. al, 2008) shows no new aging mechanism would likely be operative at 1,000 degrees C versus lower temperatures. Wu et. al, 2008, documents microstructural testing of Alloy 617 aged at temperatures up to 1,600 degrees F (871 degrees C).

Staff Evaluation

ANL/AMD-21/1, Historical Context and Perspective on Allowable Stresses and Design Parameters in ASME Section III, Division 5, Subsection HB, Subpart B dated March 2021 (ANL, 2021) indicates that the yield and tensile strength reduction factors (Table HBB-3225-2) in Section III-5 are based on the ratio of the average strength after exposure to elevated temperature to the tabulated yield strength (Table HBB-I-14.5) or tabulated tensile strength (Table HBB-3225-1) as applicable. There is no credit for strength increase so the maximum factor is 1.0.

The staff compared the data presented for aged tensile and yield strength to the tabulated tensile and yield strength from Tables HBB-3225-2 and HBB-I-14.5 of the code case, and Section II-D for the room temperature tensile and yield strength. The ratio for yield strength at all temperatures appears to be greater than 1.0. Some of the at temperature tensile strength values from 1382-1600 degrees F (750-871 degrees C) had ratios less than 1.0; however, these materials also had unaged tensile strength values below the code case values, and the tensile strength values did increase with aging time.

Alloy 617 is primarily a solid solution strengthened alloy, with a small contribution due to precipitation strengthening by the γ' phase (INL, 2021j). Therefore, it is expected to have good

microstructural stability for long-term aging. Therefore, although the aged tensile data only goes out to 20,000 hours, it is reasonable to conclude that no unexpected metallurgical transformations will occur at greater times that will cause a significant drop in strength.

Therefore, based on the data presented in the technical basis that shows no trend of a decrease in tensile or yield strength with increasing aging temperature or time, plus the relative metallurgical stability of Alloy 617, the staff finds the proposed tensile and yield strength reduction factors to be acceptable.

3.3 Article HBB-4000

The primary technical basis for this article is found in INL, 2021c.

3.3.1 HBB-4212 Effects of Forming and Bending Processes

Summary of Code Case Content

HBB-4212 of Code Case N-898 requires post-fabrication heat treatment of materials that have been formed during fabrication, that have fabrication induced strains greater than 5%. When required, N-898 states the post-fabrication heat treatments shall be in accordance with the heat treatment specified in the base material specification.

Technical Basis

The technical basis for N-898 HBB-4212 is contained in "Background Document – HBB-4212 - Effects of Forming and Bending Processes," (INL, 2021k), states that cold work alters the creep-rupture behavior of Alloy 617 for strains as low as 5%. INL, 2021k further states that specific changes to the creep and rupture behavior depend on the amount of cold work and the creep temperature; in general, the time and strain to rupture are reduced. NRC, 2021b notes that cold work lowers the recrystallization temperature of austenitic materials, when compared to materials in the annealed condition, and as a result, degrades creep properties.

INL, 2021k discusses the results of creep-rupture testing performed on Alloy 617 material with various levels of cold work. Some of these tests showed reduced creep-rupture life for material with 10-20% cold work. Other creep tests, interrupted before failure, showed reduced creep rates and creep strain for materials with 5-20% cold work compared to solution annealed material. INL, 2021k did not present any creep-rupture data for Alloy 617 material with cold work percentages of 0-5%. However, INL, 2021k states that limiting the fabrication strain to 5% in components which are not given a post-fabrication solution treatment allows incidental deformation associated with fit up and installation without deleterious effect on properties.

INL, 2021k states cold work alters the creep-rupture behavior of Alloy 617 for strains as low as 5%, and that, although specific changes depend on the amount of cold work and the creep temperature; the time and strain to rupture are both generally reduced. INL, 2021k further states that the mechanism by which these changes occur is not clear. INL, 2021k also states that it

does not appear that bulk recrystallization occurs; local recrystallization in the highly deformed region near the fracture surface of ruptured specimens has been reported even in the absence of prior cold work.

The technical basis document notes that for fabrication strains greater than 5%, a post-fabrication solution heat treatment of 2,102 degrees F (1,150 degrees C) for 20 minutes per 25 mm of thickness or 10 minutes, whichever is greater, is required by Section VIII, Division 1. INL, 2021k notes that this heat treatment will likely recrystallize the material and allow grain growth that is required for creep-rupture resistance. INL, 2021k recommended the same heat treatment for Alloy 617 with post-fabrication strains greater than 5%; however, this requirement was changed in the final code case to “in accordance with the material specification.”

Staff Evaluation

The provisions of N-898 are similar in principle to those of Section III-5, HBB-4212 for the Class A materials allowed by Section III-5. These provisions call for a post-fabrication heat treatment, or written justification for not performing a heat treatment when local strains exceed 5%. For the austenitic materials allowed for Class A components in Section III-5, a figure is provided that gives time-temperature limits for short-time high temperature transients; if these limits are exceeded, post-fabrication heat treatment is required. NRC, 2021b Section 3.6.4 contains the staff's review of the requirements of Section III-5 for forming and bending of the Class A materials allowed by Section III-5. The code case does not provide such a figure or any exemptions for Alloy 617 subjected to fabrication induced strains greater than 5%.

The staff notes that since INL, 2021k presents no rupture data for material cold worked between 0 and 5%. Rupture data at lower amounts of cold work exists for some of the other Division 5 materials; for example, some data exists for Type 304 at 4% cold work that shows creep-rupture life is not degraded by 4% cold work compared to annealed material (Gold et. al., 1975). It is likely that components that are intentionally cold worked for fabrication will have more than 5% cold work, while components with incidental cold work from fit up and installation will have low levels of cold work. For example, Moen et. al, 1976, notes that strains resulting from straightening of pipe after final heat treatment are usually below about 5%, and cold work for tube and pipe bends ranges between 10-20%. Therefore, the staff expects the effects on rupture life of small amounts of cold work (e.g. 2-3% or less) to be minimal.

The staff also notes that the Code Case N-898 heat treatment requirement is more conservative, with respect to the maximum cold work limit without heat treatment, than the heat treatment requirements of the ASME Code, Section I, “Rules for Construction of Power Boilers,” (ASME, 2021a) for Alloy 617, and the ASME Code, Section VIII, “Rules for Construction of Pressure Vessels” (ASME, 2021b). Section I requires post-cold forming heat treatment for strains exceeding 10% for design temperatures exceeding 1,400 degrees F (760 degrees C) and strains exceeding 15% for design temperatures exceeding 1,200 degrees F (650 degrees C) but less than 1,400 degrees F (760 degrees C). Section VIII, Division 1, Table UNF-79 requires heat treatment at 2,100 degrees F (1,150 degrees C) for 20 minutes/1 inch (25 mm) thickness or 10 minutes, whichever is greater, for strains up to 15% in the design temperature

range of 1000-1250 degrees F (540-675 degrees C) and for strains up to 10% for design temperatures exceeding 1,250 degrees F (675 degrees C).

For Alloy 617, the Code Case N-898 post-fabrication heat treatment requirement (in accordance with the base metal specification) is similar to the post-fabrication heat treatment requirement for the austenitic materials allowed by Section III-5. Specifically, for the austenitic materials allowed by Section III-5 for Class A components, the required post-fabrication heat treatment is the heat treatment specified in the base material specification except that Ni-Fe-Cr Alloy 800H shall be heat treated at 2,050 degrees F (1,120 degrees C). In addition, the heat treatment temperatures from the material specifications allowed by Code Case N-898 are generally similar to the Section VIII, Division 1 post-fabrication required heat treatment for Alloy 617.

The staff finds the post-fabrication heat treatment requirement for Alloy 617 to be acceptable because requiring heat treatment for materials with greater than 5% cold work will prevent deleterious effects on creep-rupture life that could result from higher amounts of cold work, and the requirement for heat treatment in accordance with the original material specification will restore the materials to the solution annealed condition. The staff further finds that the limit of 5% cold work is reasonable because it will allow for incidental deformation associated with fit up and installation; however, any component that has been fabricated by bending is likely to exceed 5% cold work and thus require post-fabrication heat treatment. The staff also notes that the heat treatment requirement of HBB-4800 of N-898 is required for all components regardless of the percentage of cold work, if those components will operate in a certain temperature range, and thus should provide redundant protection against reduced creep life for many components. See Section 3.3.2 of this report for details.

3.3.2 HBB-4800 Relaxation Cracking

Summary of Code Case Content

For components that will see service between 932 degrees F (500 degrees C) and 1,436 degrees F (780 degrees C), HBB-4800 requires heat treatment of three hours at 1,796 degrees F (980 degrees C) to eliminate relaxation cracking after post-fabrication heat treatment, if needed according to HBB-4212. HBB-4800 states that this heat treatment is required for material in either a welded or solution annealed condition.

Technical Basis

The technical basis for HBB-4800 is from "Background Document - HBB-4800 Relaxation Cracking" (INL, 2021i). The main basis for the susceptible service temperature range of 500-780 degrees C and the required heat treatment and time of 980 degrees C for three hours appears to the recommendation from "Manufacturer's Data Sheet for VDM^R Alloy 617 (Nicrofer 5520 Co), Material Data Sheet No. 4119". The staff reviewed an updated version of the same manufacturer datasheet, which contained the same recommendation (VDM Metals (VDM), 2021).

Staff Evaluation

Relaxation cracking, also known as stress relaxation cracking (SRC) or reheat cracking, is a mechanism that can lead to premature failure of austenitic stainless steel or nickel alloy components in high temperature service. The term SRC will be used here. Common characteristics of SRC include (Shoemaker et. al, 2007, van Wortel et. al, 2007):

- Failures typically occur after only one to two years of service
- Failures are characterized by brittle, intergranular fracture, often associated with voids

Factors that increase susceptibility to SRC include (Colwell et. al, 2020, Shoemaker et. al, 2007, van Wortel et. al., 2007):

- Cold formed or welded components
- Multiaxial stresses, notches (or high tensile stress constraint which reduced rupture strains)
- Service in a particular temperature range specific to the alloy, typically bounded by 930-1400 degrees F (500-760 degrees C)
- Coarse grain size

No guidance is provided in Section III-5 for mitigation of SRC in components constructed from the five materials permitted for Class A, high temperature components in Subsection HB, Subpart B.

Tung et. al, 2014 and ASME Section II-D, Appendix A-206 provide a description of the mechanism of SRC. In nickel-based alloys such as Alloy 617, the mechanism of SRC is related to precipitates that form over time at the service temperature. Certain precipitates (primarily γ' – $\text{Ni}_3(\text{Al},\text{Ti})$) form preferentially within the grains rather than on the grain boundaries, strengthening the grain interior preferentially. Carbide precipitation along the grain boundaries can also deplete the grain boundaries of certain elements and further weaken the grain boundaries. Any strains that develop (such as due to relaxation of residual stresses) therefore concentrate in the grain boundaries which can lead to rapid creep crack growth and ultimately failure of the component in a nonductile manner.

Typical preventive measures include heat treatments (stabilizing or post-weld), control of alloy composition, control of grain size, controls on welding such as minimizing restraint and joint designs that minimize stress concentrations, and low heat-input welding techniques (Colwell et. al 2020, van Wortel et. al, 2007, Shoemaker et. al, 2007).

The VDM data sheet recommendations are consistent with the information from the Joint Industrial Program in Europe to address SRC, summarized in Hans van Wortel, “Control of Relaxation Cracking in Austenitic High Temperature Components” (van Wortel, et. al, 2007).

Van Wortel et. al, 2007 notes that Alloy 617 is most susceptible to SRC at service temperatures of 1020-1290 degrees F (550 -700 degrees C). Van Wortel et. al., 2007 notes that a stabilizing heat treatment at approximately 1,800 degrees F (980 degrees C), before or after cold deformation, is very effective to avoid relaxation cracking during service, for both Alloy 617 and Alloy 800H. With respect to welded joints, van Wortel et. al., 2007 indicates that post-weld heat treatment (PWHT) is very effective for avoiding relaxation cracking.

Van Wortel et. al, 2007, explains the mechanism by which the stabilizing heat treatment mitigates SRC as follows. The additional stabilizing heat treatment of the base metal after solution annealing generates coarse carbides within the grains and on the grain boundaries. For the formation of these carbides, the elements carbon (C), titanium (Ti), niobium (Nb) etc. will be fixed. The consequence is that at the operating temperature of, for instance, 1,110 degrees F (600 degrees C), less of these elements are available for the formation of fine carbides within the grains. The consequence is a material condition which can withstand relaxation strains >2%.

A similar stabilizing heat treatment is recommended for Alloy 800H in API Technical Report 942-B (API, 2017), which recommends a stabilization heat treatment at 1,800 degrees F (982 degrees C) for 3 hours on Alloy 800H base materials after rolling, forming or other manufacturing steps. API 942-B states this heat treatment is done after the ASTM-required solution annealing. API 942-B further states that a stabilization heat treatment creates benefits by generating coarse particles within the grains and on the grain boundaries. These carbides form by reacting with age-hardening elements such as Ti, aluminum (Al), Nb, etc. The result is that at operating temperature, less of these elements are available for the formation of fine carbides within the grains. Alloy 800H is a primarily solid solution strengthened austenitic alloy as is Alloy 617, but has much higher iron content and lower nickel content, and lacks cobalt. However, in both alloys, formation of fine γ' precipitates within the grains strengthen the grain interior more than the grain boundaries is a contributor to SRC. Thus, the same type of stabilizing heat treatment recommended for Alloy 800H may be effective at preventing SRC in Alloy 617. This heat treatment would also serve to relieve weld residual stresses.

The heat treatment requirement of HBB-4800 is also consistent with the information in the data sheet for Alloy 617 from VDM (VDM, 2021), which indicates that Alloy 617 is susceptible to relaxation cracking if new solution annealed and welded semi-fabricated products are exposed to service temperatures within the range of 1020-1436 degrees F (550-780 degrees C) without a prior post-weld stabilizing heat treatment at 1,800 degrees F (980 degrees C) for three hours. VDM, 2021 further indicates that the subsequent service temperature range within which relaxation cracking may occur extends further to 932 -1,436 degrees F (500- 780 degrees C) if products are reused which have already been in service and which have been repair welded with matching Alloy 617 consumables without a following stabilizing heat treatment at 1,800 degrees F (980 degrees C) for three hours.

The heat treatment required by HBB-4800 of 1,800 degrees F (980 degrees C) for three hours is consistent, with respect to time and temperature, with that recommended by van Wortel et al, 2007, and VDM, 2021, for prevention of SRC in Alloy 617. The service temperature range for which the heat treatment is required by HBB-4800 of 1020-1436 degrees F (550-780 degrees

C) is also conservative with respect to that recommended in van Wortel et al., 2007, and consistent with the more conservative recommendation of VDM, 2021, for repair welded components. The heat treatment required by N-898 is consistent with the stabilizing heat treatment recommended for Alloy 800H in API, 2017. The staff thus expects that heat treatment required by HBB-4800 should help to mitigate the metallurgical contribution to SRC by reducing the potential for formation of fine precipitates within the grains. The heat treatment required by HBB-4800 should also partially relieve weld residual stresses.

The staff finds that requirements of Code Case N-898 with respect to SRC, specifically the heat treatment time and temperature, and operating temperature range for which components must be heat treated, are acceptable based on the cited research and vendor recommendations. However, NRC, 2021b, Section 3.9.6 in the discussion of the special strain requirements at welds in HBB-T-1710, notes that SRC has occurred in high-temperature applications from relaxation of weld residual stresses, even in regions where the weld residual stresses were partially reduced by PWHT. The staff also notes that in addition to heat treatment, weld joint design and welding techniques also influence SRC susceptibility, so specification of PWHT alone may not be sufficient to mitigate SRC. NRC, 2021b therefore recommended a limitation that when using HBB-T-1710, applicants and licensees should develop their own plans to address the potential for SRC in their designs. This limitation was therefore included in the draft regulatory guide, DG-1380. The staff notes that HBB-T-1710 addresses special strain requirements for welds, and is applicable to Alloy 617 components as well as components constructed from the five materials permitted in Subsection HB, Subpart B. Therefore, the staff recommends that the following limitation should apply to Alloy 617 components:

When applying HBB-T-1710 and HBB-4800 to Alloy 617 components, applicants and licensees should develop their own plans to address the potential for SRC in their designs. These plans should address factors such as weld joint design and controls on welding in addition to the required heat treatment of HBB-4800.

The staff interprets HBB-4800 as applicable to any component, regardless of whether it has been cold formed for fabrication, welded, or neither cold formed nor welded.

3.4 Mandatory Appendix HBB-I-14 Tables and Figures

The Mandatory Appendix HBB-I-14 Tables and Figures in Code Case N-898 provide the various materials properties and allowable stresses for Alloy 617, in the same format as the corresponding properties for the existing Section III-5 materials. These properties include the permissible base and weld material specifications, maximum allowable stress intensity for design condition calculations (S_0), allowable stress intensity values (S_{mt}), time-dependent allowable stress intensity values (S_t), yield strength (S_y) versus temperature, rupture strength (S_r), and stress rupture factors for weldments. NUREG-2245, Section 3.7 contains more explanation of these properties and how they are typically determined by ASME, as well as the staff's review of these properties for the five materials allowed by Section III-5 for Class A, high - temperature components.

3.4.1 Table HBB-I-14.1(a) Permissible Base Materials

Summary of Code Case Content

N-898 modifies Section III-5, Table HBB-I-14.1(a) to add the permissible base material specifications for Alloy 617. These are specifications SB-166 (bar and rod), SB-167 (seamless pipe and tube), SB-168 (plate sheet and strip), and SB-564 (Forgings). The Type, Grade or Class for each specification is UNS N06617.

Technical Basis

The technical basis for the permissible base materials in Table HBB-I-14.1(a) is contained in “Background Document - HBB-1-14.1(a) Permissible Base Materials for Structures other than Bolting” (INL, 2021d), which states that all the specifications permitted represent wrought and solution annealed material. A minimum material thickness of 0.125 inches (3.175 mm) is specified by Note (1) to Table HBB-I-14.1(a).

INL, 2021d indicates that the solution treatment required by these specifications produces a large grain size that contributes to the creep resistance Alloy 617. INL, 2021d also indicates that the minimum thickness is specified to prevent sections with too few grains through the cross section, to ensure that material selected for construction is well represented by the bulk properties used in developing allowable stresses for the code case. INL, 2021d further indicates that it is commonly thought that a minimum of approximately ten grains are required in the cross section for grain size effects to become negligible, and that the grain size of wrought Alloy 617 is typically in the range of 100-300 microns (μm) (0.004-0.012 in) after solution annealing. INL, 2021d states that a thickness of 3.175 mm (0.125 in) represents approximately ten grains of the maximum observed diameter.

Staff Evaluation

The staff finds the minimum thickness requirement to be acceptable because a grain diameter of 100-300 μm (0.004-0.012 in) corresponds to a very coarse grain size, which is conservative (most materials should have a finer grain size).

The staff finds that the permissible base material specifications are acceptable because they are ASME material specifications for Alloy 617 in the solution-treated condition, which will ensure a large grain size that is optimal for creep resistance. In addition, the staff finds the minimum material thickness required by N-898 acceptable because it will ensure that bulk materials properties used to develop the allowable stresses represent all the permissible materials well.

3.4.2 Table HBB-I-14.1(b) Permissible Weld Materials

Summary of Code Case Content

N-898 modifies Section III-5 Table HBB-I-14.1(b) to add the permissible weld material for Alloy 617. One filler metal, ERNiCrCoMo-1 (Alloy 617), per specification SFA-5.14, is allowed. Only gas tungsten arc welding (GTWA) is permitted per Note [1] to the table.

Technical Basis

The technical basis for Table HBB-I-14.1(b) is documented in “Background Document – HBB-I-14.1(b) Permissible Weld Materials” (INL, 2021e), which describes the qualification of a weld under ASME, Section IX. The weld was made using an automated gas tungsten arc welding (GTAW) process using ERNiCrCoMo-1 (Alloy 617). INL performed extensive property characterization on specimens machined from the reference material. INL performed tensile and bend tests as part of the weld qualification. The same weld was used for creep testing to support determination of the weld stress reduction factors in Table HBB-I-14.10F-1 of the Code Case.

Staff Evaluation

The staff finds the permissible weld material acceptable because it uses a recognized ASME weld material specification that is compatible with the base material, and the permissible weld process and material is limited to the weld filler specification and process used in property testing supporting N-898.

3.4.3 Table HBB-I-14.2 s_0 — Maximum Allowable Stress Intensity

Summary of Code Case Content

N-898 modifies Section III-5 to add maximum allowable stress intensity values, S_0 , for Alloy 617 to Table HBB-I-14.2 of Section III-5.

Technical Basis

The technical basis for the S_0 values in N-898 is provided in “Background Document – Allowable Stress Values,” (INL, 2021g). INL, 2021g indicates S_0 values correspond to the S values given in ASME Code, Section II, Part D, Table 1B. INL, 2021g states that the SI version of Table 1B only includes values up to 900 degrees C, but additional values are given in Note G29 that were used to interpolate the values proposed for 925 and 950 degrees C.

Staff Evaluation

Section III-5, Paragraph HBB-3221 defines S_0 as the maximum allowable value of general primary membrane stress intensity to be used as a reference for stress calculations under Design Loadings, and states that the allowable values are given in Table HBB-I-14.2. HBB-3221

further states that the values correspond to the S values given in Section II, Part D, Subpart 1, Table 1A, except for a few cases at lower temperatures where values of S_{mt} (defined below and given in Tables HBB-I-14.3A through HBB-I-14.3E) at 300,000 hr exceed the S values. In those limited cases, S_0 is equal to S_{mt} at 300,000 hr rather than S. Since N-898 is limited to 100,000 hours, the S_{mt} values at 300,000 are not relevant; therefore, the S_0 values should be based on the Section II, Part D, Subpart 1, Table 1B (Section II-D Table 1B) values. The staff notes that the S values for Alloy 617 in Section II-D are contained in Table 1B rather than Table 1A since Alloy 617 is considered a nonferrous material.

The staff reviewed the proposed S_0 values and verified they are consistent with the values for annealed N06617 in Section II-D, Subpart 1, Table 1B. In Table 1B there are two sets of values for each Alloy 617 specification, with one set being somewhat higher. The proposed S_0 values are based on the higher set of values.

The footnote to Section II-D, Table 1-100, which provides the criteria for establishing the S values in Tables 1A and 1B, states that:

Two sets of allowable stress values may be provided for austenitic stainless steels in Table 1A; and nickel alloys, copper alloys, and cobalt alloys in Table 1B; having an S_Y/S_T ratio less than 0.625. The lower values are not specifically identified by a footnote. These lower values do not exceed two-thirds of the yield strength at temperature. The higher alternative allowable stresses are identified by a footnote. These higher stresses may exceed two-thirds but do not exceed 90% of the yield strength at temperature. The higher values should be used only where slightly higher deformation is not in itself objectionable. These higher stresses are not recommended for the design of flanges or for other strain-sensitive applications.

The proposed set of values are apparently based on the higher set of values based on the principal that some deformation is acceptable. The technical basis for Code Case N-872 refers to footnote G5 to Section II-D Table 1B, which states:

Due to the relatively low yield strength of these materials, these higher stress values were established at temperatures where the short-time tensile properties govern to permit the use of these alloys where slightly greater deformation is acceptable. The stress values in this range exceed 66-2/3 % but do not exceed 90% of the yield strength at temperature. Use of these stresses may result in dimensional changes due to permanent strain. These stress values are not recommended for the flanges of gasketed joints or other applications where slight amounts of distortion can cause leakage or malfunction. For Section III applications, Table Y-2 lists multiplying factors that, when applied to the yield strength values shown in Table Y-1, will give allowable stress values that will result in lower levels of permanent strain.

The staff finds the S_0 values acceptable since these values are based on Section II-D, Table 1B values for S, which is consistent with the definition of S_0 in Section III-5, HBB-3221.

3.4.4 Figure and Table HBB-I-14.3F S_{mt} – Allowable Stress Intensity Values

Figure HBB-I-14.3F and Table HBB-I-14.3F contain the allowable stress intensity values, S_{mt} , for Alloy 617.

Summary of Technical Basis

Per Section III-5 Paragraph HBB-3221, S_{mt} is the allowable limit of general primary membrane stress intensity to be used as a reference for stress calculations for the actual service life and under the Level A and B Service Loadings; the allowable values are shown in Figures HBB-I-14.3A through HBB-I-14.3E and in Tables HBB-I-14.3A through HBB-I-14.3E for the five materials allowed by Section III-5. The S_{mt} values are the lower of two stress intensity values, S_m (time independent) and S_t (time-dependent). HBB-3221 further states that as described in HBB-2160(d), it may be necessary to adjust the values of S_{mt} to account for the effects of longtime service at elevated temperature.

S_m , the time independent allowable stress, is defined in Section III-5, Paragraph HBB-3221 as the lowest stress intensity value at a given temperature among the time-independent strength quantities that are defined in Section II, Part D as criteria for determining S_m ; in Subsection HB, Subpart B, the S_m values are extended to elevated temperatures by using the same criteria. As described in HBB-2160(d), it may be necessary to adjust the values of S_m to account for the effects of long-time service at elevated temperature.

The technical basis for the S_m values in N-898 is documented in INL, 2021g. In INL, 2021g, the S_m values had to be calculated based on the criteria of Section II-D, Table 2-100 since S_m values for Alloy 617 do not appear in Section II-D, Table 2B (since the alloy is currently not allowed for Section III-1 use). INL, 2021g notes that as specified in Note (1) to Table 2-100, a yield strength multiplication factor of either $\frac{2}{3}$ or 0.9 must be selected for austenitic and nickel alloys when determining the yield strength criteria above room temperature. INL, 2021g further notes that Section II-D, Appendices 1 and 2 specify that the high stress rules apply to austenitic stainless steel, nickel alloys and cobalt alloys whose yield to tensile strength ratio is less than 0.625. INL, 2021g stated that for Alloy 617 this ratio is less than 0.5 in the temperature range where this criterion governs, thus the yield strength multiplication factor of 0.9 applies.

INL, 2021c notes that above 800 degrees F (427 degrees C), S_m is governed by $0.9S_YR_Y$ up to 1,400 degrees F (775 degrees C), and by $\frac{1.1}{3}S_T R_T$ at higher temperatures, where $S_y = S_Y R_Y$ and $S_u = 1.1S_T R_T$.

R_T = ratio of the average temperature dependent trend curve value of tensile strength to the room temperature tensile strength

S_T = specified minimum tensile strength at room temperature, ksi

R_Y = ratio of the average temperature dependent trend curve value of yield strength to the room temperature yield strength

S_y = specified minimum yield strength at room temperature, ksi
 S_y = yield strength at temperature

In the technical basis, the S_y and S_u values from “Background Document – Yield and Ultimate Strength,” (INL, 2021f) were used in the above equations to determine S_m .

Staff Evaluation

The staff performed confirmatory calculations of the S_m values based on the S_y and S_u values tabulated in INL, 2021g, and obtained results closely matching the S_m values in Figure HBB-I-14.3F of the code case and Figure 3 of INL, 2021c.

Since the S_m values in the code case were calculated using the criteria of Section III-5, Paragraph HBB-3221, and the staff found the underlying S_y and S_u values acceptable (see Sections 3.1.4 and 3.1.5), the staff finds these values acceptable.

The S_{mt} values are the lower of the S_m value and S_t value for a given time, temperature and stress combination. The staff’s review of the S_t values is in Section 3.4.5. Since the staff found the underlying S_m and S_t values acceptable, the staff finds the S_{mt} values in the code case acceptable.

3.4.5 Figure and Table HBB-I-14.4 S_t – Allowable Stress Intensity Values

Summary of Code Case Content

N-898 adds Figure HBB-I-14.4F and Table HBB-I-14.4F, which provide the time-dependent allowable stress values, S_t for Alloy 617.

Technical Basis

S_t is the temperature and time-dependent allowable stress value as defined in Section III-5, Paragraph HBB-3221, which is determined based on the lowest of three quantities:

- (a) 100% of the average stress required to obtain a total (elastic, plastic, primary, and secondary creep) strain of 1%;
- (b) 80% of the minimum stress to cause initiation of tertiary creep; and
- (c) 67% of the minimum stress to cause rupture.

The technical basis for the S_t values in N-898 is documented in INL, 2021g, which indicates that the data for all three of the above quantities is obtained from creep tests. The relationship between time, temperature and stress for the three types of data was determined using the Larson-Miller Parameter (LMP), a typical method used for analysis of creep data. The LMP is

expressed as follow, where C is the Larson-Miller constant, T is absolute temperature, and t is time.

$$LMP = T(C + \log t)$$

INL, 2021g further indicates that a relationship between stress and LMP is then determined by expressing stress as a polynomial and performing regression to determine the fit. INL, 2021g uses a linear equation in log stress for the stress for 1% strain, the stress for initiation of tertiary creep, and the stress to cause rupture.

$$LMP = a_0 + a_1 \log(\sigma)$$

For the purposes of the regression analysis, the stress function is rewritten so that $\log t$ is the dependent variable and T and $\log(\sigma)$ are the independent variables:

$$\log_{10}(t) = \left[\frac{a_0 + a_1 \log_{10}(\sigma)}{T} \right] \left[\frac{a_0 + a_1 \log_{10}(\sigma)}{T} \right] - C$$

Using a least-squares fitting method, the optimum values for C , a_0 , and a_1 are determined. A “lot-centering” procedure developed by Sjodahl (Sjodahl, 1978) was employed that calculates the lot constant (C_{lot}) for each heat of material, along with the Larson-Miller constant, C , which is the average of the lot constants. A spreadsheet developed for ASME for the analysis of time-dependent materials properties was used to generate the Larson-Miller plots.

Staff Evaluation

Adequacy of Database

With respect to the adequacy of the creep database for determination of the LMP for 1% strain, tertiary creep, and stress rupture, the staff referred to Section III-5, Nonmandatory Appendix HBB-Y. Although HBB-Y is not part of the staff’s endorsement of Section III-5, it provides useful guidance with respect to the adequacy of the data for determining time-dependent properties. Specifically, the guidance of HBB-Y recommends the creep-rupture data from a minimum of three commercial heats, representing the compositional ranges, sizes, and product forms for the applications. For 1% strain, there were 220 data from 16 different heats. For tertiary creep, there were 183 data from 14 heats. For stress rupture, there were 348 data from 29 heats.

The permissible material specifications allowed by N-898 cover bar, rod, seamless pipe and tube, plate, sheet, strip, and forgings. The creep data cover most of these product forms with the exception of seamless pipe. The background document for Table HBB-I-14.1(a) states “the creep data set that has been used to generate the time dependent allowable stresses in this Code Case includes specimens from plate, sheet, rod, tube and forgings. Significant differences in creep properties have not been observed with varying product form. It is therefore reasonable to use these values for all wrought product forms.” The staff finds this argument to be reasonable.

The staff also reviewed the data to determine if the range of time to rupture, time to 1% strain, and time for onset of tertiary creep is sufficient for extrapolation to the 100,000-hour maximum life allowed by N-898. HBB-Y states that well-behaved, solid solution alloys may require data at 100 degree F or 50 degree C intervals (depending on whether determining the U.S. Customary or SI properties) extending to times that will require an extrapolation in time of no more than a factor of five to reach the intended life. The staff observes that the stress rupture data go to approximately 40,000 hours, with numerous data points in the 20,000-hour range. The 1% strain data and tertiary creep data each have several data points in the 20,000-30,000-hour range. The staff therefore judges the time range of the creep data to be adequate to support extrapolation out to 100,000 hours.

With respect to the temperature range of creep data needed, HBB-Y states that, to support development of the minimum stress-to-rupture values as a function of time and temperature, the temperatures range from the creep threshold to 100 degrees F or 50 degrees C above the maximum use temperature for the material. N-898 provides S_t values for temperatures ranging from 800-1750 degrees F or 425-950 degrees C. The temperature range covered by the three types of data is 1,099-1999 degrees F (593-1093 degrees C). The maximum temperature of the data therefore meets the HBB-Y recommendation of being 100 degrees F (50 degrees C) above the maximum use temperature.

INL, 2021g notes that the data set for creep and tensile testing has been limited to specimens with known chemistry that were tested in air. McCoy et. al, 1985 documented creep testing by ORNL that included specimens tested in helium as well as air and also specimens subject to aging heat treatments, which were excluded from the dataset for N-898. McCoy et. al, 1985, has only two data points for aged material tested in air, so this is not a significant amount of data. Kim et al, 2013 also contains creep testing data in helium that are not included in the database used to determine the allowable stresses for N-898. Shorter rupture times in helium as compared to air were documented in Kim et. al, 2013. Not including the creep data in helium is acceptable because addressing environmental effects is outside the scope of Section III-5, and the ASME practice is to test in air. Environmental effects therefore must be accounted for outside of Section III-5 rules.

Confirmatory Analysis

Using the C , a_0 , and a_1 values given in INL, 2021g for the LMP analysis of time to 1% strain, time to tertiary creep, and time to rupture, the staff calculated the stresses associated with each of these parameters for the range of times and temperatures covered by the code case S_t table (800-1750 degrees F, 425-950 degrees C). The staff then calculated the resulting S_t value for the same temperature range. The staff duplicated the code case S_t values exactly, thus confirming that the S_t values in the code case were calculated correctly from the parameters determined in the LMP analysis.

Using the data for 1% strain, tertiary creep, and stress to cause rupture in Appendixes II, III, and IV of Ref. 1, the staff performed confirmatory analysis of the LMP parameters. The staff did not have access to the spreadsheet used by ASME for analysis of time-dependent materials

properties, that was used to perform the LMP analysis for the N-898 technical basis. Therefore, there may be some differences in the regression procedures used in the staff's confirmatory analysis from the procedures used by ASME. The staff performed the regression analysis of C , a_0 , and a_1 using Microsoft Excel, with the Data Analysis add-on. The regression analysis was performed separately for each heat, and calculated an unweighted average of C , a_0 , and a_1 . Regression could not be performed for a few heats due to having insufficient data points (less than three data points), or heats having data at only one temperature. Also, in some cases some heats yielded atypical regression results, such as C values with a high negative value positive value, or a small absolute value (typical C values are in the -15 to -20 range). The heats with insufficient data points and the heats yielding atypical regression results were combined into a "pooled" heat and this was treated as a single heat. The C , a_0 , and a_1 values are therefore based on the unweighted average of all the good heats and the pooled heat.

Using the independently generated C , a_0 , and a_1 values, the staff solved for the stress values associated with the three criteria for S_t , and then determined the resulting S_t values. The staff's values were generally higher than the code case values by a maximum of 12.3% at longer times and higher temperatures. In the intermediate times and temperatures, some of the staff's S_t values were lower than the code case values but were within 10% of the code case values. For the 1st-order regression, the staff's analysis found that the S_t values were controlled either by 80% of the stress for tertiary creep or the stress for 1% strain, with no values being controlled by S_r , with tertiary creep controlling the S_t values at longer times and higher temperatures, consistent with the INL, 2021g results for the code case technical basis.

The staff also performed analysis of the LMP parameters for 1% strain, tertiary creep, and stress to cause rupture using a second-order polynomial fit rather than the first-order polynomial fit used in INL, 2021g. For the S_t values based on second-order regression, the values at longer times and higher temperatures are controlled by 80% of the stress for tertiary creep. At intermediate temperatures and times, $0.67S_r$ controls S_t , while at lower temperatures and shorter times, stress for 1% strain is controlling.

The staff's 2nd-order fit resulted in slightly lower S_t values than the code case values, with the differences becoming larger at longer times and higher temperatures. The maximum discrepancy from the code case values was 13.3% less at 1,382 degrees F (750 degrees C) and 3 hours. At 1,742 degrees C (950 degrees C) and 100,000 hours, the staff value was 10.7% less than the code case value. Most differences were less than 10%.

The staff does not find the differences in S_t values resulting from a second-order fit to be significant considering the conservatism in the Section III-5 design rules, and likely differences in regression procedures used in the staff's confirmatory analysis versus those used in the technical basis for N-898. A detailed discussion of the conservatism in the Section III-5 design rules can be found in Section 3.7.6 of NRC, 2021b.

Overall, the staff finds that the confirmatory analysis yielded sufficiently similar results in terms of the resulting S_t values to support the conclusion that the N-898 S_t values are conservative

and acceptable, especially considering likely differences in regression procedures used in the staff's analysis.

Note on Tertiary Creep Criterion

The staff notes that the tertiary creep criterion controls the S_t values at longer times and higher temperatures, as shown in Table 4 of INL, 2021g. The staff's confirmatory analysis also found the tertiary creep criterion to control S_t at longer times and higher temperature. INL, 2021g indicates that the tertiary creep criterion was adopted by ASME to address concerns related to leakage of internally pressurized tubes that leaked at times less than those predicted using analysis based on uniaxial rupture data. INL, 2021g further indicates that this criterion was developed based on the logic that the onset of tertiary creep during uniaxial testing of austenitic stainless steels is associated with extensive creep induced cavitation; thus, eliminating tertiary creep, and the associated cavitation, was presumed to represent a conservative indirect limit to minimize the potential for premature failure of tubes under multiaxial loading. However, INL, 2021g states that for many temperatures and stresses, Alloy 617 exhibits extensive tertiary creep prior to rupture, without evidence of measurable cavitation. INL, 2021g further states that this has raised questions regarding the validity of the tertiary creep criterion for the S_t value for Alloy 617 and other alloys that exhibit similar creep behavior, and that S_t would be increased over a wide range of times and temperatures if the tertiary creep criterion were eliminated. Based on the fact that the proposed S_t values are controlled by tertiary creep, yet Alloy 617 does not exhibit creep cavitation, the staff concludes the S_t values are conservative.

Independent Data

The staff performed a literature search to determine if there was additional creep data available that could be used to perform an independent analysis of the LMP parameters for S_r , stress for 1% strain, and stress for the initiation of tertiary creep. The staff found very few creep data for Alloy 617 that was not used in the technical basis for N-898. The only independent data found were the data for aged material and material tested in helium documented in McCoy et. al., 1985, and the data in air and helium from Kim et. al, 2013. The data for aged material from McCoy et al, 1985, were excluded from the technical basis for N-898. The data in air from Kim et. al, 2013, are only for one temperature, and there are only seven data points, while there are only two data for aged materials tested in air from McCoy et. al., 1985. Therefore, the number of available independent data in air was insufficient to perform a meaningful independent analysis.

Summary – S_t Values

Overall, the staff finds that the S_t values are based on a sufficient database in terms of number of data, number of heats/lots, diversity of product forms, temperature range covered, and times covered by the database (for either rupture, 1% strain, or onset of tertiary creep). The database is consistent with the recommendations of Nonmandatory Appendix HBB-Y. The determination of the relationship of time, temperature and stress was done using well-accepted techniques, specifically the LMP. The staff's confirmatory analysis also determined similar S_t values to the code case values. The fact that the N-898 S_t values are controlled by the tertiary creep criterion,

which may be overly conservative when actual material creep behavior is considered, is also conservative. Therefore, the staff finds the proposed S_t values to be acceptable.

3.4.6 Table HBB-I-14.5 Yield Strength Values, S_y

Summary of Code Case Content

N-898, Table HBB-I-14.5 adds yield strength (S_y) values for temperatures from 1050-1750 degrees F and 525-950 degrees C. Below these temperatures ($\leq 1,050$ degrees F or 538 degrees C), the table refers to Section II, Part D, Subpart 1, Table Y-1 for the S_y values.

Technical Basis

The technical basis for the yield and ultimate strength values in N-898 is documented in "Background Document for Yield and Ultimate Strength," (INL, 2021f), which states that the NDMA spreadsheet was used to determine S_y for temperatures greater than 1,000 degrees F (525 degrees C), and that fifth-order polynomial was fit to the yield strength ratio (R_Y). INL, 2021f notes that the fitted trend line for R_Y reaches a minimum at 450 degrees C and increases slightly above this, corresponding to an S_y of 23.9 ksi (164.8 MPa); however, S_y was held constant with temperature until R_Y decreases at higher temperatures. The value of 23.9 ksi is also slightly higher than the current Section II, Part D value of 23.3 ksi (161 MPa) at 1,000 degrees F and 525 degrees C, so the current code values were used in the Code Case at 1,000 degrees F and 525 degrees C and held constant until 1,500 degrees F or 800 degrees C. Above that temperature, new values based on the analysis of INL, 2021f are proposed.

General Note (b) to Section II-D Table Y-1 states in part:

The tabulated values of yield strength are those which the Committee believes are suitable for use in design calculations. At temperatures above room temperature, the yield strength values correspond to the yield strength trend curve adjusted to the minimum specified room temperature yield strength. The yield strength values do not correspond exactly to "minimum" or "average" as these terms are applied to a statistical treatment of a homogeneous set of data.

Staff Evaluation

Figure 7 of INL, 2021f shows the proposed S_y values for temperatures above 1,000 degrees F (525 degrees C) along with the Section II-D, Table Y-1 values for lower temperatures. The figure shows a smooth transition from the Section II-D, Table Y-1 values to the code case values for higher temperatures. The figure also shows the S_y at room temperature corresponds to the specified minimum yield strength, indicating the values are in keeping with General Note (b) above.

The same considerations with respect to the adequacy of the database for tensile data discussed in Section 3.1.6 apply to the determination of the yield strength values.

Based on the sufficient database of tensile data, plus the reasonable fit of the yield strength ratio R_Y to the data, the staff finds the proposed S_y values to be acceptable.

3.4.7 Figure and Table HBB-I-14.6G S_r - Minimum Stress-to-Rupture

Summary of Code Case Content

N-898 adds Figure HBB-I-14.6G and Table HBB-I-14.6G containing minimum S_r values as a function of time and temperature from 800-1750 degrees F and 425-950 degrees C, and times out to 100,000 hours.

Technical Basis

The technical basis for the S_r values in N-898 is documented in INL, 2021g, which indicates that sometimes the S_r values predicted from the LMP correlation can exceed the ultimate strength of the material. INL, 2021g indicates that in such cases, S_r was limited to $S_u/1.1$, with division by 1.1 to represent a minimum tensile stress (although not in a statistical sense), since the S_r values are minimum values.

Staff Evaluation

The staff finds that the S_r values are based on a sufficient database in terms of number of data, number of heats/lots, diversity of product forms, temperature range covered, and times covered by the database. The database is consistent with the recommendations of Nonmandatory Appendix HBB-Y. The determination of the relationship of time, temperature and stress was done using well-accepted techniques, specifically LMP analysis.

With respecting to limiting S_r to $S_u/1.1$, according to General Note (a) for Section III-5, Table HBB-3225-1, "Tensile Strength Values, S_u " neither the tensile strength nor the yield strength values correspond exactly to either average or minimum as these terms are applied to a statistical treatment of a homogeneous set of data. Therefore, the staff finds that dividing the S_u values by 1.1 a reasonable approximation of a minimum value of S_u . The staff therefore finds the upper limit applied on S_r based on $S_u/1.1$ to be acceptable since it provides a consistent minimum value of S_r and since it is philosophically consistent with S_r values being minimum values.

The staff also performed independent analysis of the LMP parameters for S_r , as detailed in Section 3.4.5 of this report, and calculated the resulting S_r values. (Note that these values were not multiplied by 0.67 as they are for the determination of S_t). The staff's calculated S_r values were either the same within a few percent of the code case values, with the maximum difference at 100,000 hours and 1,742 degrees F (950 degrees C) where the staff's value is 6% higher than the code case value. The staff therefore concludes the code case S_r values are conservative.

Based on the staff's review of the database and methods used to determine the S_r values, plus the results of the staff's confirmatory analysis, the staff finds the code case S_r values are acceptable.

3.4.8 Table HBB-I-14.10F Stress Rupture Factors for Welded Alloy 617

Summary of Code Case Content

Table HBB-I -14.10F provide stress rupture factors (SRF) for Alloy 617 welded with ERNiCrCMo-1 as a function of temperature from 800-1,750 degrees F and 425-950 degrees C. The SRFs have a value of 1.0 up to 1,550 degrees F and 825 degrees C, and 0.85 above these temperatures.

Technical Basis

The SRF is defined as the ratio of the weld metal creep-rupture strength to the base metal creep-rupture strength. This value is designated "R" in Section III-5 Paragraphs HBB-3221, and HBB-3225, and is also used in Section III-5, Paragraph HBB-T-1715. The factor is used in conjunction with the S_r values given in Figure HBB-I-14.6G and Table HBB-I-14.6G.

In Section III-5, Paragraph HBB-3221, the S_t values for weldments are defined as the lower of the tabulated S_t values from Tables HBB-I-14.4A through HBB-I-14.4E, or

$$0.8 \times S_r \times R$$

Only GTAW is permitted using weld wire Class ERNiCr CoMo-1, Spec. No. SFA-5.14, according to HBB-I-14.1(b) of N-898.

The technical basis for the SRFs for Alloy 617 is described in "Background Document – HBB-I-14.10 Stress Rupture Factors for Welded Alloy 617," (INL, 2021h). INL, 2021h described the results of creep-rupture testing of weld specimens. Specimens from a welded reference plate were tested by Argonne National Laboratory (ANL) and Idaho National Laboratory (INL), and additional weldment creep-rupture data was obtained from three other sources. The SRFs were based only on data from transverse specimens (weld direction perpendicular to the specimen axis) with welds made with the GTAW process. The base metal creep-rupture strength (S_r) for a given time, temperature, and stress combination was determined using the same LMP approach and parameters as the tabulated S_r values in the code case (see Section 3.4.7 of this report). The database for weldment creep-rupture tests covers temperature from 1,202 degrees F-1,742 degrees F (650 degrees C to 950 degrees C). The staff finds the database acceptable because it is limited to the weld process and filler allowed by the Code Case and covers an appropriate temperature range (the higher part of the allowable temperature range for Alloy 617 where reduction of weld creep strength is more likely).

INL, 2021h describes the analysis method for the SRFs as follows. The SRF is defined as $Stress_{weld}/Stress_{base}$, where $Stress_{weld}$ is the applied stress which causes creep-rupture in time t , and $Stress_{base}$ is the rupture stress of the base metal for the same time and temperature. INL, 2021h states that, ideally, the heat of the base metal is the same as that used to fabricate the weldment. In practice, the data base does not include base metal creep specimens with rupture times that match those of the weld specimens, and often does not include specimens of the same heat. Instead, an average base metal rupture stress is calculated for the time to rupture of the weldment using an LMP relation for a large, multi-heat compilation of Alloy 617 creep-rupture data. (The same LMP database and parameters used to determine the S_r values in Table HBB-I-14.6F of the Code Case was used for the average base metal rupture stress.) The result is one data point for the SRF of each weldment creep-rupture test.

Based on all the weld creep-rupture data for transverse specimens from GTAW welds, the technical basis determined SRFs of 1.0 for GTAW weldments for temperatures < 1,562 degrees F (850 degrees C). and a SRF of 0.85 at temperatures \geq 1,562 degrees F (850 degrees C). INL, 2021h indicates these factors are considered a conservative representation of the data. Figure 8 of the Background Document for the SRFs in INL, 2021h shows the individual calculated SRFs as a function of temperature, with the recommended 1.0 and 0.85 lines shown on the graph. A few data points (4 of 19) fall below the 1.0 line at temperatures \leq 1,562 degrees F (850 degrees C), with the remaining 15 points located above the line. For temperatures > 1,562 degrees F (850 degrees C) up the maximum use temperature of 1,742 degrees F (950 degrees C), only two of twenty points fall below the 0.85 line.

INL, 2021h noted that the INL reference heat used as the base metal of the INL and ANL weldment specimens tends to have creep-rupture strengths at the low end of the overall database used to determine the average base metal rupture stress. INL, 2021h states that if the SRF for the INL and ANL data points are calculated by using an LMP relation based on only creep data for the INL reference heat, the SRF values increase. INL, 2021h stated that it is not possible to apply this method to the creep data from other sources since the welded specimens have base metal from a heat that is not represented in the overall creep-rupture data base, or the heats for other sources are not specified. However, the staff notes that this suggests that the SRFs calculated using the base metal strength of the overall database are conservative since the overall database has a higher base metal creep-rupture strength.

INL, 2021h also included a plot of the SRFs as a function of rupture time for the entire database, which showed no downward trend in the SRFs with respect to time.

INL, 2021h also provided a graph of SRFs versus temperature from some additional data from EPRI, for Alloy CCA617 (also known as Alloy 617B), which were prepared in support of developing SRFs for Alloy 617 for ASME Section I use. The EPRI data include both GTAW weld and other processes. The EPRI work also proposed an SRF of 1.0 for GTAW welds in Alloy 617 for temperatures \leq 1,562 degrees F (850 degrees C). The staff reviewed the EPRI data which showed the majority of the SRFs for GTAW welds are above 1.0; however, there are two SRFs

for GTAW welds that fall slightly below 1.0 at 1,472 degrees F (800 degrees C) (between 0.85 and 0.95). Alloy CCA617 is supposed to have better high-temperature creep behavior than Alloy 617.

Staff Evaluation

The staff reviewed the determination of the SRFs, and notes that although a few SRFs for individual tests fell below the SRFs recommended in the Code Case technical basis, the additional factor of 0.8 by which the base metal S_r values are multiplied in Section III-5, Paragraph HBB-3221 provides an additional margin of conservatism. Figure 3-1 is a graph of the actual versus measured weld rupture stress from the test data used to develop the code case SRFs. The expected values are determined based on the expected base metal rupture stress, determined using the base metal LMP correlation for S_r multiplied by the applicable SRF (either 1 or 0.85). Measured weld rupture values falling above the black (one-to-one) line indicate actual values higher than expected rupture values, while those falling below indicate actual rupture values less than the expected rupture values. The green line represents the expected value multiplied by 0.8. It can be seen that the green line is below, and thus bounds all of the measured data. Figure 3-2 shows the weld rupture data for tests conducted at temperatures less than 1,562 degrees F (850 degrees C), and Figure 3-3 shows the weld rupture data for tests conducted at temperatures greater than or equal to 1,562 degrees F (850 degrees C). Figure 3-2 and 3-3 also show all the data being bounded by 0.8 times the expected rupture value. Therefore, the additional factor of 0.8 in HBB-3221 results in 100% of the test data being bounded, indicating that the proposed SRFs are sufficiently conservative for design purposes.

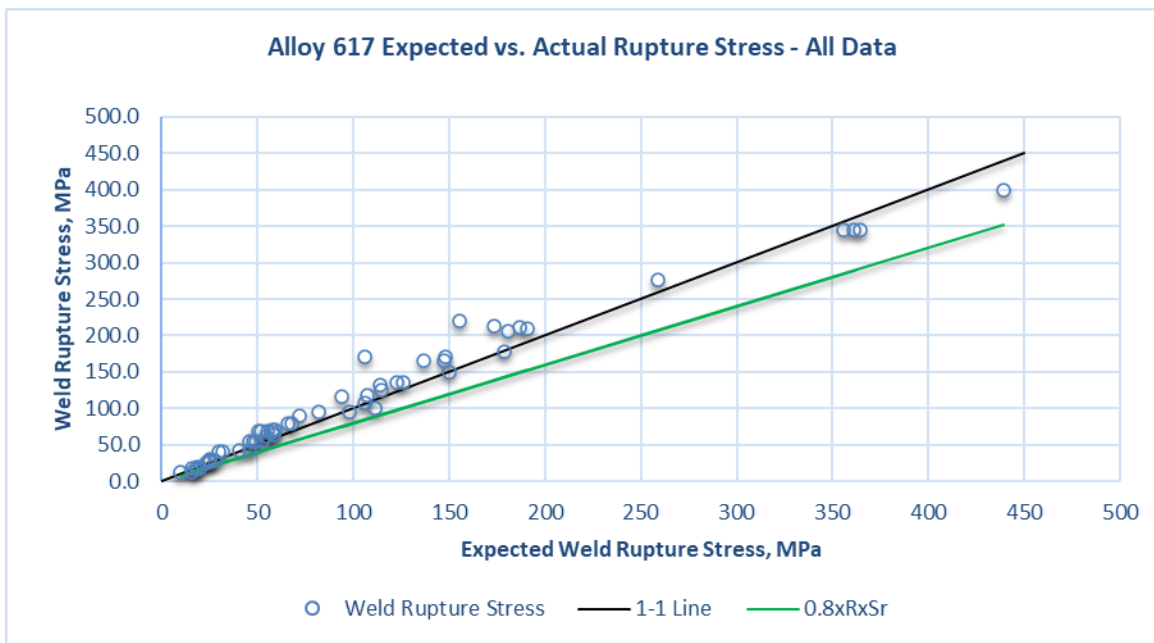


Figure 3-1 Actual vs. expected rupture stress for weld tests reported in INL, 2021h, all test temperatures

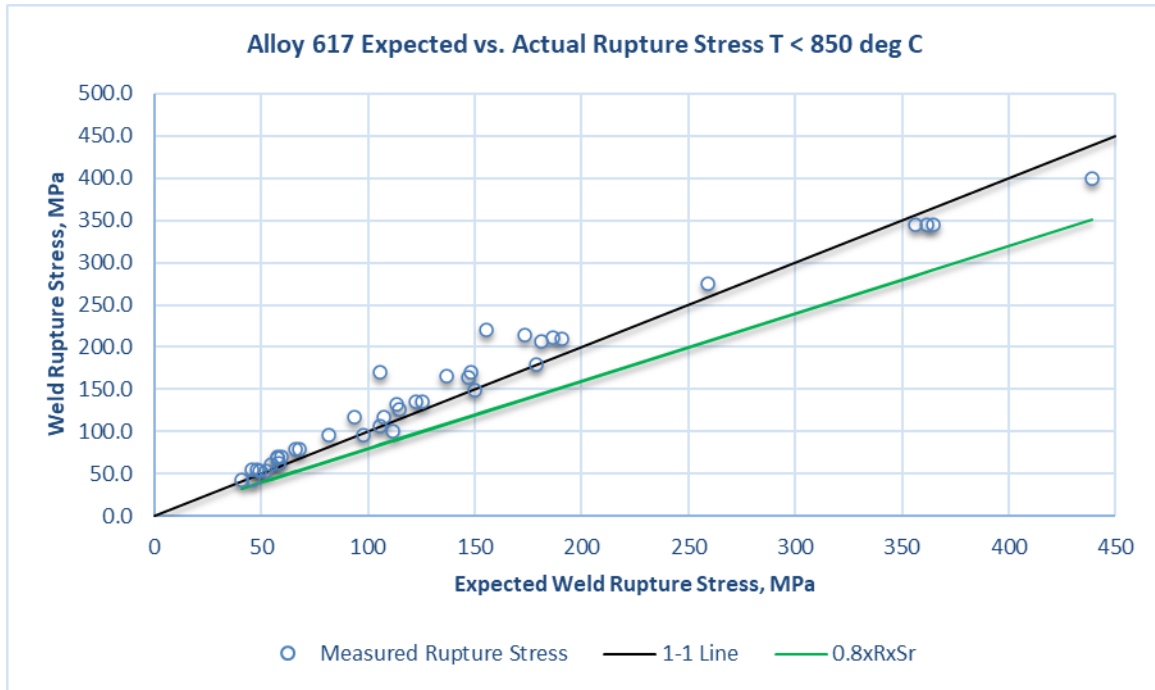


Figure 3-2 Actual vs. expected rupture stress for welds tests reported in INL, 2021h, for temperatures < 1,562 degrees F (850 degrees C)

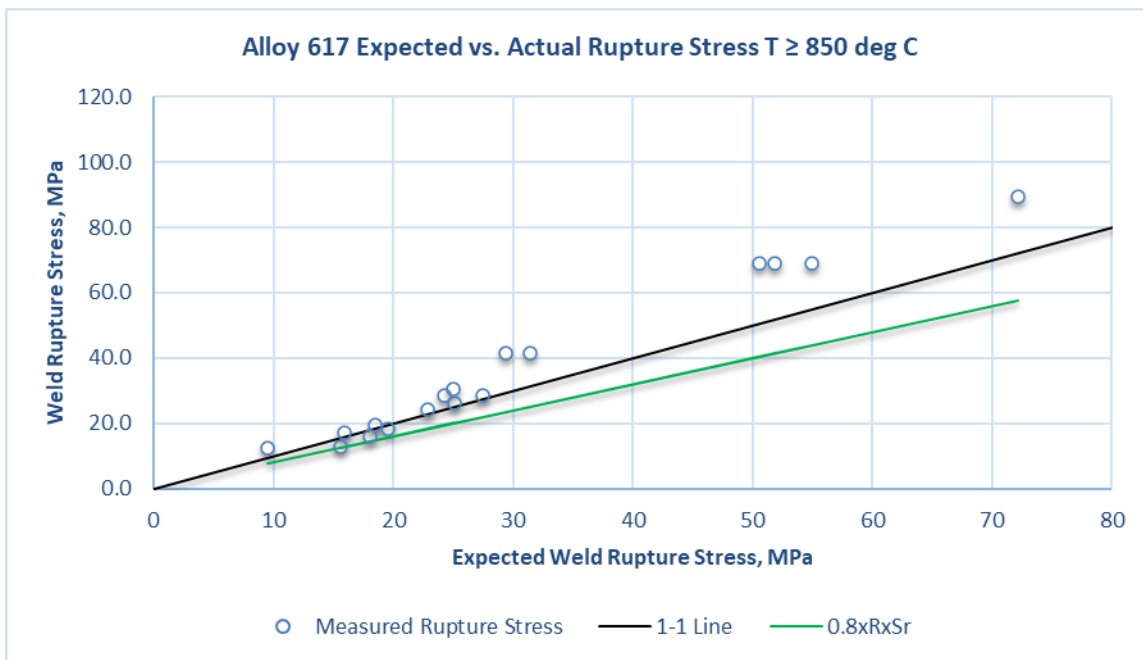


Figure 3-3 Actual vs. expected rupture stress for welds tests reported in INL, 2021h, for temperatures ≥ 1,562 degrees F (850 degrees C)

For the creep-fatigue evaluation of welds in Section III-5, Paragraph HBB-T-1715, the allowable time T_d is multiplied by the SRF (without the additional factor 0.8). However, there are additional conservatisms in the creep-fatigue evaluation of welds including dividing the stress used to determine T_d by the factor K' (which increases the stress since K' is less than one), and a factor of 0.5 applied to the allowable number of fatigue cycles N_d . Therefore, the staff judges that the proposed SRFs are also sufficiently conservative with respect to the creep-fatigue evaluation rules for welds in Section III-5.

Based on the fact that the proposed SRFs bound the majority of the SRFs determined from creep-rupture tests of welds, the appropriate database tested, and considering the additional conservatisms applied to design of welds in Section III-5 HBB, the staff finds the proposed SRFs to be acceptable.

3.5 Physical Properties

3.5.1 Coefficient of Thermal Expansion

Summary of Code Case Content

Nonmandatory Appendix A, Physical Properties Tables – Thermal Expansion, provides CTE values from 70-1,750 degrees F and 20-950 degrees C.

Technical Basis

The technical basis for the CTE values is provided in “Background Documents – Physical Property Tables for Alloy 617,” (INL, 2021i), and is identical to the technical basis for the CTE values provided in N-872, documented in INL, 2021b.

Staff Evaluation

The staff found the Code Case N-872 CTE values acceptable, which are identical to those in N-898, as documented in Section 2.6 of this report. Therefore, the staff finds the CTE values provided in N-898 to be acceptable.

3.5.2 Thermal Conductivity and Thermal Diffusivity

Summary of Code Case Content

Values of TC and TD are provided in Nonmandatory Appendix B, Thermal Conductivity and Thermal Diffusivity, Tables TCD and TCD-M for temperatures from 70-1,750 degrees F and 20-950 degrees C.

Technical Basis

The technical basis for the TC and TD described in INL, 2021i is essentially identical to the technical basis for the TC and TD values of N-872, documented in INL, 2021b. The TC and TD values in N-898 are identical to the TC and TD values tabulated in INL, 2021b.

Staff Evaluation

Since the technical basis is essentially identical and the TC and TD values in Appendix B of N-898 are identical to those in Code Case N-872, which were found acceptable by the staff as documented in Section 2.7 of this report, the staff finds the TC and TD values in N-898 to be acceptable.

3.5.3 Nonmandatory Appendix C, Modulus of Elasticity

Summary of Code Case Content

Nonmandatory Appendix C, Modulus of Elasticity, provides values of the modulus of elasticity (E) from 70-1800 degrees F and 25-950 degrees C. For the materials permitted in Section III-5, E values are found in Section II-D. Code Case N-898 provides E values for Alloy 617 since Section II-D does not provide values for Alloy 617 for the full temperature range of the code case.

Technical Basis

The technical basis for the E values in N-898 is described in “Background Documents – Modulus of Elasticity Tables for Alloy 617,” (INL, 2021m), which indicates that the basis for increasing the temperature range of the E values is twofold: extrapolation of the E values currently in the ASME Code, and confirmation from experimental measurement. INL, 2021m states that the E values currently in Tables TM-4 and TM-4M were extrapolated to 1,800 degrees F and 950 degrees C using a third-order polynomial fit. INL, 2021m, summarizes results of experimental measurements of E , which were performed using the resonant frequency in the flexural mode of vibration in 9 degrees F (5 degrees C) increments up to 1,832 degrees F (1,000 degrees C), in accordance with ASTM E1875 (ASTM, 2021). INL, 2021m shows a graph that includes the E values predicted at 1,652 degrees F (900 degrees C) and 1,742 degrees F (950 degrees C) using the third-order polynomial fit equations, the current ASME Code values, and the experimental data. The plot shows the experimental results and extrapolated results are in close agreement.

Staff Evaluation

Since the *E* values in N-898 are either identical to the values for Alloy 617 in Section II-D or were extrapolated from the Section II-D values with confirmation from experimental data, the staff finds these values to be acceptable.

3.6 ALARA Considerations (Cobalt)

Alloy 617 contains a nominal cobalt (Co) content of 13 weight %. In nuclear reactors, Co-containing alloys have the potential to release corrosion products which can become activated in nuclear reactors, resulting in high out-of-core radiation dose rates to personnel. Institut De Radioprotection et de Surete Nucleaire (IRSN), 2010, indicates that radiocobalts (the radioactive isotopes of cobalt) are found in nuclear power reactors. IRSN, 2010 indicates that radiocobalts currently account for 39% of total gamma activity discharged as liquid effluent, with a total of 2.7×10^9 Bq of ^{58}Co and 3.5×10^9 Bq of ^{60}Co from all Electricite de France plants in 2007. IRSN, 2010 states that specifically, ^{59}Co is the only stable isotope of Co, and when activated to ^{60}Co , it can result in high gamma dose rates. For this reason, Alloy 617 may be inappropriate for use in components such as reactor internals and reactor vessels. Corrosion products from components made from Alloy 617 can also release corrosion products that can be transported to the reactor, where these products become activated.

There has been a general effort to reduce Co in light water reactors (LWRs) since the 1990's. Co content is generally restricted to low levels in austenitic stainless steels intended for components in LWR primary systems. Cobalt-based alloys were originally used for wear resistant hard facing in valves. The industry has also sought to develop alloys to replace high-Co alloys in these applications. EPRI has published several guidelines on Co reduction, such as the Cobalt Reduction Sourcebook (EPRI, 2010).

Due to the potential for activation of Co, which could lead to high out-of-core radiation dose rates to personnel, designers considering use of Alloy 617 in ANLWR components should carefully consider the applications in which this alloy is used, interactions with coolants that may create transportable corrosion products, and the potential for high radiation dose rates to personnel. The staff notes that aspects of structural materials related to radiation dose are outside the scope of the ASME Code.

3.7 HBB-T-1300 Deformation and Strain Limits for Structural Integrity

The load-controlled stress limits of HBB that are discussed in Section 2.2 are mandatory, while the deformation-controlled limits in Appendix HBB-T, which is the subject of the remaining sections of this report, are not mandatory. HBB-T-1300 rules¹ provide strain limits for high-

¹ In this report, the NRC staff uses the nomenclature of the ASME Code. In general, the ASME Code is written in mandatory terms. In particular, ASME Code "rules" or "requirements" do not impose regulatory requirements unless incorporated into 10 CFR 50.55a or otherwise imposed through an NRC regulation, order, or license.

temperature design. The rules of HBB-T-1300 permit elastic analysis methods to be used which are very conservative. In addition, inelastic analyses are permitted using advanced numerical modeling methods. For the strain limits, the rules are meant to limit excessive deformations during service and to limit crack initiation. Since there is usually considerable life remaining during the crack growth phase, these rules are considered to produce designs that are quite conservative. Moreover, an extensive experience database over the years clearly shows the reliability and conservatism of the rules in HBB-T. In addition, years of experience with high-temperature service have been used to modify the rules as appropriate. This section provides discussion of the strain limit rules in Code Case N-898 for use of Alloy 617.

3.7.1 HBB-T-1320 Satisfaction of Strain Limits Using Elastic Analysis

Summary of Code Case Content

Satisfaction of strain limits for Alloy 617 is summarized in this subsection when using elastic analysis rules. The strain limit tests, which can be performed to ensure satisfaction of the limits, are not appropriate for Alloy 617 at temperatures higher than 1,200 degrees F¹ (650 degrees C) because the distinction between plastic and creep strains cannot be made and the simplified elastic design rules rely on being able to separate the strains. The strain limits are considered to have been satisfied if the limits of the three tests (A-1 to A-3) are satisfied as discussed in Section 3.7.2.

Technical Basis

The Alloy 617 code case rules for strain limits were evaluated using numerous references summarized below. These rules were evaluated in Turk (Turk, 2020a, Turk, 2020b) for the other five Section III-5 materials and a similar evaluation approach is used for Alloy 617. The strain limits in N-898, HBB-T-1300 were developed in INL, 2021o except for those of test A-3 discussed below, which were developed under INL, 2021q. Alloy 617 is a solid solution strengthened alloy which exhibits a response where separation of plastic and creep strains is not possible at higher temperatures, and it is difficult to define yield strength. The ability to clearly define yield strength is a requirement for development of the both the elastic and simplified inelastic rules in Section III-5. Corum and Blass (Corum et al, 1991) identified this

Unless otherwise noted, this document refers to “rules” or “requirements” in the sense used in the ASME Code. The same is true of ASME Code provisions that use mandatory language, e.g., where a Code provision states that an action “shall” be taken. While this NUREG often uses ASME Code nomenclature to describe the provisions of ASME Code, Section III, Division 5, such description does not mean that Division 5 or any portion of it is legally binding. Legally binding NRC requirements in NRC regulations will be identified as such in this NUREG.

¹ Note that Code Case N-898 uses 1200 degrees F and 650 degrees C as the upper limit for elastic analysis in HBB-T-1321 and elsewhere; however, the exact conversion of 650 degrees C to degrees F is 1200 degrees F. This report will use 1200 degrees F for consistency with Code Case N-898 when discussing this limit.

temperature at about 1,200 degrees F (650 degrees C) and other more recent work by Wright (Wright et. al., 2013a, Wright et. al., 2013b, Wright et. al., 2018), Messner, Phan, and Sham (Messner et. al., 2018, Messner et. al., 2019), and Messner and Sham (Messner et. al., 2021), identified this temperature to be about 1,382 degrees F (750 degrees C) using advanced analytical methods to characterize the data. For elastic analysis the tests described in HBB-T-1322 (Test A-1), HBB-T-1323 (Test A-2), and HBB-T-1324 (Test A-3) can be used to ensure that the strain limits are satisfied. For simplified inelastic analysis, the tests described in HBB-T-1332 (Tests B-1, B-2, and B-3) can be used to satisfy strain limits.

Staff Evaluation

The following summarize the conservative nature of the strain limit rules for Alloy 617. The elastic design procedures are based on accepted legacy high-temperature design procedures developed before widespread use of computational methods.

- For Alloy 617 many of the tests to ensure allowable strain limits are achieved are not permitted above 1,200 degrees F (650 degrees C), which is a very conservative temperature limit. This limit was originally developed by Corum and Blass (Corum et. al., 1991) in the first attempt to develop a code case for Alloy 617 from early data. This limit is essentially the temperature where the distinction between time independent and time-dependent strains cannot be made for Alloy 617. Recent data analysis of Alloy 617 (Messner et. al., 2021) suggests this limit could be 1,382 degrees F (750 degrees C) (or even 1,472 degrees F (800 degrees C)) showing 1,200 degrees F (650 degrees C) is quite conservative.
- The assessments using elastic analysis methods are complex to use and overly conservative because they are based on legacy elastic analysis methods. This often presents designers with challenges to meet the rules. Legacy approaches in BPV-III-5 are difficult to develop and apply for newer materials.
- The reviewers could not find any direct validation of these rules for temperatures lower than 1,200 degrees F (650 degrees C). However, below the conservative 650 degrees Celsius temperature limit a clear distinction between plastic and creep strains occur with Alloy 617. Therefore, the tests should limit the strains to the Bree regime and produce conservative strain predictions based on the arguments of O'Donnell and Porowski (1974, 1979). For these reasons, the reviewers of this document consider the elastic tests (A-1 to A-3) to be acceptable for Alloy 617 at temperatures below 1,200 degrees F (650 degrees C).

The justification for both of these sets of tests is rigorously developed by O'Donnell and Porowski (O'Donnell et. al., 1974) and Porowski and O'Donnell (Porowski et. al., 1979) with enhancements by Sartory (Sartory, 1989) and is summarized in detail in Turk et. al., 2020a in the review of Division 5 rules for other materials. This justification is equally valid for Alloy 617 in the temperature ranges permitted by this code case for temperatures below 1,200 degrees F (650 degrees C) because Alloy 617 is a solid solution strengthened alloy which does not

cyclically soften, which is one of the inherent assumptions of the tests. Therefore, while the rules do not appear to have been specifically tested for Alloy 617 below 1,200 degrees F (650 degrees C) these rules are recommended for endorsement because the strains should be limited to the Bree regime as they are for the other materials. The staff believe this is technically acceptable and conservative.

3.7.2 HBB-1322, HBB-T-1323, HBB-T-1324 Tests A-1, A-2 and A-3

Summary of Code Case Content

Three simple tests, called A-1, A-2, and A-3 are provided for elastic analysis, which if passed, satisfy the strain limit rules. Test A-1 does not change from Section III-5 rules for other materials while A-2 and A-3 provide data specific to Alloy 617 in the Code Case.

Technical Basis

The test cases were developed based on work by Bree (Bree, 1967, Bree, 1968). Bree analyzed pressurized cylinders subjected to pressure loading and a cyclic thermal gradient through the cylinder wall. This work led to the original Bree diagram that identified six regions of thermal and pressure stress combinations. Three of these regimes resulted in ratcheting even without the presence of creep straining. Two of the regions resulted in shakedown to elastic action in the absence of creep. Finally, an elastic “safe” regime was identified where no ratcheting occurs under plastic and creep conditions. The loading conditions for the analysis based on the Bree diagram were extended to account for realistic load conditions: general primary and general secondary stress. Hence, the intent of the rules is to consider the maximum value of primary and secondary loads in the ratcheting assessment, which is quite conservative. Jetter summarizes the conservative nature of these tests with extensive discussion (Jetter, 1976), pages 224–225, and the reviewers agree that these tests are indeed conservative. The yield stress used in normalizing the load stress intensities for comparison to the Bree elastic regime is the average value of the maximum and minimum wall average temperatures during the cycle under consideration. Choice of the higher temperature for yield stress would be too conservative, but the average is considered an appropriate choice (Rao, 2017). This discussion applies to Alloy 617 as well.

Tests A-1 and A-2 to satisfy strain limits can be applied regardless of the material and apply equally well for Alloy 617 although the material properties used for the test depend on the material being assessed because the tests limit the strain to the conservative Bree regime which was summarized in Turk, 2020a. The Bree diagram identifies the regions of strain where the tests will lead to limited strains and are independent of material as long as an elastic yield can be identified which for Alloy 617 is conservatively defined as below 650 degrees C. Test A-3 is material dependent based upon the s and r design factors. Test A-3 defines the s factor as 1.5 and r factor as 1.0 for performing the test. These are identical to the values used for the other solid solution strengthened alloys in Table HBB-T-1324 in Section III-5 and proposed code case. The test data developed at INL (Wright et. al., 2012, Wright et. al., 2013, Wright et. al.,

2019) demonstrates that Alloy 617 does not cyclically soften so the use of the s value for the other materials is justified ($s = 1.5$) and is a safety factor applied to S_y . The r value is taken as 1.0 which is the same as the value taken for other solid solution alloys in the code. Because these tests do not apply above 650 degrees C, these values are considered reasonable.

Staff Evaluation

This review recommends that HBB-T-1321 to HBB-T-1323 be accepted because this test ensures that the maximum value of the load-controlled stresses throughout service life and maximum secondary stresses are limited to the elastic Bree regime where ratcheting does not occur. This is ensured if one end of the temperature cycle is below the creep range. Moreover, the temperature limit of 650 degrees C is a conservative lower limit. Also, the r and s values of Table HBB-T-1324 provide additional conservatism as discussed in Jetter et al., 2011 for Test A-3. The intent of the rules is to consider the maximum value of primary and secondary loads in the ratcheting assessment, which is quite conservative for materials that have a well-defined yield stress as Alloy 617 has below 1200 degrees F (650 degrees C). Jetter summarizes the conservative nature of these tests with extensive discussion (Jetter, 1976), pages 224–225, and the reviewers agree that these tests are indeed conservative. The staff believes this is technically acceptable and conservative despite no direct validation was made because the response of Alloy 617 below 1200 degrees F (650 degrees C) should be similar to the other Section III-5 materials.

3.7.3 HBB-T-1330 Satisfaction of Strain Limits Using Simplified Inelastic Analysis

Summary of Code Case Content

Simplified inelastic analyses are based on elastic stress analysis methods that are adjusted to account for inelastic deformations. These tests extend the region of applicability of the A-1 to three tests. Three simple tests, called B-1, B-2, and B-3 are provided for simplified inelastic analysis which if passed satisfy the strain limit rules.

Technical Basis

O'Donnell and Porowski (O'Donnell et. Al., 1974) and Porowski and O'Donnell (Porowski et. al., 1979) originally developed simplified inelastic analysis methods and the corresponding tests to satisfy strain limits. Sartory (Sartory, 1989) later enhanced these methods further. The following discussion applies to all materials including Alloy 617. The tests developed by O'Donnell, Porowski, and Sartory are termed "simplified" inelastic analyses, but they are based on elastic stress analysis methods that are adjusted to account for inelastic deformations, which must satisfy the strain limits summarized in HBB-T-1310. These tests extend the range of use of the Bree diagram approach (Tests A-1 to A-3), which is limited to an elastic response to prevent ratcheting. O'Donnell and Porowski (O'Donnell et. al., 1974) recognized that the rules of elastic

analysis methods could be extended to include other regions of the Bree diagram for compliance with the strain limits. They developed simplified inelastic analysis methods using the Bree cylinder with pressure loading and cyclic thermal loading. They modified the Bree method to estimate creep ratcheting in regions of the Bree diagram where no plastic ratcheting occurs. The solution is obtained in a one-dimensional elastic-plastic creep analysis. Enforcing beam theory assumptions, plane sections are assumed to remain plane, which occurs, for practical purposes, even under inelastic straining. The bounding theorems of Frederick and Armstrong (Frederik et. al., 1966) and Leckie (Leckie, 1974) and others are used to place an upper bound on inelastic strains.¹ The bounding theorems permit extension of rules to regions of the Bree diagram beyond elastic limits. These are represented by regions S_1 , S_2 , and P of the Bree diagram (see Figure 2 of O'Donnell et. al., 1974, for example), which are outside the range of applicability of Tests A-1 to A-3 (region EE for elastic).

The concept of an “elastic core” near the middle of the wall thickness was introduced. In this core, only elastic and creep strains can occur, and bounds on creep ratcheting strains could be established under cyclic loading based on bounding theorems. This is the basis of the B series of tests in Section III-5, Appendix T. Porowski and O'Donnell (Porowski et. al., 1979) extended this concept to elastic-plastic hardening materials (instead of EPP materials), temperature-dependent yield stresses, and a limited number of severe cycles into the plastic ratcheting regime. Porowski and O'Donnell (Porowski et. al., 1979) used energy concepts to extend the applicability of the bounds to include intermittent cycling in the plastic strain ratcheting region (extending the applicability of the regions for ratcheting rules using Tests B-1 to B-3 in HBB-T). The procedures are developed for both isotropic and kinematic hardening and are therefore general. Most material response follows mixed hardening, which is bounded by isotropic and kinematic hardening.

Staff Evaluation

Although the rules do not appear to have been specifically tested for Alloy 617 below 1200 degrees F (650 degrees C) (the applicable temperature range for the tests) these rules are recommended for endorsement because the strains should be limited to the Bree regime as they are for the other materials. Moreover, the temperature limit of 650 degrees C is conservative. The staff believe this is technically acceptable and conservative for the reasons discussed above.

¹ These bounding theorems were precursors to those used to establish the validity of Code Cases N-861 and N-862.

3.7.3.1 HBB-T-1331, 1332, 1333 Tests B-1, B-2, and B-3

Summary of Code Case Content

Three simple tests, called B-1, B-2, and B-3 are provided for simplified inelastic analysis which if passed satisfy the strain limit rules.

Technical Basis

The basis for the rules were summarized in Section 3.7.3 and these rules apply to Alloy 617. The Code Case procedure consists of determining the core stress with a safety factor applied for each load block from Figures HBB-T-1332-1 and HBB-T-1332-2 for Tests B-1 and B-2, respectively. These curves were originally published by O'Donnell and Porowski (O'Donnell et. al., 1974), where they were referred to as the "O'Donnell-Porowski iso-strains" and are used to obtain the creep ratcheting strain from ISSC provided in HBB-T for different materials. Restrictions on the tests are clearly indicated in HBB-T for Tests B-1 to B-3. The original approach of O'Donnell and Porowski ignored peak thermal stress considerations as occur in a stepped-wall cylinder, for example.

Sartory (Sartory, 1989) modified Tests B-1 and B-2 to account for peak thermal stress. To this point, no geometries analyzed by Sartory using finite element analyses to examine the appropriateness of the O'Donnell and Porowski (O'Donnell et. al., 1974) approach have resulted in non-conservative results. Ignoring peak stress can lead to non-conservatism in applying the rules. The revised technique was found to be conservative in all test cases. Validation has been made using finite element methods and compared to the simplified "Bree-type" analytical solutions.

This review considers Tests B-1 to B-3 to produce conservative results for the following reasons:

- The bounding theorems ensure that conservative results are predicted.
- The strain limits of HBB-1310 are considered quite conservative.
- The methodology predicts only when crack initiation occurs. There is typically more structural life in high-temperature structures beyond crack initiation.

The strain limits tests using elastic and simplified inelastic analysis are limited to below 1200 degrees F (650 degrees C) to ensure conservatism and the temperature limit is based on the original Corum and Blass (Corum et. al., 1991) assessments. The more recent identification of 1,382 degrees F (750 degrees C) as the temperature at which there is difficulty in separating plastic and creep strains by Messner (Messner, 2019) is more realistic than the 1,200 degrees F (650 degree C) limit imposed by Corum and Blass because it is based on a more precise analysis of the data.

For the above reasons the tests B-1 to B-3 used to ensure conservative satisfaction of strain limits when using simplified inelastic analysis methods for Alloy 617 is limited to 1,200 degrees F (650 degrees C). (It is noted that test B-3 has been removed from the 2021 version of Section III-5 because it is difficult to satisfy and is rarely used). As discussed in Section 2.7.3, the justification for both of these sets of tests is rigorously developed by O'Donnell and Porowski (O'Donnell et. al., 1974) and Porowski and O'Donnell (Porowski et. al., 1979) with enhancements by Sartory (Sartory, 1989) and is summarized in detail in Turk et al., 2020a in the review of Division 5 rules for other materials. This justification is equally valid for Alloy 617 in the temperature ranges permitted by this code case because Alloy 617 is a solid solution strengthened which does not cyclically soften, which is one of the inherent assumptions of the B tests.

Staff Evaluation

These rules are recommended for endorsement for the reasons justified above. The arguments and theory behind these rules apply equally well to Alloy 617. This justification is equally valid for Alloy 617 in the temperature ranges permitted by this code case because Alloy 617 is a solid solution strengthened which does not cyclically soften, which is one of the inherent assumptions of the B tests. This is technically acceptable and conservative.

3.7.3.2 HBB-T-1340 Strain Limits Using Elastic-Perfectly Plastic Analysis

Summary of Code Case Content

The EPP procedure for satisfying strain limits is an alternative to Tests A-1 to A-3 and B-1 to B-3, which are only applicable for Alloy 617 at temperatures less than 1,200 degrees F (650 degrees C). Since Alloy 617 is likely to be used in advanced reactors at temperatures higher than 1,200 degrees F (650 degrees C) these sets of tests are very important. The method permits the use of EPP finite element analyses to assess the high temperature response to strain development.

Technical Basis

The technical basis for the EPP analysis limits proposed in this record for Alloy 617 is summarized in INL, 2021q. This was carefully evaluated using the processes and evaluation procedures used in Turk et. al., 2020b for the strain limits. The code case is essentially identical to Code Case N-861 developed for stainless steel with the definition of the steps for the ratcheting analysis and the EPP assessment identical. This is because the bounding theorems ensure conservative predictions for any high temperature response regardless of material. A short summary of the validity and conservative nature of the EPP code case is provided next. Consult Turk et al., 2020b, Section 4, for more details. In addition, Carter, Sham, and Jetter (Carter et. al., 2016) provide further discussion and validation of these simple EPP analysis procedures.

- The EPP based code case for Alloy 617 permits finite element analysis (FEA) to make the assessment as an alternative for some design features and it is permitted for all temperatures where Alloy 617 is permitted. This is considered good practice today with FEA now dominating design and analysis procedures.

In summary, the Alloy 617 EPP Code Case permits use of time independent EPP FEA to show compliance with strain limits and ratcheting. The validity of this EPP based alternative was first examined with regard to the bounding theorems (for instance those presented in Frederick et. al., 1966) which ensure the conservative bounding nature of the methods. The bounds must first be shown to be valid for Alloy 617 as they are for the materials summarized in Code Case N-861. The bounding theorems were discussed in detail in Turk et. al., 2020b as well as Sham et. al., 2015. There is no restriction on application of the EPP procedure for Alloy 617 to a temperature range (recall that the tests for satisfaction of strain limits HBB-T-1300 are applicable only below 1,200 degrees F (650 degrees C)). The limits in HBB-T-1300 have temperature limits because of the difficulty distinguishing between plastic and creep strains above this temperature. The Alloy 617 EPP analysis relies on the ISSC which provide results for total strain and thus there is no need for a distinction. Moreover, the load definitions and composite load cycle definition rules are checked along with definition of the numerical model. Finally, the requirements for the satisfaction of strain limits in HBB-1344 was carefully examined using the process discussed in Turk et al (2020b) to ensure compliance. Example analyses were performed by Sham et. al., 2015 and clearly show conservative predictions for Alloy 617 using EPP methods when compared with full inelastic analyses and test data.

Staff Evaluation

The following present some additional justification for application of the method:

- The actual cyclic high-temperature response requires material behavior, including temperature dependent creep and plasticity damage assessment. Mathematical bounding theorems (Frederick et. al., 1966, Goodall et al., 1979; Penny et. al., 1995; and Carter, 1985, and Carter et. al., 1997), originally developed in the 1960s and 1970s and enhanced in the 2000s (Carter, 2005, Carter et. al., 2011), demonstrate EPP analysis results for strain limits and ratcheting and will bound both plastic and creep strains and creep-fatigue damage in component assessments. After extensive review of these references and others they cite, the reviewers agree with these theorems and approach. This is because the bounding theorems are independent of material, even for cyclic softening materials, although Alloy 617 does not cyclic soften. Turk et. al., 2020b provides a more detailed assessment of the theory behind these methods and their validity. Moreover, Sham et. al., 2015 provides conservative validation examples for Alloy 617 by comparison to test data and inelastic analyses.
- This Code Case permits a designer to perform an EPP FEA, following the step-by-step rules in the Code Case, to assess strain limits through a simplified service load block using desktop computers. This is much simpler and practical compared to a complete inelastic computational analysis assessment using complex visco-plastic material

models that must account for each load hold cycle individually. Solutions with complete inelastic models using the complete load sequences may require high-performance computing facilities and codes that run efficiently within that framework. Vendors will undoubtedly perform this for some components, since the current computational capability of many vendors is significant.

- The methods of Code Case N-861 for Alloy 617 do not necessarily predict the actual component strain limits. However, following these procedures will ensure a conservative design basis for metallic components at high temperature to satisfy strain limits.

for improving the design process and possibly reducing conservatism Section III-5 because the bounding theorems ensure conservative predictions (possibly over conservative) the EPP method for satisfaction of strain limits for Alloy 617 is recommended for endorsement. All test comparisons shown by Sham et. al., 2015 produced conservative predictions of life using EPP methods although additional validation cases would be useful.

3.8 Article HBB-T-1400 Creep-Fatigue Evaluation

Summary of Code Case Content

HBB-T-1400 provides rules to satisfy creep-fatigue damage design requirements for combination of Level A, B, and C Service Loadings including the effects of hold time and strain rate effects. Creep-fatigue interaction strongly affects life for both crack initiation predictions (HBB-T) and for the creep-fatigue crack growth and fracture procedures (currently under development) in Section XI and Division 5 (which are not part of the design rules for HBB-T since cracks are not permitted).

Technical Basis

The creep-fatigue rules for Alloy 617 were summarized in INL, 2021p and several references discussed below. In addition, Turk et al (2020a) provides a detailed discussion III-5 approach to creep-fatigue design along with the history of the development. Creep-fatigue interaction strongly affects life for both crack initiation predictions. Despite the approximations with this creep-fatigue design procedure the methods have repeatedly been shown to be conservative over the years according to Jetter, 2017 based on work performed by Severud (Severud, 1978, Severud, 1991) – see Section 4 of Turk et. al., 2020a. Moreover, the rules guard against crack initiation, and there is often considerable life remaining after crack initiation occurs in a component making this approach quite conservative. Most material data are developed using uniaxial test specimens. The provisions of HBB-T-1411 (Section 3.8.1) to account for multiaxial effects for evaluating creep damage using the Huddleston approach has also been sufficiently validated (see Section 3.8.1 below). As discussed by Turk et. al., 2020a many possible approaches were considered in the 1970s before development of the current HBB-T approach to creep-fatigue assessment in Division 5 and the precursor Code Cases. Ultimately, the simple bilinear creep-fatigue interaction approach was chosen because it is easy for designers to use, and the material data requirements are the simplest among all approaches considered.

With the creep-fatigue interaction approach, creep damage is accounted for on a time-fraction basis, and fatigue damage is accumulated using Miner's rules independent of strain rate (as done in Subsection NB). The combined damage is limited to a bilinear interaction damage value that is determined empirically (see Section 3.8.2 for the definition of the damage envelope for Alloy 617). This interaction curve must be used for both inelastic and elastic analysis methods discussed in Sections 3.8.3 and 3.8.4, respectively.

The Alloy 617 code case rules for creep-fatigue were evaluated using numerous references summarized below. These rules were evaluated in Turk et. al., 2020a, and Turk et. al., 2020b for the other five materials and a similar evaluation approach is used for Alloy 617. The design fatigue curves for Alloy 617 (in Figure HBB-T-1420-1F) were examined for their appropriateness for use within the HBB-T rules. The creep-fatigue interaction damage envelope of Figure HBB-T-1420-2 proposed for Alloy 617 was examined as well. These are proposed to be the same as Grade 91 and 2.25Cr-1Mo in the proposed code case (0.1, 0.1) for fatigue and creep interaction. These are shown to be conservative below based on discussion of the safety factors employed in the methods along with test data comparisons.

The creep-fatigue interaction damage value, which is determined empirically and, for Section III-5, is more conservative compared to the procedures in the Japanese code (DDS) (JAERI, 2010), the U.K. code (BEGL (R5), 2008, and the French code (RCC-MR, 2002) for most materials including Alloy 617. The Section III-5 rules for Alloy 617, with the Appendix T safety factors, provide conservative results, with the conservatism decreasing as strain range and rate decrease (i.e., where creep dominates) (Severud, 1991).

The cyclic life is reduced due to the accumulation of creep damage during the hold times of the cycle. The methods used for performing creep-fatigue within Section III-5 were developed in the 1970s and are still used today. A complete history of development of this procedure, along with other alternative methods that were originally considered are provided in Turk et. al., 2020a and the many references cited therein.

The material data requirements for the bilinear damage interaction rules chosen for use in HBB-T were by far the simplest to achieve, and this ultimately led to this choice for the code. The bilinear damage fatigue approach used in the code is non-conservative unless adequate safety factors are used on load definitions for both fatigue and creep assessments and with the use of conservative fatigue curves. Indeed, as discussed in detail in Turk et. al., 2020a there are more accurate methods to design for creep-fatigue interaction but the bilinear damage fraction rules in the code are simple to use and to develop data for. This will also carry over the design rules for Alloy 617 because the same safety factors used are the same.

Staff Evaluation

The creep-fatigue rules of Code Case N-898 are recommended for approval with details provided in the subsections below. The creep-fatigue interaction diagram approach has been

shown to be conservative for Alloy 617 from comparison to numerous tests performed at INL with details discussed below.

3.8.1 HBB-T-1411 Huddleston Parameter for Multiaxial Creep Failure Criterion

Summary of Code Case Content

The creep-fatigue rules require the consideration of multiaxial stress states during the creep-fatigue assessment. The method for doing this is based on the work of Huddleston and is described in INL, 2021o, and the additional references discussed below. The definition of the multiaxial equivalent stress and strain ranges are provided here for use in the creep-fatigue assessment.

Technical Basis

Most fatigue data is obtained on uniaxial test specimen so inclusion of multiaxial effects using the Huddleston criterion is used and shown to be conservative but not overly conservative compared to using a von Mises multiaxial criteria. HBB-T-1411 provides design rules for components operating under creep-fatigue conditions to satisfy deformation-controlled limits and employs a multiaxial failure criterion developed by Huddleston (Huddleston 1984, Huddleston 1993). Multiaxial effects for the creep part of the damage failure are based on work by Huddleston (Huddleston, 1984, Huddleston, 1993). The Huddleston equivalent stress accounts for compressive stresses, which are not as damaging as tensile stresses (for most materials), and it reduces over conservatism in the creep damage portion of the assessment. The use of the Huddleston criteria reduces over conservatism for components with significant compression in the load cycles. Turk et. al., 2020a provides further details for the other five materials.

Code Case N-898, HBB-T-1411 provides the Huddleston parameters which define multiaxial effects on creep-fatigue evaluation in HBB-T-1411. The Huddleston C parameter used for defining the equivalent stress is proposed to be '0.24' which is identical to that used for austenitic steels. The C value is the parameter which modifies the failure surface size in compression when compared with von Mises (when C is zero the von Mises criteria results). Moreover, the K' parameters defined in Table HBB-T-1411-1 are 0.9 for elastic analysis and 0.67 for inelastic analysis, which are identical to all other materials except 9Cr-1Mo-V. K' less than one is conservative because stress is divided by this factor before entering the ISSC to determine the allowable time duration for the cycle. The K' parameter is the safety factor on load. These are considered adequate for reasons listed next.

The choice of the value of $C = 0.24$, which is a simple factor used to modify the standard von Mises Yield criteria is discussed in the Huddleston papers (1984, 1993, 2003) and was originally developed based on data for Alloy 600 which is similar to Alloy 617 as both are nickel base solution annealed alloys. Validation of the choice of C for Alloy 617 based on data for Alloy 600

is documented in INL, 2021o based on data for tests performed on Alloy 617 specimens subjected to compression holds at INL. Huddleston, 2003 provides details on the calculation of C for 304 and 316 stainless steel and Alloy 600 based on tensile and compression tests. Huddleston found the value of C to be 0.25 for Alloy 600. The detailed calculations of C for Alloy 617 are provided in Wright et. al., 2012 following the method defined by Huddleston, 2003. These calculations determined a C value of 0.25. This derivation method to obtain this constant follows Huddleston and is considered valid and accurate. Use of the value of 0.24 for Alloy 617 in Table HBB-T-1411 is slightly conservative and this value is recommended for endorsement in the Alloy 617 code case.

The second part of the Huddleston parameter review is concerned with the safety factors used for the creep hold damage portion of the cycle (K' factors) again for inelastic analysis procedures. The safety factors are used by dividing the maximum stress during the creep hold portion of the cycle at the time of interest and are defined in Table HBB-T-1411-1 for Alloy 617 in Code Case N-898. Jetter, 2017 discusses the historical development of the K' safety factor values. This factor is also used in the EPP analyses to add additional conservatism into the EPP based predictions (discussed below). As discussed by Turk et. al., 2020a, these factors were modified after assessment of steam pipe failures in the mid-1980s. The values used for elastic analysis (0.9) and inelastic analysis (0.67) for Alloy 617 are identical to those for the other Division 5 materials except for 9Cr-1Mo-V, which for elastic analysis is 1 (or used with no safety factor). For Alloy 617 these same K' factors are used in the validation example problems discussed by Sham et. al., 2015. These validation problems included EPP simulations, comparison to creep-fatigue test results and comparison to Simplified Model Tests (SMT) which are meant to examine elastic follow-up effects among other conditions. In addition, comparisons were made to full inelastic solutions. While these example problems are not extensive these reviewers believe the use of these same factors for Alloy 617 is acceptable since conservative predictions were made for all of these cases. In addition, the use of these factors with the stress-to-rupture curves of Figure HBB-I-14.6G, which are log-log relationships, provide even more conservatism. Finally, these safety factors on load hold time have been validated for these materials over many years and these same factors should apply equally well for Alloy 617 even without extensive service experience with this material to date (see Turk et al 2020a).

Staff Evaluation

The values of the Huddleston parameters in Table HBB-T-1411 are recommended for endorsement since all comparisons to test data and inelastic analyses have shown predictions to be conservative using the Huddleston multiaxial parameters as discussed above.

3.8.2 Figure HBB-T-1420-2, Creep-Fatigue Damage Diagram

Summary of Code Case Content

The bilinear creep-fatigue interaction curve for use with Alloy 617 using the creep-fatigue damage equation of HBB-T-1411 is defined here. The interaction diagram is shown in Figure 3-

2. Creep damage is accumulated on the vertical axis and fatigue damage is accumulated on the horizontal axis. The combined damage must be below the bilinear line.

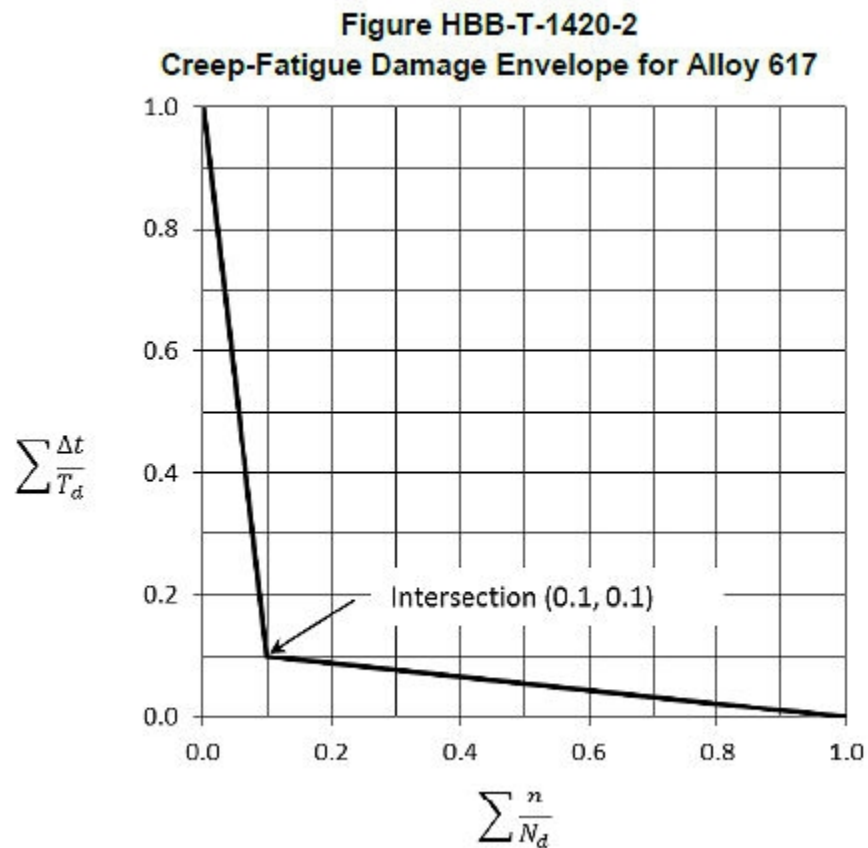


Figure 3-4 Creep-fatigue damage envelope for Alloy 617.

Reproduced from INL, 2021p.

Technical Basis

The original test data used to verify the interaction rule with intersection point (0.1, 0.1) for Alloy 617 was developed by Corum and Blass (Corum et. al., 1991) based on an early set of test data compiled by Yukawa (Yukawa, 1991). In addition, INL, 2021p, which is based on the work with data published in Wright et. al., 2016 shows that 15 of 103 data points are outside the failure locus diagram (e.g., to the right or above the lines on Figure 2-2) (see Figures 11-13 in Wright et. al., 2016) for many test cases. On the fatigue axis, a few points are on or inside the failure locus diagram in Wright et. al., 2016. The staff finds that having a few points inside the line does not indicate the creep-fatigue diagram is unacceptable because, as stated in INL, 2021p, the creep-fatigue damage envelope generally represents the average trend of the interaction between the creep damage and fatigue damage. McMurtrey et. al., 2018 shows similar

conservative comparisons to the failure envelope. Finally, Dewa, et. al., 2018 also show that creep-fatigue test data developed in Korea all fall outside the Alloy 617 failure envelope for the proposed interaction diagram for Alloy 617.

Staff Evaluation

The creep-fatigue failure envelope is recommended for endorsement because comparison to test data consistently shows conservative results which fall outside of the failure envelope.

3.8.3 HBB-T-1420 Limits Using Inelastic Analysis

Summary of Code Case Content

This section defines the rules to use when performing a creep-fatigue analysis using inelastic analysis methods. This includes the use of the inelastic safety factor of Table HBB-T-1411-1 for the creep damage portion of the assessment and the creep-fatigue interaction diagram of Figure HBB-T-1420-2.

Technical Basis

Full inelastic analysis involves performing a finite-element-based analysis of the creep-fatigue problem for the component of interest, using a proper constitutive law that handles combined creep and plasticity (visco-plastic behavior for Alloy 617) as functions of temperature throughout the service load history. The entire history of loading is included to perform the assessment. In the original code case developed by Corum and Blass (Corum et. al., 1991) a visco-plastic constitutive law proposed by Robinson (Robinson, 1984) was recommended with material properties defined up to 982 degrees C. Messner and Sham (Messner et. al., 2019, Messner et. al., 2021) also developed a visco-plastic constitutive law for temperatures up to 1,742 degrees F (950 degrees C). Either of these can be used in the inelastic analyses if they can be shown to be representative of Alloy 617 high temperature material behavior.

With the inelastic analysis approach, one performs this analysis and obtains the creep damage term via integration (HBB-T-1420 (a)) and similarly obtains the strain ranges for fatigue from the FEA, as corrected for multiaxial effects in accordance with HBB-T-1413 or HBB-T-1414. This type of analysis requires finite element expertise to apply to components subjected to real service loads. For this reason, the more conservative elastic analysis procedure of HBB-T-1430 was developed, which is discussed in Section 3.8.4.

It is anticipated that current vendors will use the inelastic approach for several their ANLWR component designs in the future because of the advances in computer technology and the use of high-performance computing. Discussions with some vendors during ASME Code meetings indicate that high-performance computers capable of performing large complex analyses rapidly are available and will be used extensively for next-generation ANLWR design.

Figure HBB-T-1420-1F provides design fatigue curves for determining the fatigue damage fraction as a function of temperature including Alloy 617 and the validity of these curves is discussed in more detail in INL, 2021r. These data were obtained from fully reversed loading conditions at temperature, and safety factors were applied to the curves before implementation into the code. As is the case for lower temperatures covered by Subsection NB, the design curve is constructed by reducing the best-fit curve of continuous cycling fatigue data by a factor of two on total strain range or a factor of 20 on life, whichever results in a minimum value. This is considered quite conservative and is consistent with the lower temperature fatigue curves developed and used in Subsection NB. The design allowable in Section HB, Subpart B, is presented as total strain range versus cycles compared to Subsection NB where the design allowable is stress amplitude versus cycles.

The fatigue curves were originally compiled during the development of the previous draft Alloy 617 code case (Corum et. al., 1991). This fatigue data was augmented by new test data developed at INL (Wright et. al., 2012 and INL, 2021p) along with tensile, creep, and constitutive data. The additional data developed by Wright et al (2012) for continuous cycling (no hold times) is similar to that produced for the data used for the original code case (Corum et. al., 1991) for similar applied strain ranges and this is consistent with this older data INL, 2021r describes the data sources used to develop the code case fatigue curves in HBB-T-1420-1F. The new INL data are consistent with the original data from the 1991 code case. It is noted that mean stress effects at high temperatures were shown to be unimportant for Alloy 617, and are not included in the curves, because of rapid stress relaxation during the high temperature portion of the hold time.

The assumptions used for the creep-fatigue design analysis approach are quite conservative. To summarize, these conservative assumptions include: (i) the maximum metal temperature during the cycle is used for the assessment; (ii) the fatigue curves in Figure HBB-T-1420-1F are constructed by reducing the best-fit curve of continuous cycling fatigue data reduced by a factor of two on total strain range or a factor of 20 on life, whichever results in a minimum value; (iii) the value of stress for determining T_d from rupture curves divided by K' (0.67 for inelastic analysis) increases conservatism, (iv) among other conservative rules.

Staff Evaluation

This review recommends that HBB-T-1420 be accepted for the reasons discussed in the previous paragraph because the choice of the interaction diagram is very conservative as seen with the discussion of predictions using the model with test data discussed in Section 3.8.23.8.4. The validity of the inelastic constitutive models must be demonstrated to produce accurate inelastic response. The creep-fatigue damage envelope, with damage intersection point (0.1, 0.1), proposed for Alloy 617, will provide conservative predictions when used with the safety factors. This definition of the failure locus was originally proposed by Corum and Blass (1991) in the original attempt to put together a code case for Alloy 617 based on test data compiled from sources at the time and is validated in the work at INL and references cited therein (Cabet et. al., 2013, Wright et. al., 2016, Wright et. al., 2018) by comparison to extensive creep-fatigue test

data. There is consensus (Suzuki et. al., 2011) that creep-fatigue life is dominated by fatigue at the lower end of the temperature range for Alloy 617 and by creep at the higher temperature end of the application.

3.8.4 HBB-T-1430 Limits Using Elastic Analysis

Summary of Code Case Content

This section defines the rules to use when performing a creep-fatigue analysis using elastic analysis methods. HBB-T-1431 of the code case modifies Section III-5 by adding a reference to the design fatigue curve for Alloy 617 in Figure HBB-T-1420-1F of the code case, a reference to the creep-fatigue interaction diagram for Alloy 617 of Figure HBB-T-1420-2 of the code case, and also prohibits the use of elastic analysis at temperatures greater than 1,200 degrees F (650 degrees C) for Alloy 617. References to the ISSC and design fatigue curves for Alloy 617 are also added in HBB-T-1432 and HBB-T-1433. Additionally, HBB-T-1433 adds references to the minimum stress-to-rupture curve for Alloy 617 and the elastic safety factor of Table HBB-T-1411-1 for Alloy 617.

Technical Basis

A brief summary of the elastic analysis technical basis provided in Turk et al 2021a is provided here as it is appropriate for Alloy 617 for temperatures less than 1,200 degrees F (650 degrees C) where plastic and creep strains can separate. This method is applicable for temperatures less than 650 degrees C which is a temperature upper limit where Alloy 617 is unlikely to be used in an ANLWR component due to cost and the availability of other Section III-5 materials. This method can only be used if the elastic ratcheting rules of HBB-T-1320 (Tests A-1 to A-3) or HBB-T-1330 (Tests B-1 to B-3) discussed in Sections 3.7.1 or 3.7.3, respectively, are passed.

As discussed in Jetter, 2017 and Severud, 1991, the original elastic analysis rules were unduly conservative in the original creep-fatigue design procedure because of redundant counting of creep damage. Severud, 1991 and the references cited in that work address this issue, and the current rules for creep-fatigue assessment using elastic analysis methods are based on this work. The carefully developed arguments of Severud (Severud, 1978, Severud, 1991) are based on years of work and vetting by the ASME Code Section III Division 5 committee, are considered conservative, and are the reason the articles for creep-fatigue discussed below are recommended for endorsement.

Elastic analysis methods exist in the code because some designers did not have the background and experience to perform detailed inelastic analysis of the creep-fatigue component design process in the 1970s when the rules were originally developed. This is not likely the case today. In addition, EPP methods, described next, can also be used to satisfy creep-fatigue life design. A series of inelastic finite-element-based analyses performed by Becht (Becht, 1989) examined the effect of stress relaxation at structural discontinuities (e.g., at a pipe reducer) subjected to mechanical and thermal load combinations. This work considered 10 different configurations in piping and vessels with different discontinuities that are typical of in

service components. The results led to important additions to HBB-T in which pressure-induced secondary stresses are now considered as primary stresses for creep-fatigue analysis purposes. Becht (Becht, 1989) referred to this as “creep follow up” rather than “elastic follow-up,” but the code was modified to classify secondary stresses for ratcheting and creep-fatigue.

WRC Bulletin 366 (Datta, 1991) summarizes the procedures of accounting for elastic follow-up, which are based on so-called “adjusted secant for piping” methods. In addition, Jawad and Jetter (Jawad et. al., 2009) provide detailed examples along with discussion of the rationale behind the rules. Elastic follow-up must be included in the elastic analysis rules to account for stress relaxation due to creep, which is often only partial in complex components such as piping systems. The methods identify the fraction of stress necessary to be included as primary stress due to restrained thermal expansion for both strain limits (discussed above) and creep-fatigue damage. The K' safety factor of Table 1411-1 (0.9) must also be used for the creep damage portion. In addition, the fatigue curves have the safety factors discussed above.

The fatigue curves for the other five Section III-5 materials were established long ago, before 1985 according to the former chair of the ASME Code, Section III Subsection NH (the precursor to Division 5 during that time). This procedure has been used with success for many years for all materials.

The test data used to verify the interaction rule with intersection point (0.1, 0.1) was originally developed by Corum and Blass (Corum et. al., 1991) with additional data published in Wright et. al., 2016 as seen in Section 3.8.2. While these comparisons of the method to the test data were made at temperatures above 1,200 degrees F (650 degrees C) for use with inelastic and EPP analysis, the legacy elastic creep-fatigue rules for Alloy 617 should apply since they are so conservative.

The assumptions used for the elastic creep-fatigue design analysis approach are quite conservative. To summarize, these conservative assumptions include: (i) the maximum metal temperature during the cycle is used for the assessment and must be less than 650 degrees C; (ii) the fatigue curves in Figure HBB-T-1420-1F are constructed by reducing the best-fit curve of continuous cycling fatigue data reduced by a factor of two on total strain range or a factor of 20 on life, whichever results in a minimum value; (iii) the value of stress for determining T_d from rupture curves divided by K' (0.9 for elastic) increases conservatism, (iv) among other conservative rules.

Staff Evaluation

This review recommends that HBB-T-1430 be accepted because of the careful arguments discussed in the above references and the conservative results expected. Moreover, additional conservatism is ensured because the elastic ratcheting rules of HBB-T-1320 must be satisfied before the approach in HBB-T-1430 can be used. Finally, elastic follow-up is addressed by classifying certain secondary stresses as primary for the assessment.

3.8.5 HBB-T-1440 Limits Using Elastic-Perfectly Plastic Analysis – Creep-Fatigue Damage

Summary of Code Case Content

This section of the Code Case provides an alternative method for evaluating creep-fatigue damage and shakedown to satisfy compliance with Section III-5, Subsection HB, Subpart B. This is termed a simplified method because it does not require the use of comprehensive full inelastic constitutive equations that account for both time independent plasticity and time-dependent creep.

Technical Basis

As an alternative, creep-fatigue limits can be satisfied using the EPP methods. These methods provide conservative estimates of creep-fatigue life based on bounding theorems of Frederick and Armstrong (Frederick et. al., 1966), Goodall et al., 1979), (and others) and discussed in detail in Turk et. al., 2020a where it is shown that conservative results will result when using the EPP modeling methods. This series of bounding concepts reflect the tradeoff between problem complexity, accuracy, and the guaranteed conservative nature of the bounds when using EPP methods. For Alloy 617 these same bounding theorems apply equally well as they do for all the other materials. The applicability of the EPP method to Alloy 617 is discussed in INL, 2021p. This method can be used for Alloy 617 for temperatures up to 954 degrees C and is not limited to below 650 degrees C as is the elastic method of HBB-T-1431. Validation of the EPP method for creep-fatigue is provided by Sham et. al., 2015 by comparison of the EPP results to test data and to full inelastic analysis predictions.

Detailed discussion of all steps required to perform the EPP analysis are provided in Section 4.3 of Turk et. al., 2020b where a discussion and justification of all steps of the analysis procedure are provided. The arguments, which apply for Alloy 617, used for the general case of thermal-mechanical loading and creep-plasticity are based on the self-evident assumption for a structure under general loading—from the bounding theorems (Goodall et al., 1979, and Penny et. al., 1995) - “Reducing the perfectly plastic yield stress does not reduce the deformation.” Rather, it should increase the deformation. In addition, reducing the yield stress by using ISSCs and conducting EPP analysis produces larger deformation compared with the corresponding full inelastic solution. Applied to the plastic rapid cycle solution (rapid cycle neglects creep since EPP is performed), this statement means that the cyclic increment in the deformation of a structure is not reduced if the yield stress is reduced, all other factors being unchanged. Therefore, if the yield stress is reduced to the point where ratcheting in a cyclic problem is imminent, then the cyclic incremental deformation is not less than for the original yield stress. Therefore, the energy dissipation and deflection for the reduced yield stress case provide an upper bound of the energy dissipation and deflection in the original cases. This ensures not only ratcheting but cyclic shakedown, which is the basis of Code Case N-862 (creep-fatigue), ensuring that the bounding theorems for the creep damage fraction provide conservative predictions.

Further discussion of the basis for the Code Case is expressed in terms of energy bounding theorems (Carter et. al., 2012b, Carter et. al., 2016) and discussed here also. A “hierarchy” of bounding concepts reflects the tradeoff between problem complexity and bounding accuracy. Problems with mechanical load cycles may be bounded by external work, and those with thermal (secondary stresses) and mechanical load cycles may be bounded by internal energy dissipation. The application for displacement-type loading is generally more conservative than for purely mechanical problems, since high internal energy dissipation may be associated with zero net deflection. In both cases, the opportunity for a simplified analysis arises from the use of the “rapid cycle” concept. Rapid cycles have no creep relaxation during the cycle, and no hold times, but they generally have the most advantageous residual stress system, which ensures that deformation rates over the cycle are as low as possible. In terms of deformation and strain accumulation over time, rapid cycles are more conservative than slow cycles. Therefore, if creep-fatigue limits can be demonstrated for rapid cycles, slower cycles with relaxation will also satisfy the creep-fatigue limits. The references cited above further discuss this application to the Code Cases in more detail, and general bounding theorem papers provide higher level proofs.

The use of a time independent analysis to assess high temperature processes is not intuitively obvious so the judicious use of the bounding theory proofs is essential for complex high temperature design and life assessment. Sham et. al., 2015 provides both theoretical and practical discussion regarding the conservative nature of the EPP method for creep-fatigue of Alloy 617. Moreover, example problems are presented where comparison of EPP predictions to the SMT results, are presented. The SMT test specimen mimics the effects of elastic follow-up in pressure boundary components which is an important concern in real reactor piping systems. The EPP predictions were conservative compared to the test results including validation of the shakedown predictions using EPP.

Staff Evaluation

The use of EPP methods for Alloy 617 ensure conservative predictions because of the bounding theorems and comparison to test data was always conservative and this method is recommended for endorsement. In addition, predictions of shakedown were made using EPP, which also produced conservative predictions, for a large number of standard creep-fatigue tests performed by Carroll et. al., 2010 and Cabet et. al., 2013. The EPP methods bounding theorems do not have material dependent validity. Therefore, some of the validation cases discussed in the references summarized in Turk et. al., 2020b for austenitic steels apply to validation of the methods for Alloy 617 as well. However, it would be useful to see additional validation tests for Alloy 617 to ensure the conservative nature of the EPP methods for Alloy 617. Indeed, the EPP method for creep-fatigue assessment may be overly conservative based on the comparisons shown in Sham et. al., 2015. The EPP method for the satisfaction of creep-fatigue for Alloy 617 is recommended for endorsement for the reasons summarized above.

3.9 Article HBB-T-1500 Buckling and Instability

The buckling and instability requirements for design to prevent buckling are summarized in this section.

3.9.1 HBB-T-1510 General Requirements

Summary of Code Case Content

The general requirements for buckling and instability for high temperature nuclear design are provided in this article. The consideration of both time independent buckling and creep buckling is necessary and this requires that buckling loads or strains be calculated for all cases where compressive loads may lead to instability for Alloy 617.

Technical Basis

The technical basis for these rules is discussed in INL, 2021n. The design rules for buckling, along with the design factors for time-dependent buckling, have been significantly enhanced from the original rules from Code Case 1,592 for all materials. Some of the original guidance from RG 1.87 for buckling (Section C, Regulatory Position 2, Code Case 1592-d(1) and d(3)) is no longer needed because the new rules are more specific, especially with the temperature limits defined in Figures HBB-T-1,522-1 to HBB-T-1,522-3. The current rules require use of the load-controlled buckling factors for conditions where strain and load-controlled buckling may interact or for conditions where significant elastic follow-up may occur. The general requirements in this article apply to all materials including Alloy 617.

The stability limits for buckling of Alloy 617 pertain only to specific geometric configurations under specific loading conditions. For instance, column buckling is not evaluated. These conditions consist of cylinders under axial compression, and cylinders and spheres under external pressure. Distinction is made between load and strain-controlled buckling. Load-controlled buckling occurs with continued application of the load through the post-buckling regime leading to collapse. Strain-controlled buckling is characterized by load reduction as deformation instability occurs and is therefore self-limiting. However, strain-controlled buckling must be avoided to guard against fatigue and excessive strain.

The rules permit use of NB buckling rules when creep buckling is not a concern. Griffin (1980, 1996, 1999) developed a rationale and temperature limit charts (Figures HBB-T-1522), which when satisfied, permit use of the time independent rules of Subsection NB to satisfy buckling design. The methods summarized by Griffin (Griffin, 1996, Griffin, 1999), which are based on use of the buckling equations using time-dependent material parameters defined from ISSC for the lifetime of the component. Section VIII, Code Case 2,964, provides the method of Griffin (Griffin, 1996, Griffin, 1999) to perform time-dependent buckling analysis to develop the temperature limit charts. As discussed by Griffin (Griffin, 1996, Griffin, 1999) the method used to produce the temperature limit charts has been validated for a number of buckling tests for the other code materials. When the temperature limit charts are exceeded, the owner must perform

inelastic analyses, using the load factors specified in Code Case N-898 (Record 16-996) for Alloy 617 to ensure that the component does not experience creep buckling over the design life. The method used to perform the inelastic analyses is not specified and is up to the owner. However, it is expected that many vendors will use inelastic finite element analyses, using the proposed constitutive law for Alloy 617, including initial imperfections, to show that creep buckling is not a concern.

Staff Evaluation

The general requirements in HBB-T-1510 apply to all materials including Alloy 617 and is thus recommended for endorsement.

3.9.2 HBB-T-1520 Time-Dependent Buckling

Summary of Code Case

The design requirements to protect against load-controlled time-dependent buckling creep buckling are provided in HBB-T-1520. It shall be demonstrated that time-dependent instability will not occur during the component lifetime for load histories which include load factors discussed below.

Technical Basis

The portion of Code Case N-898 was developed under INL, 2021n. As discussed in a recent review of HBB-T rules for buckling Turk et. al., 2020a, load and strain-controlled rules for time independent and time-dependent buckling are provided in Appendix HBB-T-1500 and remain an important design consideration for components that operate under compression loading at high temperature (see Reference Section III-5 (2021)). HBB-T-1500 requires consideration of both time independent buckling and creep buckling and requires that buckling loads or strains be calculated for all cases where compressive loads may lead to instability for the current five materials. Subsection NB-3133 may be used for cylindrical and spherical shells for instantaneous buckling and includes the effects of initial imperfections and temperature effects on properties but not creep. Time independent load factors are defined to provide margin for load or strain that may occur instantaneously at any time with time independent material properties at the time of loading.

The technical basis for the HBB-T-1500 buckling rules is based on very thorough work by Griffin (Griffin, 1996, Griffin, 1999) who extended earlier work by Gerdeen and Sazawal (Gerdeen et. al., 1973), Berman and Gupta (Berman et. al., 1976), and Gerard, (Gerard, 1962) and the many references cited therein. The design factors and the methods were carefully validated and ensure conservative buckling predictions when compared to extensive test data. The rules provide limits on temperature and load time (or geometry) that define when the Section III NB-3133 external pressure design charts (which have NRC endorsement) can be used without the need for consideration of creep buckling. The buckling charts in NB-3133 permit buckling assessment up to high temperatures for short high temperature excursions where creep has no

time to occur. Griffin's original rules were designed to be simple to use and so a number of conservative assumptions were made to accommodate this simplicity. If the temperature and time limits in Figures HBB-T-1522-1 to -3 are not satisfied inelastic analyses must be performed to ensure creep buckling is not an issue. Prior experience with high temperature design suggests that many designs to prevent creep buckling can use the Section III NB-3133 rules.

A short summary of the rationale behind the rules is provided next. The critical buckling stresses originally developed by Griffin (Griffin, 1996, Griffin, 1999), and also used for the Alloy 617 rules are calculated for instantaneous and creep buckling using classical stability theory for perfect shells and the time-dependent isochronous stress-strain curves (ISSC) which include elastic, plastic, and creep strains without using an explicit creep law. Griffin (Griffin, 1996, Griffin, 1999) used classical buckling formulas augmented with the tangent and secant moduli from the ISSC to predict time-dependent buckling. These methods were validated with extensive test data. The following lists the rationale for the rules and the conservative assumptions inherent in the rules.

- For cylinders under external pressure the ASME Section III-5 design rules are developed for long shells so that the allowable stress depends only on radius and thickness. Shorter length shells have higher buckling stresses, so this is conservative and makes the rules simpler to apply.
- The classical elastic buckling stresses are used but modified by a reduced modulus to account for plasticity and creep from the isochronous curves and a factor to account for initial imperfections and dividing by a design factor to ensure conservatism. As discussed in Griffin, 1999 and Gerard, 1962 use of isochronous curves and the corresponding tangent and secant modulus for this purpose provides conservative predictions of buckling and has been verified with extensive test data. Therefore, the equations for time independent plastic buckling can be used directly using the appropriate ISSC.
- Much of the test validation of the buckling stresses were made with aluminum, stainless steel, titanium alloys, and other materials, and for Alloy 800 (Livingston, 1987). This included stiffened shell tests. The buckling equations equally apply for Alloy 617 since they are material independent and depend on use of the ISSC. Some test data has been developed for Alloy 617 shells by Schulze, R. and Seehafer, H.J., (Shulze et. al., 1977).
- The limits of HBB-T-1521 for time independent buckling, and the limits of HBB-T-1522 for time-dependent buckling must both be satisfied. The critical stresses used for development of the temperature time charts use the HBB-T-1800 code ISSC, which are average data curves rather than minimum. The minimum is conservatively estimated by multiplying the average curves by 0.8.
- The time-temperature limits also depend on radius to thickness ratio. However, as shown in Griffin, 1996 and Griffin, 1999, this dependence is not strong for cylinders under axial compression and spheres under external pressure. Therefore, the charts for these were developed for radius to thickness ratios of 150 without introducing excessive

conservatism and this makes using the charts easier. Higher limits could be provided for lower radius to thickness ratios but was not done for the sake of simplicity.

- For cylindrical shells under external pressure the radius to thickness ratio must be included in the charts because the critical stress is proportional to the square of the thickness to radius ratio. For this case the radius to thickness temperature limits also depends on load time but this dependence is not strong. For Alloy 617 the temperature time chart was developed for isochronous stress-strain curve at 100,000 hours. This was shown to be adequate for the other Division 5 materials and should apply for Alloy 617 also.
- It is noted that the method used to develop the time-temperature curves for Alloy 617, using the method of Griffin (Griffin, 1996, Griffin, 1999), were verified by the code case authors by reproducing the buckling charts for 304H and 316H stainless steel that are currently in Division 5.

Jawad et. al., 2009 provides practical examples on use of the HBB-T-1500 rules for buckling assessment. It is noted that NASA has recently performed extensive testing and modeling work on shell buckling (Hilburger et. al., 2018 and numerous references cited therein). This NASA work was focused on modifying the 'knock down' factors that have been used for buckling design in aerospace shells since the early 1960s when buckling launch failures occurred during preparation for the moon launch. These 'knock down' factors are completely analogous to the conservative load factors provided in the Section III-5 code for buckling. The work clearly shows that computational modeling of buckling, where the shell initial imperfections are included in the models, provides very accurate predictions of buckling predictions when compared to full scale testing. However, the NASA work was limited to temperatures where creep does not occur, but it shows that computational modeling of the buckling process, when initial imperfections are included, is quite accurate. It is anticipated that ANLWR vendors will use computational methods for buckling assessment and the full inelastic constitutive material models that are now being added to the code for code materials, including Alloy 617. Therefore, accurate results are expected for vendors that use full inelastic analysis for HBB-T-1500 buckling design.

Section VIII Code Case 2964, "Allowable Compressive Stress in the Time Dependent Regime," has many assumptions and approximations and is used for non-nuclear buckling design such as in refineries but cannot be used for nuclear designs. However, the Griffin methods of Code Case 2964 were used to develop the temperature time charts of Figures HBB-T-1522-1 to HBB-T-1522-3 and these methods are considered valid and conservative. The methodology of Code Case 2964 at elevated temperature is very similar to the methodology used in BPV-III-NC for temperatures below creep.

Time-dependent buckling rules are meant to account for uncertainties in initial deformation and material creep uncertainty. For Alloy 617 buckling the temperatures must be less than 1,742 degrees F (950 degrees C) and service time is limited to 100,000 hours. For strain-controlled buckling lower safety factors are imposed because stresses relax as deformation occurs. Griffin (Griffin, 1980, Griffin, 1996) showed that strain-controlled buckling limits can be handled from

time independent limits as long as the ISSC are used for the design time. In distinguishing between load and strain-controlled buckling care must be taken to ensure that the designer properly interprets the situation correctly. If it is not certain that strain. Designers should assume load-controlled buckling controls then if there is uncertainty as to which type of buckling is predominant, because load-controlled buckling is most conservative. This restriction essentially ensures that if there is any question about whether a buckling situation is load or strain control then one must assume load control rules.

For combined load and strain-controlled buckling, if there is interaction, the load control factors must be applied to ensure conservative results if the distinction between loads is not clear. This is required because, although strain-controlled buckling is self-limiting, it can result in a shape change that affects load-controlled buckling.

Staff Evaluation

Based on work by Schulze and Seehafer (Schulze et. al., 1977) on Alloy 617 the effect of initial imperfections for creep strains up to the limits permitted in the code are small. Moreover, the temperature time curves introduced for Alloy 617 for cylindrical shells loaded axially, and spheres and cylinders loaded with external pressure, used the procedure of Griffin (Griffin, 1996, Griffin, 1999). Since load factors for Alloy 617 are identical to those for the other materials, conservative predictions using the HBB-T-1500 rules are ensured and the code case record is recommended for endorsement. Details are provided in INL 2021n and corresponding technical basis documents and references were carefully examined to assess the Alloy 617 code case for appropriateness of design for buckling of this material. This includes the assessment of the appropriateness of the distinction between time independent buckling (Section III, Division 1, NB-3133) and time-dependent rules to be added in HBB-T-1520 for this Code Case. The time-dependent buckling charts in Figures HBB-T-1522-1, -2, and -3 have the curves for Alloy 617 included. HBB-T-1500 is recommended for endorsement as rules are conservative and verified with experimental test data.

3.10 HBB-T-1820 Isochronous Stress-Strain Relations

Summary of Code Case

ISSC are used in a number of the design rules for both HBB and HBB-T to account for creep deformations. INL, 2021o discusses the ISSC curves and equations for use with Alloy 617. Appendix I provides discussion of the conservative nature of using ISSC to assess creep effects.

Technical Basis

The ISSC, and corresponding temperature dependent creep equations proposed for Alloy 617 in HBB-T-1800, were carefully examined and reviewed in this effort. The ISSC for the other five materials in HBB-T-1800 were examined by the report authors in Appendix A of Turk et. al., 2020a. The assessment of Alloy 617 ISSC was performed in this assessment in a similar format

as done in Turk et. al., 2020a. The equations from INL, 2021o were programmed in a spreadsheet and compared to the isochronous curves proposed in Code Case N-898 directly (some comparisons are shown in Appendix I). Additional material data obtained from the literature (as available) was also plotted on these curves as was done in Appendix A of Turk et. al., 2020a for Alloy 617. The additional data, when plotted on these curves, provides supporting validity to the proposed curves in HBB-T-1800 for Alloy 617 as seen in Appendix I here.

ISSC are used as a simplified method to account for creep damage effects in design during hold portions of the load cycles. The detailed justification for use of ISSC were provided in Turk et. al., 2020a, Appendix A based on theoretical discussions provided in Marriott, 2011 and the many references cited therein. The isochronous stress-strain curve is a long-established method of representing creep data in a manner that provides a quick and often surprisingly accurate approximate solution to time-dependent structural problems. Despite criticisms of the foundations of the method, it has survived over the years because it has either been the only method feasible at the time, or it can provide solutions that are often good enough for practical purposes (Marriott, 2011).

Traditionally Section III-5 (and its predecessor NH) have provided the ISSCs in graphical form where the designer visually interpolates over the curves for a given temperature, stress, and time of interest. ASME Section III-5 provides the total strain versus stress and temperature equations and these are provided for each material in the code in addition to the graphical curves. This permits one to use the exact equations as an alternative to visual interpolation over the curves for design. For the other five materials in the code the validity of the curves was examined in Turk et. al., 2020a, Appendix A by providing spot checks of additional material data not used to produce the curves that were recently gathered from the literature. This is also performed here in Appendix I although extensive data at some temperatures was not available for comparison purposes. This assessment is provided in Appendix I here as well for Alloy 617. It is noted that an error was observed in the plastic strain portion of the equations in Code Case N-898 and this will be corrected (see Appendix I for more details).

The U. S. Department of Energy has supported a project through the ART Program to develop and gather the required data to support the adoption of Alloy 617 as a Class A material in Section III, Division 5 of the ASME Code for high temperature reactor components. Cabet et. al., 2013, Rabin, et. al., 2013, Wright et. al., 2013a, Wright et. al., 2013b, and Wright, et. al., 2013c, summarize much of this data for development of ISSC and the other design parameters necessary for the code case. The technical basis for the ISSC methodology proposed for Alloy 617, with validation, is provided in Appendix I.

Staff Evaluation

The equations used to calculate the ISSC for Alloy 617 were independently programmed by the current authors into a spreadsheet. The ISSC code assessment of the data and spot checks of the data provided in Appendix I show that the Alloy 617 ISSC curves are adequate, and endorsement is recommended. Indeed, the ISSC curves from the presently produced

spreadsheet are identical to those in Code Case N-898 and INL, 2021o for every temperature and stress value. In addition, the spot checks in Appendix I clearly show conservative ISSC curves are provided in INL, 2021o. The ISSC are recommended for endorsement.

4 CONCLUSIONS

4.1 Code Case N-872 Conclusions

The staff reviewed Code Case N-872, which provides permissible product specifications, allowable stresses, mechanical and physical properties for use in construction of low temperature Alloy 617 components for Section III, Division 5, Subsection HB Subpart A (Class A) and Subsection HC, Subpart B (Class B). The staff finds the permissible product specifications acceptable because they are ASME material specifications, all of which have properties listed in Section II-D/II-D-M, and are generally allowed for use in other code portions of the ASME Code such as Section III-1. The staff found all the proposed allowable stresses and mechanical properties acceptable because these are generally consistent with the corresponding values of these properties and allowables in Section II-D, for design of components of equivalent safety significance, or have been determined consistently with the procedures of Section II-D, when explicit values were not included in Section II-D. The staff found the proposed thermal properties acceptable, because the properties are generally based on a sufficient amount of experimental data, reasonable mathematical fits to the data are used to define the temperature versus property relationship, and the proposed properties have been benchmarked against values of these properties for similar alloys, or other investigations of Alloy 617.

Like Section III-5, Subsection HB Subpart A and Subsection HC Subpart A, Code Case N-872 does not address environmental effects such as corrosion or irradiation on component integrity; therefore, these topics are outside the scope of the staff's approval of Code Case N-872.

4.2 Code Case N-898 Conclusions

4.2.1 Limitations

Code Case N-898 is recommended for endorsement with the following two limitations:

- When applying HBB-T-1710 and HBB-4800 to Alloy 617 components, applicants and licensees should develop their own plans to address the potential for stress relaxation cracking in their designs. These plans should address factors such as weld joint design and controls on welding in addition to the required heat treatment of HBB-4800.
- When applying HBB-T-1836(2)(-b), the equation for plastic strain in the code case should be replaced with the following equation:

$$\text{for } \sigma > \sigma_1, \varepsilon_p = -\frac{1}{\delta} \ln \left(1 - \frac{\sigma - \sigma_1}{\sigma_p - \sigma_1} \right)$$

The following summarizes the basis for these limitations:

- Guidance for mitigation of SRC provides a stabilizing heat treatment that should address the metallurgical contributors to SRC and also relieve weld residual stresses and cold work residual stresses that contribute to SRC. The heat treatment required for mitigation of SRC is in addition to the heat treatment for components with greater than 5% cold work. However, the staff found that heat treatment alone may not be sufficient to mitigate the potential for SRC; therefore, the staff identified the limitation stated above.
- The staff determined that the isochronous stress-strain curves (ISSC) for Alloy 617 (HBB-T-1800) provide conservative predictions of stress and strain compared to the data for the same temperature and time as shown in Section 3.10 and Appendix I where spot checks on the curves were made. The ASME Code has identified a typographical error in the equation for plastic strain in HBB-T-1836. The correct equation is provided in Section I.2 as Equation I-1 and a limitation is recommended that this equation be used instead of the equation in Code Case N-898, HBB-T-1836(2)(-b).

The following subsections summarize the conclusions and basis for endorsement for each major topic covered by Code Case N-898.

4.2.2 Material Properties and Allowable Stresses

Sections 3.2 through 3.5 of this report contain the staff's review of permissible materials specifications, materials properties and allowable stresses, heat treatment requirements for cold worked components and for mitigation of SRC, and physical properties.

Permissible materials specifications, materials properties and allowable stresses are included in Sections HBB-2000, HBB-3000, and Mandatory Appendix HBB-T-14 of the code case. Table HBB-3225-1 provides the yield and tensile strength reduction factors and Table HBB-3225-2 provides ultimate tensile strength (S_u) values. Mandatory Appendix HBB-T-14 of the Code Case lists the permissible weld and base metal material specifications for Alloy 617. HBB-T-14 of the code case also contains tables and figures with time independent and time-dependent allowable stresses for Alloy 617, including S_0 , S_{mt} , S_t , S_r , along with the material yield strength S_y . HBB-T-14 also contains the SRFs (R factors) for welds. The staff found the permissible weld and base metal specifications acceptable because these are recognized ASME material specifications for Alloy 617 and its matching weld filler material. The staff found the tensile and yield reduction factors, allowable stresses and R factors have been determined from a sufficient and representative material database using techniques consistent with those generally used by ASME to determine the properties of the other materials allowed by Section III-5. Additionally, the staff's confirmatory analysis of the allowable stresses yielded consistent values to the Code Case. When applicable (such as for S_0 and S_{mt}), the allowable stresses are consistent with those listed for Alloy 617 in Section II, Part D.

HBB-4000 of the code case contains requirements to address the effects of forming and bending process that induce cold work (HBB-4212) and for mitigation of SRC (HBB-4800). The staff found the requirements for heat treatment for cold worked components are consistent with

requirements for the other materials permitted in Section III-5, and should mitigate the deleterious effects on creep-rupture life caused by cold work. The staff found the required heat treatment to mitigate SRC is based on manufacturer's recommendations and is consistent with industry research for this material and similar materials, and is therefore acceptable. However, the staff found that heat treatment alone may not be sufficient to mitigate the potential for SRC; therefore, the staff identified the following limitation:

When applying HBB-T-1710 and HBB-4800 to Alloy 617 components, applicants and licensees should develop their own plans to address the potential for stress relaxation cracking in their designs. These plans should address factors such as weld joint design and controls on welding in addition to the required heat treatment of HBB-4800.

Nonmandatory Appendixes A and B of the code case contain thermal properties for Alloy 617 and Nonmandatory Appendix C contains modulus of elasticity values. The thermal properties are identical to and share the same technical basis as those in Code Case N-872, and are therefore acceptable, for reasons summarized in Section 4.1 of this report. The staff found the modulus of elastic values acceptable because they are either identical to the values for Alloy 617 in Section II-D, or were extrapolated from the Section II-D values with confirmation from experimental data.

Like Section III-5, Subsection HB Subpart B, Code Case N-898 does not address environmental effects such as corrosion or irradiation on component integrity; therefore, these topics are outside the scope of the staff's approval of Code Case N-898.

4.2.3 ALARA Considerations

Section 3.6 briefly discusses considerations related to minimizing radiation doses to personnel. As a Co-containing alloy, Alloy 617 has the potential to cause high out-of-core dose rates around the reactor coolant system due to activation of Co corrosion products in the reactor core. The staff therefore recommends designers considering use of Alloy 617 in ANLWR components should carefully consider the applications in which this alloy is used, interactions with coolants that may create transportable corrosion products, and the potential for high radiation dose rates to personnel.

4.2.4 HBB-T Strain Limits and Creep-Fatigue

ASME Section III Division 5 provides design rules and material data for five materials that operate at high temperatures where creep damage may occur for ANLWRs. These materials must support components operating in the creep regime. The materials currently allowed in Section III-5 are 304 and 316 stainless steel, Ni-Fe-Cr (Alloy 800), 2.25 Cr-1 Mo, and Grade 91 (9Cr-1Mo-V). Alloy 617 (the subject of this review) has now been added to the code in the form of Code Case N-898. The effort to qualify Alloy 617 for use with Section III-5 began circa 2010 with much of the work being done by DOE supported by national labs (mainly ORNL, ANL, and INL for Alloy 617). The code also introduced high temperature constitutive models for some of the materials (with the others to be added) since many new designs will use finite element-

based analysis tools and require use of accurate material models. The visco-plastic material model for Grade 91, with temperature dependent material constants, has been approved by Section 3 and will appear in the 2023 code. Balloting for Alloy 617 and 316H will begin soon and the hope is that these material laws will also appear in the 2023 code. The constitutive model for Alloy 800H is being developed and the hope is that this material will appear in the 2023 code. It is doubtful that the other two materials (2.25Cr-1Mo or 304H) will make the 2023 edition but should in 2025.

The purpose of this effort was to examine the appropriateness of the Alloy 617 code case for possible NRC endorsement. There is currently ongoing pressure to add other materials in future versions of the code as well. This report provides a review of the code case technical design rules in the form of records which describe the rules. The record descriptions along with technical background material were carefully reviewed to provide the assessments. In addition, numerous additional technical reports and publications were also used to augment the review conclusions. For each of the records examined here the references used to make the assessments are provided. A short summary for each new design rule for the additions to HBB-T are provided below.

HBB-T-1300 Strain Limits – Rules for satisfaction of strain limits for Alloy 617 are introduced in HBB-T-1300. Some of the strain limit tests, which can be performed to ensure satisfaction of the limits, are not permitted for Alloy 617 at temperatures higher than 650 C which is a conservative limit. In addition, the simplified EPP analysis methods for satisfying strain limits can be used as an alternative at any temperature. This method is also ensured by invoking the bounding theorems discussed in the Creep-Fatigue record. Full inelastic analysis methods can always be used to satisfy strain design limits for Alloy 617 if the material constitutive rule used is validated. These rules are recommended for endorsement because the methods provide conservative predictions when compared to either test data or full inelastic analysis results as discussed in Section 3.7. Because this material will likely be used at temperatures greater than 650 degrees C for ANLWR components most strain limit rules will be satisfied using the validated EPP methods in the code case or full inelastic analysis.

HBB-T-1400 Creep-Fatigue – Creep and fatigue damage interact, and Code Case N-898 provides the interaction diagram constants and the general creep-fatigue assessment procedures using both elastic and inelastic analysis methods. Multiaxial fatigue rules provide design methods to consider fatigue under multiaxial stress states using a Huddleston equivalent stress approach and the choice of the Huddleston 'C' constant for Alloy 617 also. In addition, the Code Case also provides a procedure for evaluating damage using the alternative EPP creep-fatigue analysis procedure. Mathematical bounding theorems ensure conservative results with the EPP method for Alloy 617. The EPP methods provide a simple alternative procedure for satisfying the rules. Full inelastic analysis methods can always be used to satisfy creep-fatigue design limits. The fatigue design curves are constructed by reducing the best-fit curve of continuous cycling fatigue data by a factor of two on total strain range or a factor of 20 on life, whichever results in a minimum value. This is considered quite conservative and is consistent with the lower temperature rules in Subsection NB. The creep-fatigue rules for Alloy 617 are

recommended for endorsement based on the summaries provided in Sections 3.8. Comparisons of the rules, which include the need for safety factors, with experimental data, show consistent conservative predictions using the code rules. Moreover, the use of the EPP methods is also considered valid as discussed in Section 3.8.5 based on both theoretical reasons and comparisons with test data.

HBB-T-1500 Buckling Limits – The rules for buckling consider time independent and time-dependent buckling and the distinctions between load-controlled conditions, which are most severe, and strain-controlled buckling. Strain-controlled buckling is less severe because compressive buckling stresses relax due to creep. The rules permit use of NB buckling rules when creep buckling is not a concern. Figure HBB-T-1522 provide temperature limit charts which when satisfied, permit use of Subsection NB for the buckling assessment. The validity of these charts was discussed in Section 3.9. When the temperature limit charts are exceeded, the owner must perform inelastic analyses, using the load factors specified in this record for Alloy 617 to ensure that the component does not experience creep buckling over the design life. The method used to perform the inelastic analyses is not specified and is up to the owner. However, it is expected that many vendors will use inelastic finite element analyses, using the proposed constitutive law for Alloy 617, including initial imperfections, to show that creep buckling is not a concern. Based on experimental validation of the buckling rules shown in Section 3.9 the buckling rules were recommended for endorsement.

HBB-T-1800 Isochronous Stress-Strain Curves – The ISSC that were developed for Alloy 617 were thoroughly examined. Some spot checks of these curves are provided with data that were not used in developing the code basis. Moreover, the ISSC proposed for Alloy 617 were shown to provide conservative predictions of stress-time for the allowable temperatures as shown in Section 3.10 and Appendix I where spot checks on the curves were made. The ASME Code has identified a typographical error in the equation for plastic strain in HBB-T-1836. The correct equation is provided in Section I.2 as Equation I-1 and is recommended to be used instead of the equation in Code Case N-898, HBB-T-1836(2)(-b). This is recommended as a limitation on the staff's endorsement of Code Case N-898. With this one limitation, HBB-T-1800 is recommended for endorsement.

5 REFERENCES

- AESJ, 2008 Atomic Energy Society of Japan, "Code on Implementation and Review of Nuclear Power Plant Ageing Management Programs": AESJ-SC-P005E, ISBN: 978-4-89047-420-2
- ANL, 2021 ANL/AMD-21/1, Historical Context and Perspective on Allowable Stresses and Design Parameters in ASME Section III, Division 5, Subsection HB, Subpart B dated March 2021 (ADAMS Accession No. ML21090A033).
- API, 2017 Material, Fabrication, and Repair Considerations for Austenitic Alloys Subject to Embrittlement and Cracking in High Temperature 565 degrees C to 760 degrees C (1050 degrees F to 1400 degrees F) Refinery Services API Technical Report 942-B First Edition, May 2017, Effective Date November 1, 2017
- ASME, 2016 Code Case N-872, "Use of 52Ni-22Cr-13Co-9Mo Alloy 617 (UNS N06617) for Low Temperature Service Construction, Section III, Division 5. (Approval Date: October 20, 2016)
- ASME, 2019 Code Case N-898, "Use of Alloy 617 (UNS N06617) for Class A Elevated Temperature Service Construction, Section III, Division 5." (Approval Date: October 6, 2019)
- ASME, 2021a ASME Boiler and Pressure Vessel Code, Section I, Rules for Construction of Power Boilers, 2021, American Society of Mechanical Engineers, New York, NY
- ASME, 2021b ASME Boiler and Pressure Vessel Code, Section VIII, Rules for Construction of Pressure Vessels, 2021 American Society of Mechanical Engineers, New York, NY
- ASTM, 2021 ASTM E1875-20a, "Standard Test Method for Dynamic Young's Modulus, Shear Modulus, and Poisson's Ratio by Sonic Resonance," American Society for Testing and Materials, March 2021.
- Becht, 1989 Becht, C. (1989). "Behavior of Pressure-Induced Discontinuity Stresses at Elevated Temperature," *ASME Journal of Pressure Vessels and Piping*, Volume 111, pp. 322–325.
- BEGL (R5), 2008 BEGL, "An Assessment Procedure for the High Temperature Response of Structures", British Energy Generation Ltd., R5 Issue 3, 2008.
- Berman, et. al, 1976 Berman, I., and Gupta, G.D. (1976). "Buckling Rules for Nuclear Components," *Journal of Pressure Vessel Technology*, Vol. 98, Series J, No. 3, pp. 229–231.

- Bree, 1967 Bree, J. (1967). "Elastic-Plastic Behavior of Thin Tubes Subjected to Internal Pressure and Intermittent High-Heat Fluxes with Applications to Fast Nuclear Reactor Fuel Elements," *Journal of Strain Analysis*, Vol. 2, No. 3.
- Bree, 1968 Bree, J. (1968). "Incremental Growth Due to Creep and Plastic Yielding of Tubes Subjected to Internal Pressure and Cyclic Thermal Stresses," *Journal of Strain Analysis*, Vol. 3, No. 2.
- Cabet et. al, 2013 Cabet, C., Carroll, L., and Wright, R. C., (2013), "Low Cycle Fatigue and Creep-Fatigue Behavior of Alloy 617 at High Temperature", *Journal of Pressure Vessel Technology*, 135(6):061401, 2013.
- Carroll, et. al, 2013a Carroll, L. J., Cabet, C., Carroll, M. C., and Wright, R. N., (2013) "The development of microstructural damage during high temperature creep-fatigue of a nickel alloy," *International Journal of Fatigue*, Vol. 47, pp. 115 125.
- Carroll, et. al, 2013b Carroll, M. C., and Carroll, L. J., (2013), "Developing Dislocation Subgrain Structures and Cyclic Softening During High-Temperature Creep-Fatigue of a Nickel Alloy," *Metallurgical and Materials Transactions*, Vol. 44, No. 8, pp. 3592 3607.
- Carter et. al, 2016 Carter, P., Sham, T. L., and Jetter, R. I., (2016), "Overview of Proposed High Temperature Design Code Cases", *Proc. ASME 2016 PVP conference*, Vancouver, BC, Paper PVP2016-63559.
- Carter, 1985 Carter, P. (1985). "Bounding Theorems for Creep Plasticity," *Int. J. Solids and Structures*, Vol. 21, No. 6, pp. 527-543.
- Carter et. al, 1997 Carter, P. (1997). "Bounding Theorems, Extremum Principles and Convexity," *Recent Developments in Computational and Applied Mechanics* (B.D. Reddy, ed.), CIMNE, Barcelona, Spain.
- Carter, 2005 Carter, P. (2005a). "Analysis of Cyclic Creep and Rupture. Part 1: Bounding Theorems and Cyclic Reference Stresses," *Int. J Press & Piping*, Vol. 82, pp. 15-26.
- Carter et. al, 2011 Carter, P., Sham, T.-L., and Jetter, R.I. (2011). "Simplified Analysis Methods for Primary Load Designs at Elevated Temperatures," *Proc. ASME PVP Conference*, Baltimore, MD, paper PVP2011-57074.
- Carter et. al, 2012a Carter, P., Jetter, R.I., and Sham, T.-L. (2012a). "Application of Elastic-Perfectly Plastic Cyclic Analysis to Assessment of Creep Strain," *American Society of Mechanical Engineers, Pressure Vessels and Piping Division (Publication) PVP*, PVP Paper No. 2012-78082, 1:749-760.

- Carter et. al, 2012b Carter, P., Jetter, R.I., and Sham, T.-L. (2012b). "Application of Shakedown Analysis to Evaluation of Creep-Fatigue Limits," *American Society of Mechanical Engineers 2012 Pressure Vessel and Piping Conference, July 15–19, 2012*, PVP Paper No. 2012-78083, pp. 761–770.
- Carter et. al, 2016 Carter, P., Sham, T.-L., and Jetter, R.I. (2016). "Overview of Proposed High Temperature Design Code Cases," *Proc. ASME PVP 2016*, Vancouver, BC, paper PVP2016-63559.
- Chen et. al. 2010 B. Chen, D. J. Smith, M.W. Spindler, P.E. Flewitt, "Effect of Thermal-Mechanical History on Reheat Cracking in 316H Austenitic Stainless Steel Weldments," PVP2010-25088, in Proceedings of the ASME 2010 Pressure Vessels & Piping Division / K-PVP Conference PVP2010 July 18-22, 2010, Bellevue, Washington, USA.
- Clinard, 1979 Clinard, J.A. (1979). "Analytical Investigation of the Applicability of an Isochronous Method for Predicting Creep Deformations in Structures at Elevated Temperatures," ORNL/TM-6673, Oak Ridge National Laboratory, Oak Ridge, TN.
- Colwell et. al, 2020 Colwell, Richard, Shargay, Cathleen, "Alloy 800H: Material and Fabrication Challenges associated with the Mitigation of Stress Relaxation Cracking," PVP2020-21842, in Proceedings of the ASME 2020 Pressure Vessels & Piping Conference.
- Corum et. al, 1991 J. M. Corum and J. J. Blass, "Rules for Design of Alloy 617 Nuclear Components to Very High Temperatures," ASME PVP Vol. 215, American Society of Mechanical Engineers, New York, NY, 1991, p.147.
- Datta, et. al, 1991 Datta, A.K., Roche, R.L., and Nagate, T. (1991). "Recommended Practices in Elevated Temperature Design: A Compendium of Breeder Reactor Experiences (1970–1987)," Volume III, "Inelastic Analysis," *WRC Bulletin 365*, Welding Research Council, New York, NY.
- Dewa et. al, 2018 Dewa, R. T., Park, J. H., Kim, S. J., and Lee, S. Y., (2018), "High Temperature Creep-Fatigue Behavior of Alloy 617", *Metals*, 8, 103, pp 1-15.
- EPRI, 2010 Cobalt Reduction Sourcebook, EPRI Product ID 1021103, December 21, 2021, Electric Power Research Institute, Palo Alto, CA.
- Frederick, et. al, 1966 Frederick, C.O., and Armstrong, P.J. (1966). "Convergent Internal Stresses and Steady Cyclic States of Stress," *Journal of Strain Analysis*, Vol. 1, No. 2.

- Gerard, 1962 Gerard, G., (1962), "A Unified Theory of Creep Buckling of Columns, Plates, and Shells," *Proc. International Council Aero. Sci.*, Third Congress, Stockholm-1962, Spartan Books Inc., Washington, D.C.
- Gerdeen et. al, 1973 Gerdeen, J. C. and Sazawal, V. K., (1973), "A Review of Creep Instability in High-Temperature Piping and Pressure Vessels," *Welding Research Council Bulletin 195*, 1973.
- Goodall et. al, 1979 Goodall, I.W., Leckie, F.A., Ponter, A.R.S., and Townley, C.H.A. (1979). "The Development of High Temperature Design Methods Based on Reference Stress and Bounding Theorems," *J. Eng. Materials and Technology*, Vol. 101, pp. 349–355.
- Griffin, 1980 Griffin, D.S. (1980). "Design Limits for Creep Buckling of Structural Components," *Creep in Structures, 3rd IUTAM Symposium*, pp. 331–348, Leicester, United Kingdom.
- Griffin, 1996 Griffin, D.S. (1996). "Temperature Limits for ASME Boiler & Pressure Vessel Code External Pressure Design Charts," Report from Pressure Vessel Research Council (PVRC) on Grant 92–06.
- Griffin, 1999 Griffin, D. S. "Design Limits for Elevated-Temperature Buckling." In *Welding Research Council Bulletin 443 External Pressure: Effect of Initial Imperfections and Temperature Limits*, pp. 11-26, 1999.
- Hilburger et. al, 2018 Mark W. Hilburger, Michael C. Lindell, William A. Waters, and Nathaniel W. Gardner. 2018, "Test and Analysis of Buckling-Critical Stiffened Metallic Launch Vehicle Cylinders", AIAA/ASCE/AHS/ASC Structures, Structural Dynamics, and Materials Conference, AIAA SciTech Forum, (AIAA 2018-1697).
- Huddleston, 1984 Huddleston, R.L. (1984). "An Improved Multiaxial Creep-Rupture Strength Criterion," *Trans ASME*, Vol. 107, pp. 313–338.
- Huddleston, 1993 Huddleston, R.L. (1993). "Assessment of an Improved Multiaxial Strength Theory Based on Creep-Rupture Data for Type 316 Stainless Steel," *Trans ASME, Journal of Pressure Vessel Technology*, pp. 177–184.
- Huddleston, 2003 Huddleston, R. L., (2003), "Two-Parameter Failure Model Improves Time Independent and Time Dependent Failure Predictions", Lawrence Livermore National Laboratory report, UCRL-TR-202300.
- INL, 2021a Wright, Richard, "Draft ASME Boiler and Pressure Vessel Code Cases and Technical Bases for Use of Alloy 617 for Construction of Nuclear Components Under Section III, Division 5," INL/EXT-15-36305, Revision 2, December 2021, Idaho National Laboratory, Idaho Falls, Idaho <https://doi.org/10.2172/1836553>

INL, 2021b Appendix 3, Background for Draft Code Case: Use of Alloy 617 (UNS N06617) for Low Temperature Service Construction, to Wright, Richard, "Draft ASME Boiler and Pressure Vessel Code Cases and Technical Bases for Use of Alloy 617 for Construction of Nuclear Components Under Section III, Division 5," INL/EXT-15-36305, Revision 2, December 2021, Idaho National Laboratory, Idaho Falls, Idaho <https://doi.org/10.2172/1836553>

INL, 2021c Appendix 5, Background for Draft Code Case: Use of Alloy 617 (UNS N06617) For Class A Elevated Temperature Service Construction, to Wright, Richard, "Draft ASME Boiler and Pressure Vessel Code Cases and Technical Bases for Use of Alloy 617 for Construction of Nuclear Components Under Section III, Division 5," INL/EXT-15-36305, Revision 2, December 2021, Idaho National Laboratory, Idaho Falls, Idaho <https://doi.org/10.2172/1836553>

INL, 2021c contains the following individual background documents:

(Note, INL, 2021d through k are individual background documents in the Background Document – Record No. 16-994)

INL, 2021d	Background – Table HBB-1-14.1(a) Permissible Base Materials for Structures other than Bolting
INL, 2021e	Background – Table HBB-I-14.1(b) Permissible Weld Materials
INL, 2021f	Background – HBB-3225-1 Tensile Strength Values, S_u , for Alloy 617 and HBB-I-14.5 Yield Strength Values, S_y , for Alloy 617
INL, 2021g	Background – Allowable Stress Values
INL, 2021h	Background Document – HBB-I-14.10F-1 Stress Rupture Factors for Welded Alloy 617
INL, 2021i	Background – HBB-4800 Relaxation Cracking
INL, 2021j	HBB-3225-2 Tensile and Yield Strength Reduction Factor Due to Long Time Prior Elevated Temperature Service
INL, 2021k	Background – HBB-4212 Effects of Forming and Bending Processes
INL, 2021l	Background Document – Physical Property Tables for Alloy 617 (Record No. 16-995)
INL, 2021m	Background Document – Modulus of Elasticity Tables for Alloy 617 (Record No. 16-995)

INL, 2021n	Background Document – Record No. 16-996
INL, 2021o	Background Document – Record No. 16-997
INL, 2021p	Background Document – Record No. 16-998
INL, 2021q	Background Document – Record No. 16-999
INL, 2021r	Background Document – Record No. 16-1000
INL, 2021s	Background Document – Record No. 16-1001
IRSN, 2010	Radionuclide Fact Sheet – Cobalt-60 and the Environment, 11/10/201, Institut De Radioprotection et de Surete Nucleaire (IRSN).
JAERI, 2010	JAERI, "Design of High Temperature Engineering Test Reactor," JAERI-1332, 1994.
Jawad et. al, 2009	Jawad, M.H., and Jetter, R.I. (2009). <i>Design and Analysis of ASME Boiler and Pressure Vessel Components in the Creep Range</i> , ASME Press, New York, NY.
Jawad et. al, 2016	Jawad, M., Swindeman, R., Swindeman, M., and Griffin, D. (2016). "Development of Average Isochronous Stress-Strain Curves and Equations and External Pressure Charts and Equations for 9Cr-1Mo-V Steel," Report STP-PT-080, ASME Standards Technology, LLC.
Jetter, 1976	Jetter, R.I. (1976). "Elevated Temperature Design—Development and Implementation of Code Case 1592," <i>Journal of Pressure Vessel Technology</i> , Vol. 98, Series J, No. 3, pp. 222–229.
Jetter et. al, (2004)	Jetter, R. I., and McGreevy, T. E., "Simplified Design Criteria for Very High Temperature Applications in Generation IV Reactors", Oak Ridge National Laboratory report, ORNL/TM-2004/308.
Jetter et. al, 2011	Jetter, R.I., Sham, T.L., and Swindeman, R.W. (2011). "Application of Negligible Creep Criteria to Candidate Materials for HTGR Pressure Vessels," <i>Journal of Pressure Vessel Technology</i> , Vol. 133.
Jetter, 2017	Jetter, R.I. (2017). "Division 5—High-Temperature Reactors," in Rao, K.R. (ed.), <i>Companion Guide to ASME Boiler & Pressure Vessel Codes</i> , Fifth Edition, Volume 1, Chapter 17, pp. 17-1 to 17-43, ASME Press, New York, NY.
Kan, 2019	Kan, K., et al (2019), "Assessment of Creep Damage Models in the Prediction of High-Temperature Creep Behavior of Alloy 617", <i>Int. J. of Pressure Vessels and Piping</i> , Vol. 177.
Kim et. al., 2013	Kim, W., Lee, G., Park, J., Hong, S., Kim, Y., "Creep and Oxidation Behaviors of Alloy 617 in Air and Helium Environments at 1173 K," 6 th

- International Conference on Creep, Fatigue and Creep-Fatigue Interaction (CF-6)
- Knezevic, 2013 Knezevic, V., Schneider, A., and Landier, C., (2013), "Creep Behaviour of Thick-Wall Alloy 617 Seamless Pipes for 700 degree C Power Plant Technology", *Procedia Engineering* 55, pp 240-245.
- Leckie, 1974 Leckie, F.A. (1974). "A Review of Bounding Techniques and Shakedown and Ratcheting at Elevated Temperature," WRC Bulletin No. 195, Welding Research Council, New York, NY.
- Livingston, 1987 Livingston, J. M., (1987), "Creep Buckling Design Limits for Hollow Circular Cylinders Under Axial Compression and External Pressure," MS Thesis, Univ. of Pittsburgh, Pittsburgh, PA.
- Marriott, 2011 Marriott, D. (2011). "Isochronous Stress/Strain Curves—Origins, Scope and Applications," *Proc. ASME 2011 PVP Conference*, Paper PVP2011-57130, Baltimore, MD.
- McCoy et. al, 1985 McCoy, H.E., and King, J.F. (1985). "Mechanical Properties of Inconel 617 and 618," ORNL/TM-9337, Oak Ridge National Laboratory, Oak Ridge, TN.
- McMurtrey, et. al, 2018 McMurtrey, M. D., Messner, M., and Barua, B., (2018), "Continuation Report: Creep-fatigue Behavior and Damage Accumulation of a Candidate Structural Material for Concentrating Solar Thermal Receiver", INL Report, INL/EXT-18-52306-Revision 0.
- Messner et. al, 2018 Messner, M.C., Phan, V.T., and Sham, T.L. "A Unified Inelastic Constitutive Model for the Average Engineering Response of Grade 91 Steel," *Proc. ASME PVP Conference*, Paper PVP2018-84104, Prague, Czech Republic.
- Messner et. al, 2019 Messner, M.C., Phan, V.T., and Sham, T.L. "Evaluating and Modeling Rate Sensitivity in Advanced Reactor Structural Materials: 316H, Gr. 91, and Alloy 617," *International Journal of Pressure Vessels and Piping*, Vol. 178, 103997.
- Messner et. al, 2021 Messner, M. C., and Sham, T. L., (2021), "Reference Constitutive Model for Alloy 617 and 316H stainless steel for use with the ASME Division 5 Design by Inelastic Analysis Rules", Argonne National Laboratory Report ANL-ART-225.
- Mo et. al., 2011 Mo, K., Lovicu, G., Tung, H., Chen, X., Stubbins, J., "High Temperature Aging and Corrosion Study on Alloy 617 and Alloy 230, *Journal of Engineering for Gas Turbines and Power*, Vol. 133/052908-1, 2011, ASME

- Narayanan, et. al, 2017 Narayanan, A., Dubey, K., Davies, C. M., and Dear, J. P., (2017), "The creep of Alloy 617 at 700degrees C: Material Properties, Measurement of Strain and Comparison Between Finite Element Analysis and Digital Image Correlation", *International Journal of Solids and Structures* 129, pp195-203.
- NRC, 2021a DG-1380, "Acceptability of ASME Code, Section III, Division 5, High Temperature Reactors," draft for public comment, August 31, 2021 (ADAMS Accession No. ML21091A276).
- NRC, 2021b NUREG-2245, "Technical Review of the 2017 Edition of ASME Code, Section III, Division 5, High Temperature Reactors," Draft for Public Comment, August 31, 2021 (ADAMS Accession No. ML21223A097)
- O'Donnell, et. al, 1974 O'Donnell, W.J., and Porowski, J.S. (1974). "Upper Bounds for Accumulated Strains Due to Creep Ratcheting," *Trans ASME, Journal of Pressure Vessel Technology*, Vol. 96.
- Penny et. al, 1995 Penny, R.K. and D.L. Marriott (1995). *Design for Creep*, Second Edition, Chapman and Hall.
- Porowski, et. al, 1979 Porowski, J.S., and O'Donnell, W.J. (1979). "Creep Ratcheting Bounds Based on Elastic Core Creep Concept," *Transactions of 5th International SMiRT*, Vol. L.
- Pritchard et. al, 2013 Pritchard, P. G., Carroll, L., and Hassan, T., (2013), "Constitutive Modeling of High Temperature Uniaxial Responses of Alloy 617," *Transactions of the American Nuclear Society*, Vol 109, pp. 562-565.
- Rabin et. al, 2013 "Thermophysical Properties of Alloy 617 from 25 to 1000degrees C", B. H. Rabin, W. D. Swank and R. N. Wright, *Nuclear Engineering and Design Journal*, vol. 262, p. 72, 2013
- Rao, 2017 Rao, K.R. (ed.) (2017). *Companion Guide to the ASME Boiler and Pressure Vessel Code*, Fifth Edition, ASME Press, New York, NY.
- RCC-MR, 2002 RCC-MRx Code, "Design and Construction Rules for Mechanical Components of FBR Nuclear Islands and High Temperature Applications, Appendix A16: Guide for Leak Before Break Analysis and Defect Assessment", AFCEN, Appendix A16, 2002.
- Robinson, 1984 Robinson, D., N., "Constitutive Relationships for Anisotropic High Temperature Alloys," *Nuclear Engineering and Design*, 83 (1984), pp. 389-396.
- Sartory, 1989 Sartory, W.K. (1989). "Effect of Peak Thermal Strain on Simplified Ratcheting Analysis Procedures," PVP–Vol. 163, "Structural Design for Elevated Temperature Environments—Creep, Ratchet, Fatigue, and Fracture," Book No. H00478-1989.

- Schulze et. al, 1977 Schulze, R. and Seehafer, H.-J., (1977), "Creep Buckling Analysis of Cylindrical HTR-Components," *Transactions of the 4th International Conference on Structural Mechanics in Reactor Technology*, Vol. L, San Francisco.
- Severud, 1978 Severud, L.K. (1978). "Background to the Elastic Creep-Fatigue Rules of the ASME B&PV Code Case 1592," *Nuclear Engineering and Design*, Vol. 45, pp. 449–455.
- Severud, 1991 Severud, L.K. (1991). "Creep-Fatigue Assessment Methods Using Elastic Analysis Results and Adjustments," *Transactions of the ASME*, Vol. 113, pp. 34–40.
- Sham et. al, 2015 Sham, T. L., Jetter, R. I., Hollinger, G., Pease, D., Carter, P., Pu, C., and Wang, Y., (2015), "Report on FY15 Alloy 617 Code Rules Development", ORNL yearly report ORNL/TM-2015/487.
- Sjodahl, 1978 L. H. Sjodahl, "A Comprehensive Method of Rupture Data Analysis With Simplified Models," in *Characterization of Materials for Service at Elevated Temperatures*, New York, NY: American Society of Mechanical Engineers, 1978, pp. 501–516.
- Special Metals, 2005 Special Metals Corporation, "Inconel Alloy 617" Publication Number SMC-029, 2005
- Tung et. al, 2014 David C. Tung, John C. Lippold, "Modeling a Stress Relaxation Cracking Test for Advanced Ultra Supercritical Alloys," in *Advances in Materials Technology for Fossil Power Plants*, Proceedings from the Seventh International Conference, October 22-25, 2013, Waikoloa, Hawaii, 2014, D. Gandy, J. Shingledecker, editors. Electric Power Research Institute, Inc. distributed by ASM International
- Turk et. al., 2020a Turk, R., Brust, F. W., Wilkowski, G., Krishnaswamy, P. , "Technical Input for the US NRC Commission Review of the 2017 Edition of the ASME Boiler and Pressure Vessel Code, Section III, Division 5, High Temperature Reactors: HBB-T, HBB-II, HCB-II, Nd HCB-III for Metallic Components", Technical Letter Report, NRC ADAMS Accession number ML20349A003, December.
- Turk, et. al., 2020b Turk, R., Brust, F. W., Wilkowski, G., Krishnaswamy, P. "Technical Input for the US NRC Commission Review of the 2017 Edition of the ASME Boiler and Pressure Vessel Code, Section III, Division 5, High Temperature Reactors: Review of Code Case N-861 and N-862: Elastic-Perfect Plastic Methods for Satisfaction of Strain Limits and Creep-Fatigue Damage Evaluation in SECTION III-5 Rules", Technical Letter Report, NRC ADAMS Accession number ML20349A002, December.

Van Zanten, 2017 Van Zanten, P., (2017), "Thermal Cycling and Creep Behavior of Alloy 617 Behavior of Alloy 617 Boiler Components", Master's Thesis, Delft University of Technology, The Netherlands.

VDM, 2021 Manufacturer's Data Sheet for VDM^R Alloy 617 (Nicrofer 5,520 Co), Material Data Sheet No. 4,119, Revision 01, July 2021

Wright et. al, 2012 Wright, j. K., Carroll, L. J., Cabet, C., Lillo, T. M., Benz, J. K., Simpson, J.A. Lloyd, W. R., Chapman, J. A., and Wright, R. N., (2012), "Characterization of Elevated Temperature Properties of Heat Exchanger and Steam Generator Alloys", Nuclear Engineering and Design, 251m 252-260.

Wright et al, 2013a Wright et al, "Low Cycle Fatigue of Alloy 617 at 850 and 950C", Proceedings of ASME 2016 PVP conference, Vancouver, BC, paper PVP2016-63704.

Wright et al, 2013b Wright, J. K., Carroll, L. J., and Sham, T. L., "Determination of the Creep-Fatigue Interaction Diagram For Alloy 617", Journal of Engineering Materials and Technology, Vol. 135.

Wright et al, 2013c Wright, J. K., Lybeck, N. J., and Wright, R. N., (2013b), "Tensile Properties of Alloy 617 Bar Stock." Technical report, Idaho National Laboratory, INL/EXT-13-29671, 2013.

Wright et. al, 2016 Wright, J. K., Carroll, L. J., Sham, T. L., Lybeck, N. J., Wright, R. N., (2016), "Determination of the Creep-Fatigue Interaction Diagram For Alloy 617", Proceedings of ASME 2016 PVP conference, Vancouver, BC, paper PVP2016-63704.

Wright et al, 2018 Wright et al, "Creep and Creep-Rupture of Alloy 617", Nuclear Engineering and Design, Volume 329, April, Pages 142 – 146.

Wu et. al 2008 Q. Wu, H. Song, R. W. Swindeman, J. P. Shingledecker, and V. K. Vasudevan, "Microstructure of Long-Term Aged IN617 Ni-Base Superalloy," *Metallurgical Transactions*, Vol. 39A, 2008, pp. 2569-2585.

Shoemaker et al, 2007 Lewis E. Shoemaker, Gaylord D. Smith, Brian A. Baker and Jon M. Poole, "Fabricating Nickel Alloys to Avoid Relaxation Cracking" Proc. Corrosion 2007, NACE International, Paper No. 07421.

Suzuki et. al, 2011 Suzuki, K., Asayama, T., Swindeman, R. W., and Marriott, D. L., (2011) "New Materials For ASME Subsection NH", ASME LLC report STP-NU-042

Van Wortel et al., 2007 Hans van Wortel, "Control of Relaxation Cracking in Austenitic High Temperature Components" Proc. Corrosion 2007, NACE International, Paper No. 07423.

Yukawa, 1991

Yukawa, S., (1991), "Elevated Temperature Fatigue Design Curves for Alloy 617", 1st JSME/ASME Joint International Conference on Nuclear Engineering, Tokyo, Japan.

APPENDIX I

MATERIAL PROPERTY ASSESSMENT OF ISSC FOR ALLOY 617

This appendix examines the material data used to develop the ISSC listed in HBB-T-1820. As shown in Figure I-1, the curves are constructed from total strain data (elastic, plastic, and creep - top of Figure I-1) where the stresses are picked off at constant time values (isochronous or “constant time”) and plotted as seen on the bottom illustration in the figure. Starting with the 2021 version of Section III-5 the equations for each curve are shown for each material (five original materials) in HBB-T-1830 and the Alloy 617 curves and equations are shown in HBB-T-1836 in Code Case N-898 along with plots of the curves up to 954 degrees C. Such curves are plotted at various temperatures as seen in HBB-T-1836 of the record with a set of curves for each temperature of interest in the design.

The isochronous stress-strain curve is a long-established method of representing creep data in a manner that, under certain circumstances, provides a quick and often surprisingly accurate approximate solution to time-dependent structural problems. Indeed, it is another legacy-based procedure which was practical to use before the use of numerical methods which provide predictions using advanced constitutive material laws. Despite criticisms of the foundations of the method, it has survived over the years because it has either been the only method feasible at the time, or it is capable of providing solutions that are often good enough for engineering purposes. The alternative is to use full inelastic analysis where an accurate visco-plastic constitutive model is used within the context of nonlinear finite element modeling. Such analyses are possible today by some of the vendors who have access to high-performance computing power.

Marriott, 2011 provides an excellent overview of the life prediction methods based on isochronous stress-strain curve approaches and corresponding justification and validation. These methods permit creep analyses to be performed by using the isochronous stress-strain, defined for a given temperature and hold time, by performing a pseudo ‘elastic-plastic’ analysis using the appropriate curve. Comparison of predictions using the ISSC approach with full inelastic analysis are discussed by Marriott (see references cited therein). Several efforts over the years have shown that the use of isochronous curves to estimate total creep strains is reasonable and can provide conservative predictions (e.g., Clinard, 1979) by comparing predictions made using this approach to full elastic-plastic-creep finite element models. An isochronous curve simply presents, in a plot of stress against strain, the locus of total strains accumulated when different constant stresses are applied for a fixed time.

The curves have been traditionally used over the years graphically, and this is the case in the 2021 Edition of the ASME Code and in INL, 2021o. However, the 2021 ASME Code also include equations that will permit the use of either the graphical curves or the equations as desired. Use of equations will be preferred as visual interpolation between curves can be difficult for arbitrary times, temperatures, stresses, and strains by designers. It is noted that the

US NRC now has software (ASME Section III, Division 5 Design Tool Software*) which incorporates the Code Case N-898 equations for their future licensing assessments.

The remainder of this appendix discusses the isochronous curves in HBB-T-1836 for Alloy 617 provided in INL, 2021o. The code's ISSC are compared to other data to verify the conservative nature of the code as well. The isochronous stress-strain curves include elastic, plastic, and creep strains. Because creep data are highly variable with a large statistical scatter, the validation provided relies on some interpretation by the ISSC developers.

The isochronous curves in the code are meant to be "average" curves or represent data averaged over different tests. However, in reality, parts of the curves were developed from only a few sets of data. In general, as shown below, this review considers all the isochronous curves in INL, 2021o to be conservative and adequate. For Alloy 617 the maximum time permitted is 100,000 hours rather than 300,000 permitted for the other five code materials.

To develop the comparisons in the rest of this appendix, a spreadsheet was developed that can produce the isochronous curves for any temperature and time for Alloy 617. This spreadsheet will be provided to the U.S. NRC staff so that, during license review, HBB rules, many of which rely on isochronous curves, can easily be assessed.

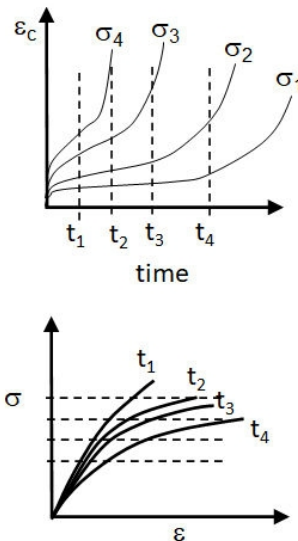


Figure I-1 Schematic of isochronous stress-strain curves

* For information the ASME Section III, Division 5 Design Tool Software, go to <https://www.nrc.gov/about-nrc/regulatory/research/safetycodes.html> and for information on obtaining the software, see <https://www.nrc.gov/about-nrc/regulatory/research/obtainingcodes.html>

I.1 Alloy 617 Data Source

INL, 2021o provides the equations that are used to develop the isochronous stress-strain curves in Figures HBB-T-1836. ISSCs are meant to provide the total strain (elastic, plastic, and creep) as a function of stress, time, and temperature for Alloy 617. These curves are used to meet the deformation-controlled design quantities for Appendix HBB-T. The curves are also used to estimate stress relaxation which occurs during load hold times for creep-fatigue assessment. The data were developed in a series of reports and papers published by INL as well as use of appropriate data from the literature. The data are meant to represent average experimentally measured stress versus strain and assume additive decomposition of the strains into elastic, plastic, and creep. The ISSCs were developed at temperatures from 800-1750 degrees F (425 - 954 degrees C) at 50 degree F (28 degree C) intervals, which is rather extensive compared to some of the other materials in the code.

Here a direct comparison of the ISSC equations to the data and curves in the code case is provided. It is noted that the work hardening behavior of Alloy 617 above 1,382 degrees F (750 degrees C) changes from a Ramberg-Osgood to Voce flow model where the distinction between plasticity and creep does not occur. However, as discussed above, the Alloy 617 code case has chosen this temperature to be 1,200 degrees C (650 degrees C) to provide more conservatism in the high temperature design rules. Much of the creep data for Alloy 617 was collected from tests on the same heat of material and the data are not extensive. Therefore, the limited INL creep data from essentially one heat of material was augmented with additional data found in the literature using simplified metrics (for instance using average creep rates reported to a given creep strain up to 2%). The additional data used to augment the data were obtained from Huntington Special Metals (the main producer of Alloy 617) and older data developed by Oak Ridge National Laboratory (ORNL). Therefore, some additional data validation is provided from different literature data found by the authors. The procedure for this is described in the background document and is based on a Kocks-Mecking diagram and is considered adequate for this purpose. The gamma precipitation aging effect on creep at temperatures above 1,382 degrees F (750 degrees C) is discussed in detail in INL, 2021o and is considered adequate. This is considered adequate although the additional data were specifically referenced in INL, 2021o were provided directly to the ISSC developers prior to publication.

Much of the original ORNL data was reported in McCoy et. al., 1985 for Alloy 617 base and weld metal and included the effects of aging for 20,000 hours. Three heats of material were tested. Elastic-plastic and creep data were obtained at 1,099, 1200, 1300, 1400 and 1,600 degrees F (593, 649, 704, 760, and 871 degrees C) under as received and after aging with some limited data on Alloy 617 welds also summarized. In addition, Corum et. al., 1991 also presents data that apparently were not used for the data set for ISSC curves here. Corum and Blass (Corum et. al., 1991) developed an early code case for Alloy 617 that was never approved at that time because approval efforts from ASME Code committees were stopped because of termination of the associated Very High Temperature Reactor programs at that time as discussed in the INL white paper (2012).

The INL data were developed from a number of reports and papers developed by the team led by Wright (2013 and the other references cited therein) with much higher temperature data 1742-1832 degrees F (750 C-1,000 degrees C) summarized in Kan et. al., 2019 in their assessment of the R5 type ductility exhaustion models. The data source for Alloy 617 also is described in Carroll et. al., 2013a, Carroll et. al., 2013b, Pritchard et. al., 2013, and the many references provided therein along with INL, 2021o. Messner et. al., 2019 also describes the development of the Alloy 617 ISSC curves.

In addition, the material data and Alloy 617 constitutive and creep response can also be observed in Messner et. al., 2019 and Messner et. al., 2021 (and references cited therein) during the development of the advanced visco-plastic constitutive that will be included in the 2023 version of Section III-5.

I.2 Alloy 617 Curves Validation

HBB-T-1836 provides the equations for the elastic, plastic, and creep strains which are used to produce the ISSC curves in the record. An error in the plastic strain definition (the term $1/\delta$ should be negative) has been identified and is being tracked under ASME Code Record No. 21-1256. For completeness the corrected equation only affects the plastic strain term in HBB-T-1836 for temperatures higher than 1,382 degrees F (750 degree C) in (2) (-b) as shown below in Equation I-1:

$$\text{for } \sigma > \sigma_1, \varepsilon_p = -\frac{1}{\delta} \ln\left(1 - \frac{\sigma - \sigma_1}{\sigma_p - \sigma_1}\right) \quad \text{[I-1]}$$

Since Code Case N-898 may not be revised to correct this error prior to the publication of this TLR, the staff recommends a limitation on Code Case N-898 that HBB-T-1836, Equation (2)(-b) should be replaced by the equation above.

The ISSC curves were reproduced and compared directly with the curves in INL, 2021o. Some of these will be shown below along with some limited data showing that the curves match other data as well. An example curve with comparisons to the code curves are shown in Figures I-2 to I-4 for 1,099, 1400, and 1,749 degrees F (593, 760, and 954 degrees C), respectively. These figures show the ISSC curves from the code case to the curves developed from the spreadsheet and they lay on top of each other verifying the mathematical equations provided in the code case. In the following ISSC plots 'E+P' represents the hot tensile curve (no creep) and 'E+P+C' included creep effects and depends on time.

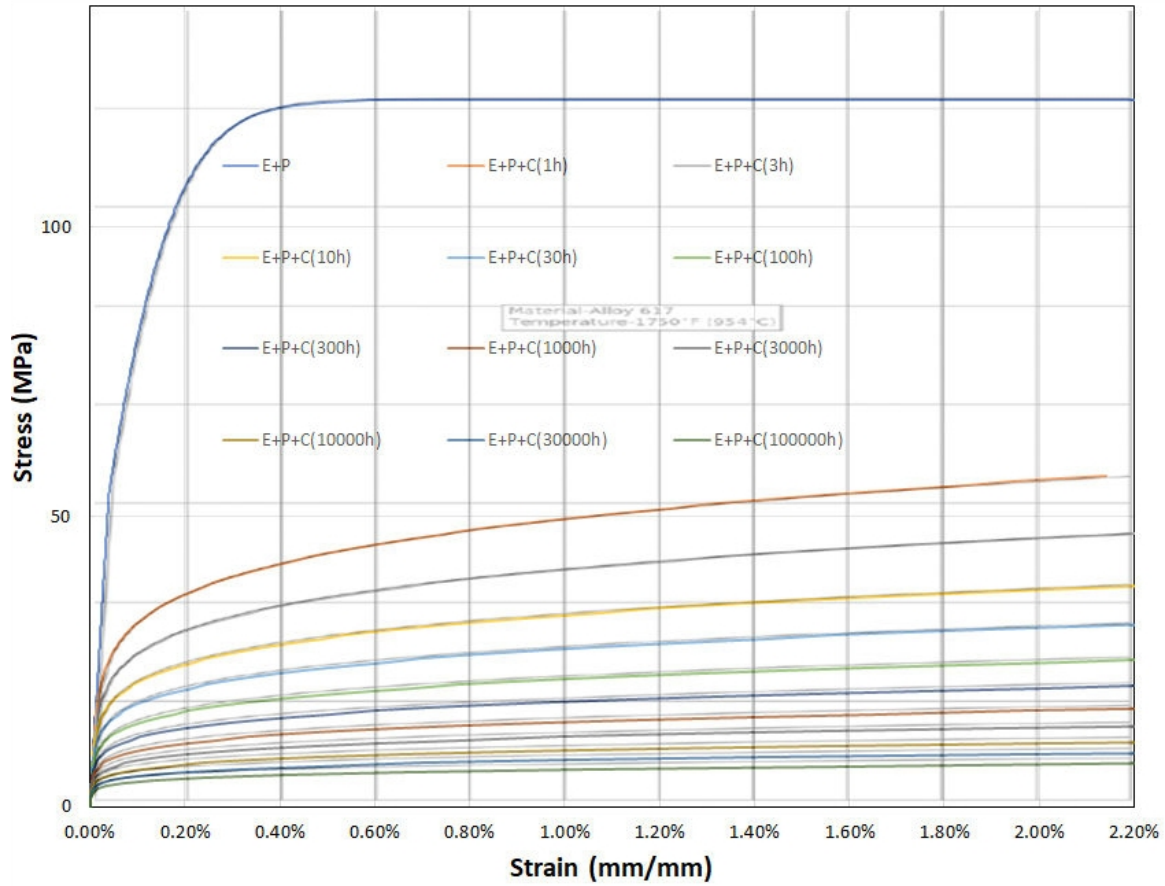


Figure I-2 Calculated ISSC for Alloy 617 at 1,749 degrees F (954 degrees C).

The calculated isochronous stress-strain curve is in color and the Record number curve is in gray. They are identical and on top of each other.

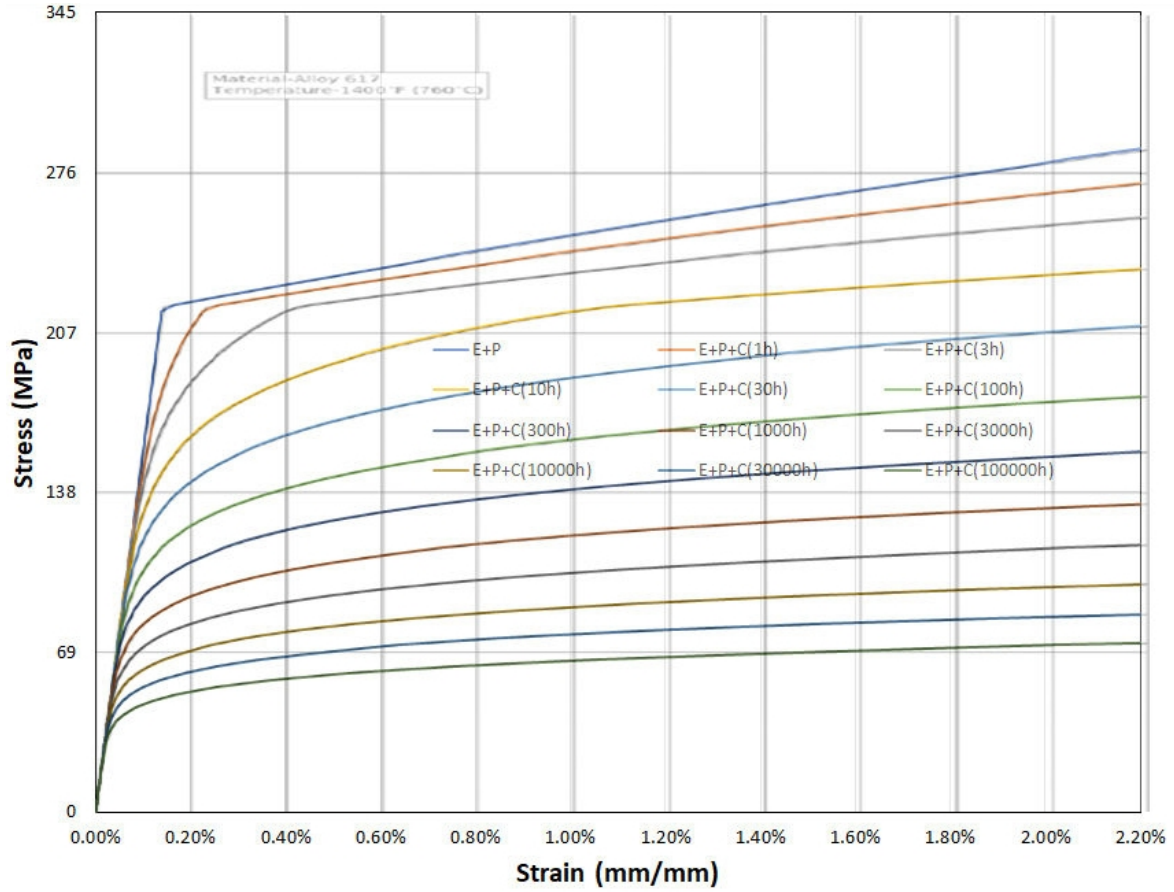


Figure I-3 Calculated ISSC for Alloy 617 at 1,400 degrees F (760 degrees C).

The calculated isochronous stress-strain curve is in color and the Record number curve is in gray. They are identical and on top of each other.

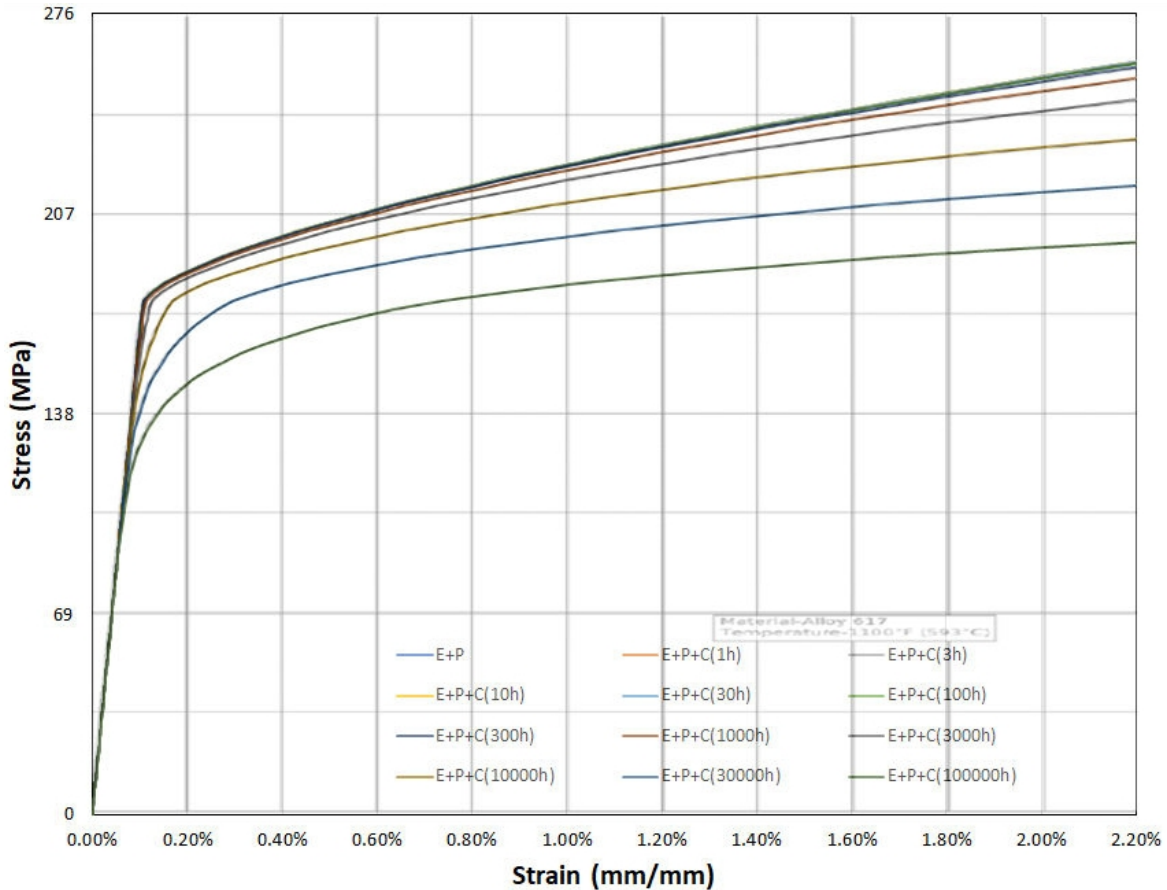


Figure I-4 Calculated ISSC for Alloy 617 at 1,099 degrees F (593 degrees C).

The calculated isochronous stress-strain curve is in color and the Record number curve is in gray. They are identical and on top of each other.

I.3 Spot Checks of ISSC for Alloy 617 with other data

Spot checks of the ISSC curves are provided here. Several data set points and curves that were not used to develop the ISSC curves in INL, 2021o are compared with the code curves. As will be seen below, the comparisons with additional data in the literature from sources that were not used to produce the code ISSC curves show code curves are conservative. Alloy 617 material has ranges of component elements that define the material type. Different heats of material produce different plastic and creep strain response at different temperatures and results in data scatter. The spot comparisons below for Alloy 617 show the inherent scatter in the data and illustrate that the data used to produce the ISSCs in the code, which are meant to be average data, are likely lower bound data compared to some of the literature data. It is not known why this is the case.

The first set of additional data comes from the Davies group at Imperial College (Narayanan, et. al., 2017). Figure I-5 compares the Davies data with the ISSC curves in the code at 700 degrees C. It is seen that the Davies data points are all above the code ISSC curves indicating

conservatism. In addition, data from Knezevic et. al., 2013 also plotted on this curve for 700 degrees C are also conservative as the points are higher than the corresponding ISSC curve in the code.

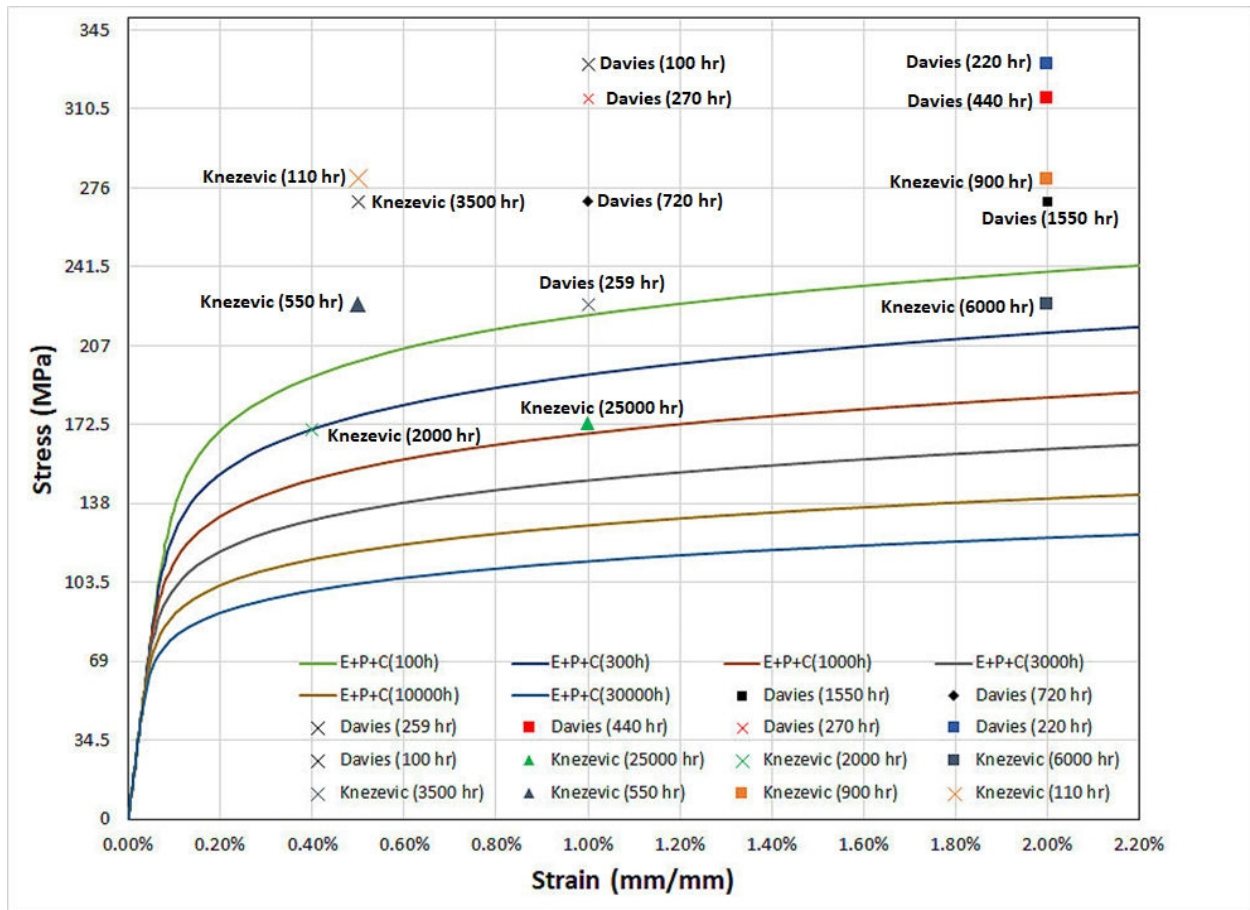


Figure I-5 Comparison of Code Case N-898 ISSC curve at 1,292 degrees F (700 degree C) to data from Narayanan, et. al., 2017 (Davies) and Knezevic, 2013.

A second set of comparisons is made with ISSC curves that are presented in Corum et. al., 1991 and Jetter et. al., 2004. Figure I-6 shows the comparison at 649 degrees C of the ISSC from Code Case N-898 and Corum et. al., 1991. It is seen that the curve for 1,000 hour from Corum et. al., 1991 is higher, for 10,000 hour the curves are rather close, and for 100,000 hours the Corum et. al., 1991 curve is a little lower. Further discussion of the 100,000 curves is useful. Robinson (1984) developed the unified constitutive model at that time from tensile testing data on one heat of material. However, the ISSC curves in the code are meant to be average curves from many heats of material. Therefore, Corum used the Robinson model equation to develop ISSC curves at different times, including 100,000 hours. Corum then adjusted those curves by using Huntington Alloy data for yield and stress to produce 1% strain from many heats. Therefore, the ISSC curves from Figure 7 in Corum et. al., 1991, which are compared to in Figure I-6 in below, are from the Robinson model of one heat of material adjusted in an attempt to make the data average. However, Robinson did not have actual data

up to 100,000 hours. Hence the long time curves are from the Robinson model at 100,000 hours adjusted to try to make it an average curve. For these reasons, this is considered within the scatter band of creep data for the 100,000 curve.

Comparison is also made with data from Jetter et. al., 2004 in Figure I-7 to the ISSC curves in the code case. For all times shown in this plot the ISSC curves from the code case are slightly more conservative and the curves are very close at the time of 100,000 hours. Finally, in Figure I-8 a comparison is made between the code case ISSC curves at 982 degrees C (1,800 degrees was F) and the models presented by Corum et. al., 1991. The comparison shows that the code case ISSC curves are conservative relative to the Corum et. al., 1991 model. . It is noted that the INL, 2021o ISSC curves are only permitted to be used up to 954 degrees C but the curves were calculated at 982 degrees C using the equations included in the code case.

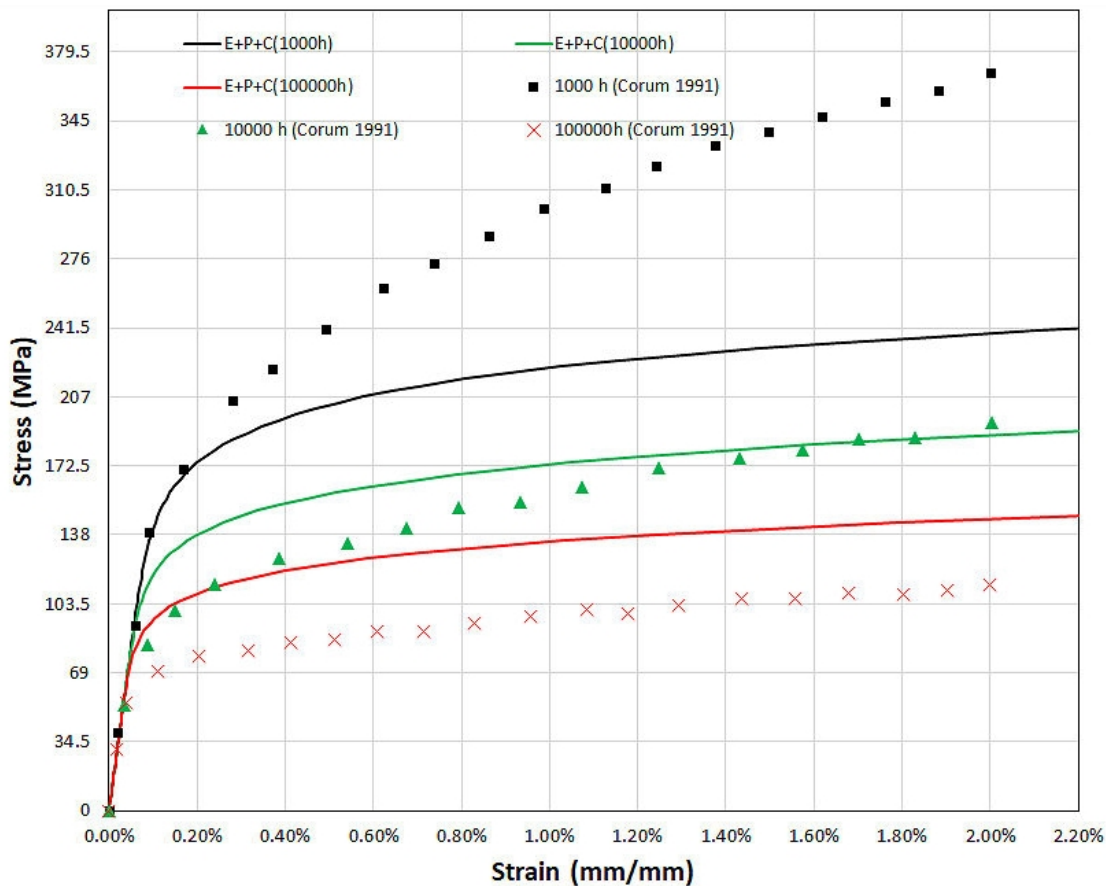


Figure I-6 Comparison of Code Case N-898 ISSC curve at 1,200 degrees F (649 degree C) to model predictions from Corum et. al., 1991.

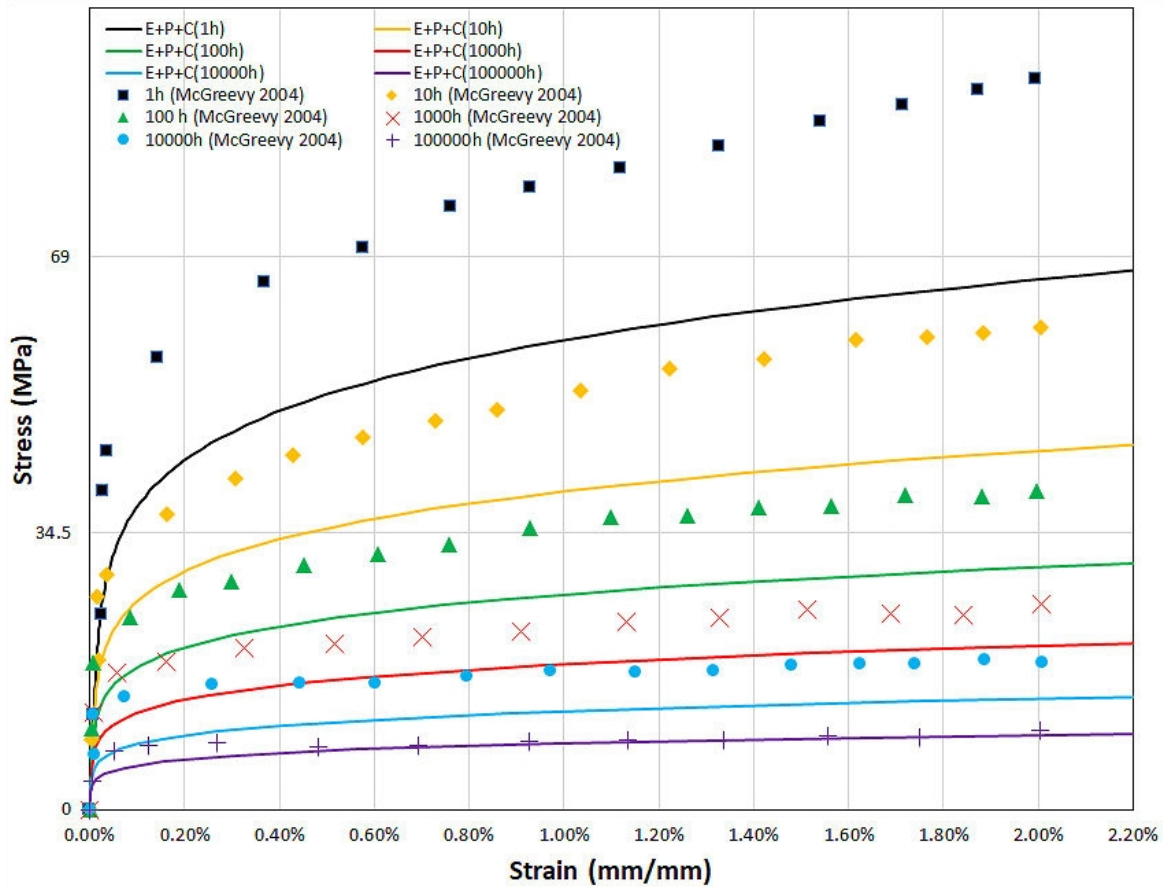


Figure I-7 Comparison of Code Case N-898 ISSC curve at 1,701 degrees F (927 degree C) to model predictions from Jetter et. al., 2004.

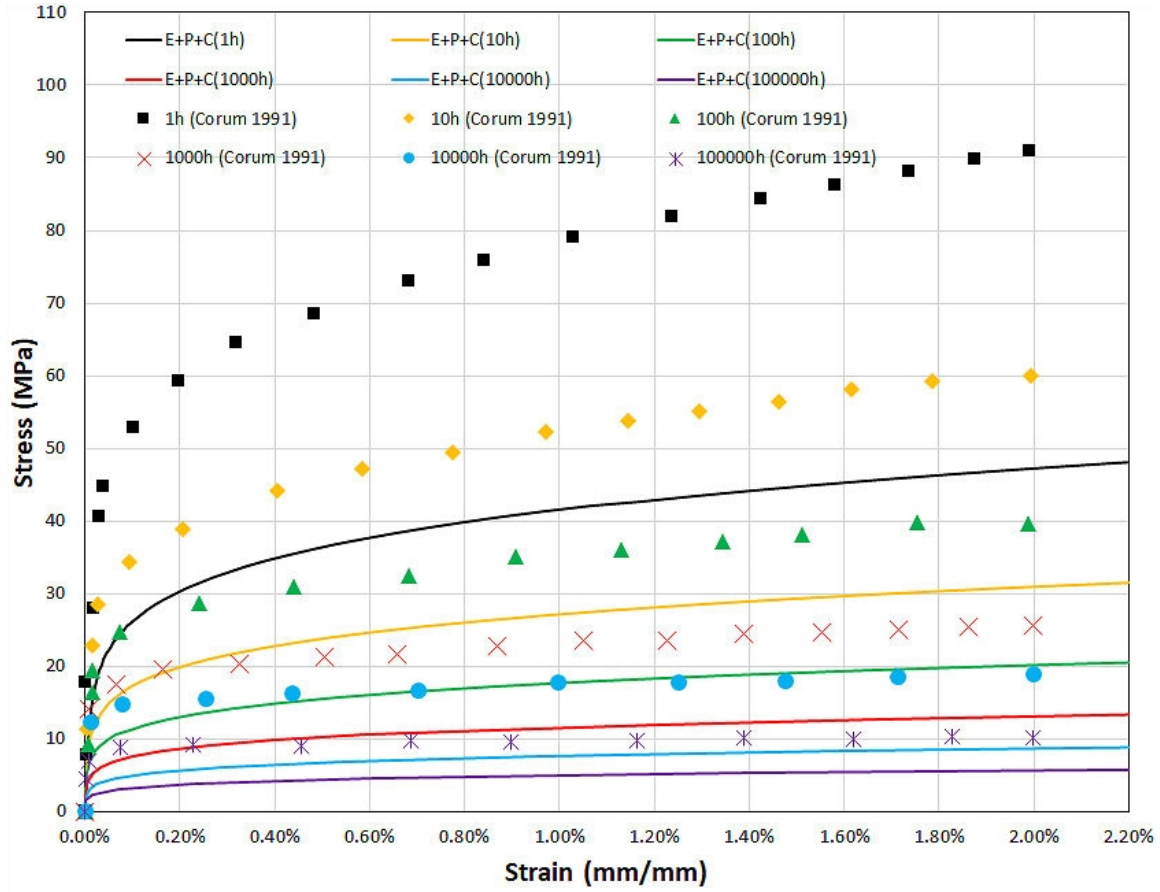


Figure I-8 Comparison of Code Case N-898 ISSC curve at 982 degree C to model predictions from Corum et. al.,1991.